DESIGN OPTIMIZATION OF GEOSYNTHETIC REINFORCED EARTH WALLS USING HARMONY SEARCH ALGORITHM

by

Mohammad Motalleb Nejad

A thesis submitted to the Faculty of the University of Delaware in partial fulfillment of the requirements for the degree of Master of Civil Engineering

Spring 2017

DESIGN OPTIMIZATION OF GEOSYNTHETIC REINFORCED EARTH WALLS USING HARMONY SEARCH ALGORITHM

by

Mohammad Motalleb Nejad

Approved: _____
Kalehiwot Nega Manahiloh, Ph.D.
Professor in charge of thesis on behalf of the Advisory Committee

Approved: _____
Harry W. Shenton III, Ph.D.
Chair of the Department of Civil and Environmental Engineering

Approved: _____
Babatunde A. Ogunnaike, Ph.D.
Dean of the College of Engineering

Approved: _____
Ann L. Ardis, Ph.D.
Senior Vice Provost for Graduate and Professional Education

ACKNOWLEDGMENTS

Next to Allah, I thank my father and my mother for giving me the opportunity to live without any expectations other than my success. I dedicate this thesis in memory of my father who passed away two years ago, but continued to live in my heart. I thank my wife who endured all difficulties in my academic and personal life. Thanking her is the least I can do for the love, support, and encouragement she gave unconditionally.

My sincere gratitude goes to Dr. Kalehiwot Nega Manahiloh for his encouragement, guidance, personal, professional and financial support throughout my academic endeavors at the University of Delaware. It was an honor being part of his research team. I learned, from Dr. Manahiloh, the skill of breaking down complex problems into smaller pieces and constructing results into a bigger solution.

I thank the graduate students with whom I shared office space and friendship. They are too many to name here, but I am forever grateful for their friendship. I also thank Drs. Meehan and Kaliakin for every contribution they offered in my graduate student life. I am thankful for their support, encouragement, and advice.

I am thankful to the staff in the Department of Civil and Environmental Engineering. Their heart-felt welcome and assistance is something that I will cherish for many more years.

TABLE OF CONTENTS

LIST OF TABLES

LIST OF FIGURES

ABSTRACT

Compared to other civil engineering structures. The cost of construction for earth structures is enormous. This is not only because of the large dimension of such structures, but also because of the high safety factors applied to reconcile the driving forces and prevent any possible failures. The fact that stringent policies specify very high safety factors is indicative of the paramount durability needed in earth structures. These policies, to some extent, are not irrational if one considers the extent of life and monetary loss associated with failure of such structures. Traditionally, the analysis and design of earth structures is done following the working stress design principles. Recent developments have led to the application of Load and Resistance Factor Design (LRFD) in the analysis and design of such structures. In the broader engineering world, there are many optimization techniques that can be adopted in the analysis and design of earth structures. Once such technique namely, harmony search algorithm, falls under the category of metaheuristic optimization. In this study, harmony search algorithm is adopted and successfully applied in the design optimization of mechanically stabilized earth (MSE) walls reinforced with geosynthetic. The effects of using non-uniform length and spacing of reinforcement layers, on cost and design of the MSE walls, has been investigated. Results of this study showed that harmony search optimization algorithm is successful in optimally reducing the cost of construction of geosynthetic-reinforced MSE walls.

Chapter 1

INTRODUCTION

1.1 Reinforced Earth Walls

Reinforced earth walls (also called mechanically stabilized earth walls or MSE walls) are soil walls constructed with artificial reinforcing. They can be used for retaining walls, bridge abutments, seawalls, and dikes. The primary constitutive elements of reinforced earth walls are the consecutive layers of engineered soil and layers of reinforcements. In fact, reinforced earth is a composite material consisting of cohesionless soil and flexible reinforcement. The most popular flexible reinforcing materials are metal strips and polymeric materials. A confined soil usually has high compressive strength but yields weak tensile performance. The tensile strength of the reinforced earth system is provided by frictional and mechanical interlocking between soil and reinforcement. Structurally, the least significant component of reinforced wall systems are the facing elements. Facings play the role of enhancing the aesthetics aspects of such structures. The facing blocks are usually prefabricated from concrete, steel sections, treated timber, or wire mesh. The analysis and design of a reinforced earth wall takes into account an integrated mass that acts cohesively, while supporting its own weight and applied loads.

The concept of reinforcement in earth walls dates back to ancient times. Two examples of ancient reinforced soils are the wooden reinforcement used in the Babylonian Gods temples in the ancient city of Dur-Kurigalzu, Iraq (Figure 1.1) and Beacon Tower in Western China. Straw, sticks, and branches were used in such structures to reinforce adobe bricks and mud dwellings. The modern form of these mechanically stabilized earth walls (MSE walls) was introduced by a French architect and engineer, Henry Vidal, in the 1960s. In 1968 and 1969, MSE walls were actively used during the construction of mountainous freeways in France. The first MSE wall in the United States was constructed in 1971 near Los Angles. Since then, more than 23,000 MSE walls have been built around the world (Nicholson 2015).

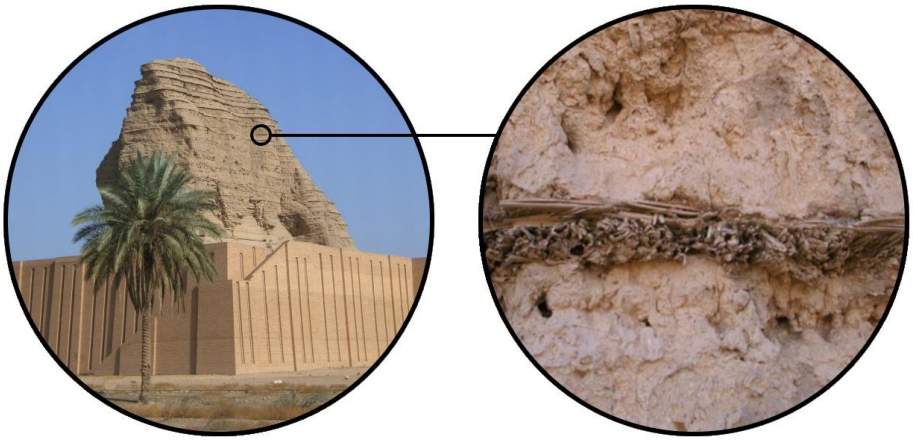

Figure 1.1 Babylonian Gods temple in ancient city of Dur-Kurigalzu ,Iraq [Modified from www. treasurenet.com]

Reinforced earth walls are extensively used in highways, abutments of bridges, railroads and subways, docks, airports, industrial sites, and commercial and residential

landscaping projects. For such pervasive applications, reinforced earth walls are considered cheaper alternatives to other types of retaining walls. In addition, reinforced earth walls are known to be reliable solutions for projects with space limitations, weak ground conditions, and underground networks of utility lines.

The significant benefits gained from reinforced earth walls include:

- Economic efficiency
- Low construction time
- absence of need for complex construction tools and facilities
- absence of need for expensive foundations
- superior flexibility under seismic loads
- Insensitivity to differential settlements
- Durability and neat look
- Constructability in limited spaces
- Environmental friendly

Geosynthetic reinforcements are engineered from strong and durable polymers. These materials offer MSE walls the capacity to withstand tensile loads, while deformations are kept under allowable values for over the design life of such structures. In addition, their integral behavior along with high flexibility and corrosion resistance makes them superior alternatives to steel reinforcement. The length of geosynthetic reinforcements can easily be extended beyond the potential failure surfaces of a soil mass. Any tensile force in the reinforced earth system is carried by

the geosynthetic layers. The geosynthetic layers also serve the purposes of confining the soil and offering resistance to movement, thus providing additional shear strength. The performance of geosynthetic reinforcements has seen growth due to the recent advancements in the polymer and material industry. One such advancement is in the area of maximizing the interaction efficiency between reinforcements and the confined soil layers. While the general MSE construction industry enjoys the perks of these recent advancements, this study looks into further optimizing the cost of construction of MSE walls reinforced with geosynthetic materials. Subsequent sections will briefly discuss the concepts behind the optimization methods.

1.2 Optimization Methods for the Design of Reinforced Earth Walls

Construction cost is one of, if not major, the decisive factors in engineering projects. Although the cost of construction for MSE walls is relatively low compared to gravity walls, the conventionally adopted design procedure, which is based on controlling the safety factors against the failure mechanisms for the initial design, does not allow for optimized design of MSE walls. Usually, the initial design is very conservative and satisfies all the required safety factors. In some cases, the obtained safety factor for one mechanism is close to the minimum allowable safety factors defined in design standards. On the other hand, safety factors for other mechanisms are very high. Such a design philosophy, even though results in a safe design, doesn't necessarily result in an economical (i.e., optimum) design. Optimum engineering design should give due regard to the cost of projects in addition to safety. One way of

achieving an optimized design is by setting a target function (e.g., cost function) and optimizing it with appropriate techniques while the minimum safety requirements are preserved.

Cost function in optimization problems is defined as a function that needs minimization or maximization, based on sought outcome, to obtain optimal performance of a given system. Cost function can be defined as an equation consisting of design variables and constants specified for the problem at hand. For instance, the constant specifications for reinforced earth walls are the unit weight of the soil, wall height, and the cost of reinforcement and embankments. Also, the tensile strength and length of the reinforcements are key design variables. For reinforced earth wall construction project, the cost function that is defined as a function of the variables listed above, is optimized by setting cost minimization as a target.

Generally, optimization problems can be divided into two categories. The first category consists of problems where the variables in the cost function are not subjected to any constraint. Each variable can take any value without any limitation; however, the optimum value for the cost function is obtained for one single set of variables. The second category includes problems where some of the variables, or specific combinations of variables, are subjected to constraints. For example, the safety factors in the design of reinforced earth walls impose several constraints that need to be enforced. If a set of variables optimize the cost function but violates any of the safety factors, there should be a prognosis approach that prevents such variables.

The existence of such problems necessitated the development of robust techniques to account for constraints emerging in some problems.

1.3 Metaheuristic Optimization Methods

As mentioned in the previous section, MSE walls are among the structures that need enforcement of constraints emanating from required safety factors. When constraints constitute a set of linear algebraic equations, utilization of linear programming and simple technics such as the "Complex Method" (Box (1965), Guin (1968)) result in a single deterministic solution for the problem. On the contrary, quadratic functions and highly nonlinear and multimodal optimizations subjected to complicated constraints cannot be easily solved by using simple conventional methods. Metaheuristic optimization methods are simple mathematical probabilistic methods that are inspired by natural and artificial phenomena. Mother Nature have been successfully optimizing the evolution of the world and have been giving birth to new, evolved creatures to bring the world into balance. Although the results of the metaheuristic optimization methods are probabilistic, the measure of their performance can be correlated with that of the harmony Mother Nature has been able to keep since the creation of life. In addition, most of the metaheuristic methods have been applied for more complicated functions. The complexity in the formulation of these methods is minimized and only the behavior of a natural phenomenon is translated into their mathematical forms or algorithms. The first widely used metaheuristic method, known as Genetic Algorithm (GA), was developed by John

Holland in the 1960s (Holland 1992). GA relies on bio-inspired operators such as mutation, crossover, and selection. Table 1.1 shows a list of popular and commonly used metaheuristic methods that have been widely used in engineering optimization problems.

Table 1.1 Commonly used metaheuristic methods.

Method	Developer	Inspired by
Simulated Annealing	Kirkpatrick et al. (1983)	Metal annealing processing
Genetic Algorithms	Holland in 1960s (Holland 1992)	Biological systems
Differential Evolution	Storn and Price (1997)	Biological systems
Ant Colony Optimization	Marco Dorigo 1992 (Dorigo and Stützle 2004)	foraging behavior of social ants
Bee Algorithms	Pham et al. (2005)	foraging behavior of bees
Particle Swarm	Kennedy and Eberhart (1995)	swarm behavior observed in nature
Tabu Search	Fred Glover in 1970s (Glover and Laguna 1997)	uses memory and the search history
Harmony Search	Geem et al. 2001 (Geem et al. 2001)	improvisation process of a musician
Firefly Algorithm	Yang 2008 (Yang 2014)	flashing behavior of fireflies
Cuckoo Search	(Yang and Deb 2009)	brood parasitism of some cuckoo species

1.4 Research Motivation

In the engineering world, the construction of earth structures is very expensive and the design procedures use controlling approaches to evaluate the performance of the initial design. In most cases, the initial design is accepted when it satisfies the criteria imposed by factors of safety. Therefore, following the conventional methods results in a highly conservative design and imposes remarkable costs. An efficient optimization method is required to obtain a reliable economical design, where safety is ensured by satisfying constraints imposed based on standard codes.

The cost function for MSE walls is nonlinear and is influenced by several complicated constraints. These constraints make optimization unachievable with conventional methods. Harmony Search algorithm is a relatively new metaheuristic method that is known for using less complex mathematical operators and for employing the concept of "memory" to obtain the best harmony among the possible harmonies resulting from different combinations of variables.

Most of the studies that have been done by previous researches were based on complicated optimization methods (e.g. Basaduhar et al. (2008)) that are not suitable for practical problems. Also, previous works lacks the possibility of having non-uniform geosynthetic layers. Non-uniformity can be defined as different vertical spacing and length of geosynthetic. In this study, an attempt has been made to integrate harmony search algorithm with design considerations for MSE Walls reinforced with geosynthetics layers and optimize their design.

1.5 Organization of the Thesis

The remainder of this thesis will provide lengthy, yet informative details on the process utilized to successfully optimize the cost of construction for MSE walls reinforced with geosynthetic layers, where the design considerations and the criteria defined by safety factors are satisfied. Chapter 2 is composed of background information that is necessary for understanding the logic and reasoning behind the MSE walls and optimization approaches in geotechnical engineering. The first section of this chapter focuses on different types of MSE walls. A number of popular systems

are introduced and the benefits and disadvantages of each one is described. Finally, the superiority of the geosynthetic reinforced earth walls compared to other systems is discussed. The last portion of this chapter presents the history of optimization methods applied to geotechnical engineering problems. Chapter 3 focuses on the optimization of design parameters and the cost of geosynthetic-reinforced earth walls using the Harmony Search algorithm. Chapter 4, titled Optimum Design of Earth Walls Reinforced with Non-uniform Geosynthetic Layers, expands on the previous Chapter 3. Most notably, a new system has been proposed in this chapter, where both the lengths and distances between geosynthetic layers are not required to be uniform. This chapter also includes an introduction to a new modified Harmony Search technique that enables the optimization algorithm to utilize a vector consisting of variables of the same type as a single input variable. Lastly, Chapter 5 presents the conclusions drawn from the work done in Chapters 3 and 4. In addition, the Matlab codes and the subroutines, developed during the implementation of Harmony Search and Improved Harmony Search Algorithms, are provided in Appendices A and B.

Chapter 2

BACKGROUND

2.1 Rigid Retaining Walls

Based on their mode of load resistance, retaining walls can broadly be subdivided into two groups, namely rigid and flexible walls. Rigid retaining walls use their stiffness to support the lateral pressures imposed by the retained soil mass. In other words, the rigid wall restrains the soil, by virtue of stiffness and no deformation, to a slope that is larger than the slope associated with the shear strength of the soil (i.e., the angle of response). There are six rigid retaining walls that are popular and intensively used in geotechnical engineering, these are:

- Gravity walls
- Semi gravity walls
- Cantilevered walls
- Sheet piles
- Bored piles
- Anchored walls

Figure 2.1 shows the various types of rigid retaining walls. Gravity walls rely on their mass to resist lateral pressures, which forces the wall to move horizontally, and remain stable against any overturning moments. The gravity walls are often made from mortarless stone or concrete units. A rigid footing is used below the wall to

maximize the stability of the wall. Gravity walls can also be built as composite structures where cellular confinement units are employed to enhance their flexibility.

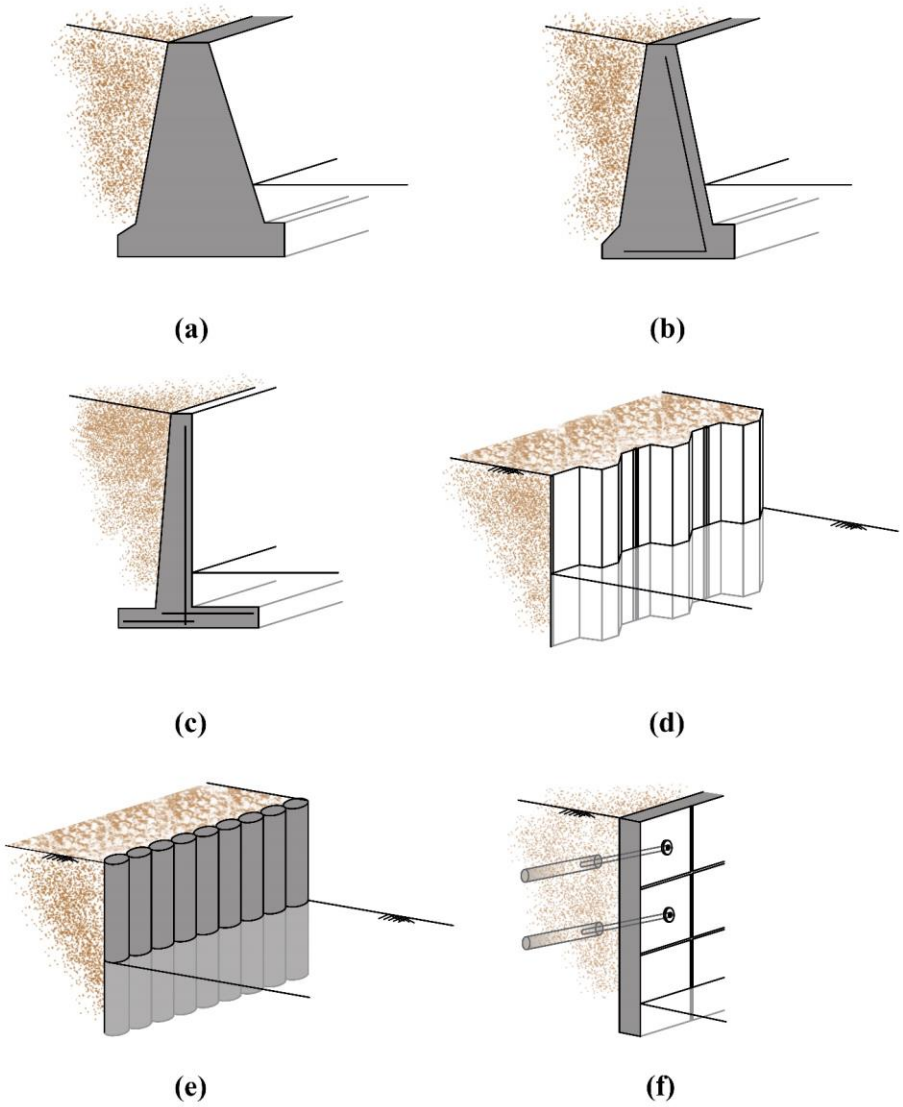

Figure 2.1 Different types of rigid retaining walls: (a) Gravity wall; (b) Semi gravity walls; (c) Cantilevered wall; (d) Sheet pile; (e) Bored pile; (f) Anchored walls.

Semi-gravity retaining walls are a specialized form of gravity walls that include tension reinforcing steel bars to minimize the thickness of the wall without requiring extensive reinforcement (Figure 2.1(b)). The concept of reinforcement in these walls are borrowed from cantilevered walls.

Due to the utilization of significant reinforcing steel bars, wall thickness is significantly reduced in cantilevered walls (Figure 2.1(c)). A relatively thin stem and a base slab are the main elements of the cantilevered wall. The base slab subdivides into the "heel" and "toe" slabs that join below the stem. Although cantilevered walls use much less concrete than monolithic gravity walls, more precision and precaution is required for successful design and construction of such walls. During service, the lateral pressures imposed by the soil are transferred, via a cantilever effect, to the footing slab and passed to the foundation soil below. When high lateral loads are expected or the height of the wall is relatively high, cantilevered walls employ buttresses on the front or counterfort on the back to facilitate the load transfer to the footing (Figure 2.2). Overall, these walls consume much less concrete compared to conventional gravity walls.

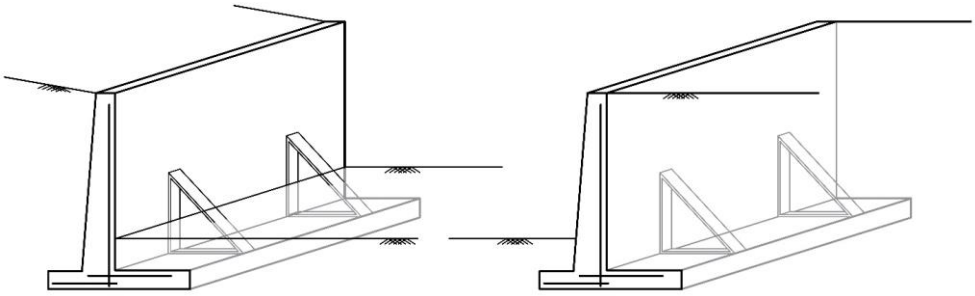

Figure 2.2 Buttressed cantilevered (left) and counterfort (right) walls.

When a retaining wall is required for soft soil or there is a space limitation, sheet piles become the best choice. Sheet piles (Figure 2.1(d)) are customarily fabricated from steel or wooden material and driven into the ground, with approximately two thirds of the height of the sheet piles embedded in the ground.

For proper construction of a bored pile retaining wall, a sequence of bored piles operations is installed in place and excavation of the soil proceeds on the desired side of the piles. The pile material could be timber, steel, or concrete.

Anchors are components of a retaining system that can be integrated with any of the walls discussed above. Generally, anchoring of a retaining wall is performed by attaching a high-tensile-capacity cable or a tie-rod to the retaining wall and extending it to a location where sufficient friction is mobilized, to counterbalance the acting loads. The interlock of the anchor is ensured by either: grouting cement mortar around the tie-rod, or tying it to a "deadman" - a concrete block deep-seated in the soil mass.

2.2 Mechanically Stabilized Earth (MSE) Walls

As mentioned before the second broad class of retaining walls are the flexible retaining walls. Mechanically stabilized earth walls (MSE walls) is a common synonym to flexible retaining walls. In MSE walls, soil’s shear strength is enhanced by reinforcing and/or confining it with artificial materials. The interaction between soil and the reinforcement makes up a composite system that monotonously serves as a retaining wall. Figure 2.3 shows some application areas of mechanically stabilized earth (MSE). As can be seen, MSE systems can be used to support pile foundations,

shallow foundations (footings), road bases, and abutments. They also can be employed in sinkhole bridging.

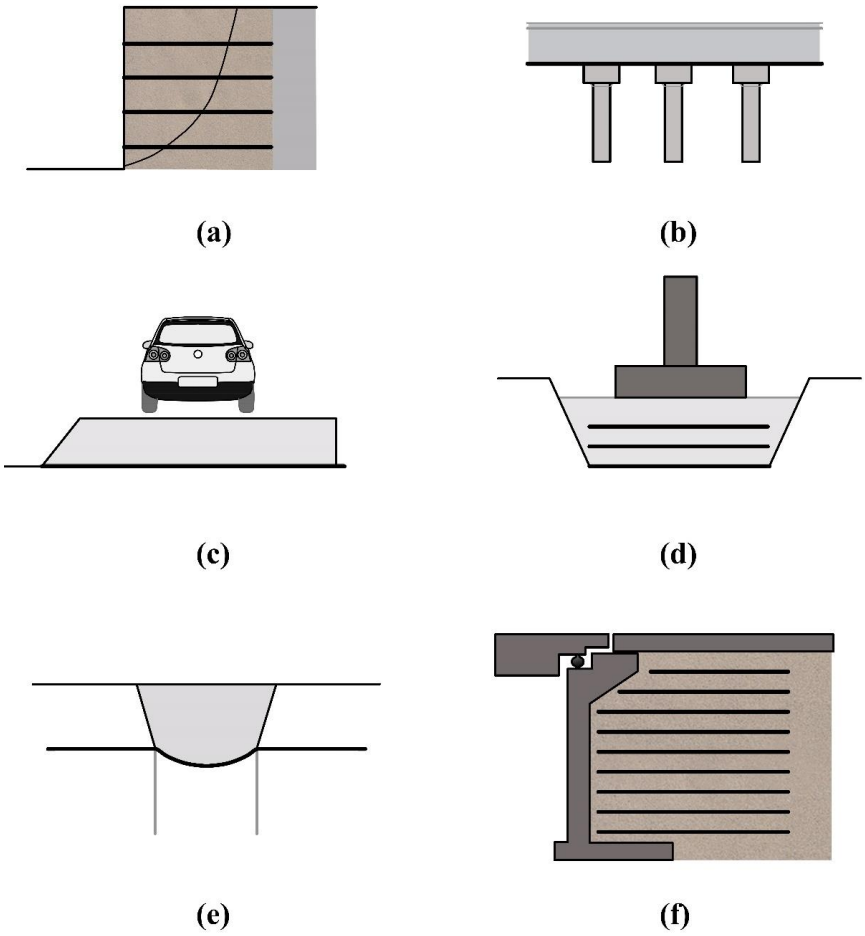

Figure 2.3 Different applications of MSE in geotechnical engineering (a) Retaining walls; (b) pile foundations; (c) road bases; (d) shallow foundations; (e) sinkhole bridging; and (f) abutments.

Figure 2.3 (a) shows a very simplified schematic of the shape of a mechanically stabilized earth wall. As seen in the figure, the reinforcements are

extended beyond the failure surface of the soil, to create a monolithic mass that provides the required strength to resist failure. The failure mechanisms for reinforced earth walls will be described in detail later in Chapters 3 and 4. In the current section, different types of MSE walls are described from the construction point of view. Figure 2.4 depicts the general, basic components of MSE walls.

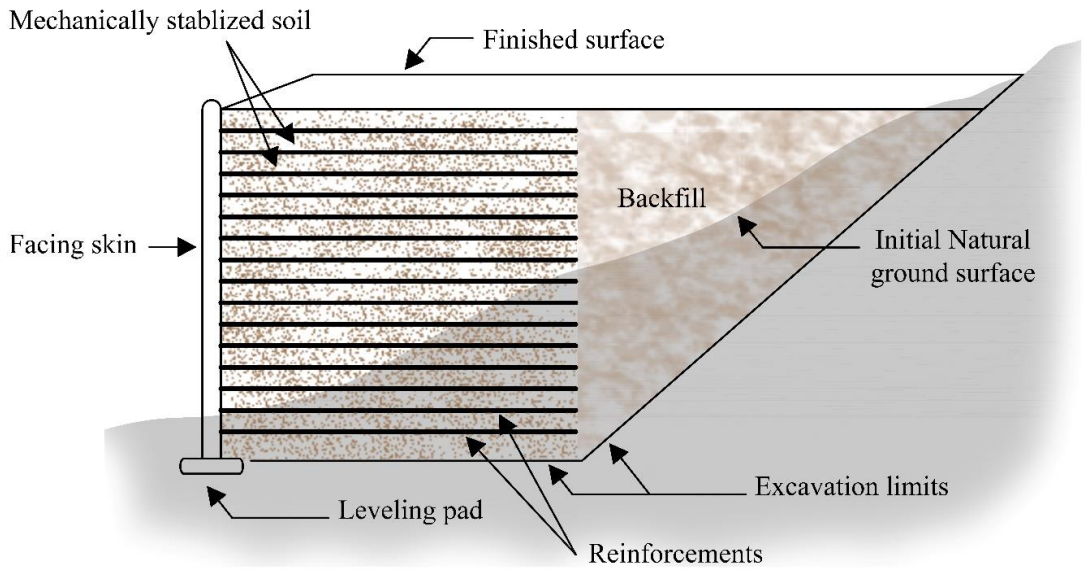

Figure 2.4 Basic elements of MSE walls.

From Figure 2.4, it can be seen that a MSE wall consists of two important elements, the reinforcement material and a selected frictional soil. The interlocking and frictional interaction between these two elements gives birth to a monolithic mass that behaves like a composite material with enhanced shear strength.

2.2.1 Different types of reinforcements for MSE walls

MSE walls employ different types of reinforcements to stabilize the soil. A simplified depiction of a reinforced soil wall is shown in Figure 2.5. Figure 2.5 (a) shows basic elements and configuration of a reinforced earth wall. A layer of engineered length of reinforcing strips, fabricated from metallic or polymeric material, is placed above and below each compacted soil layer. The horizontal (S_h) and vertical (S_v) spacing of the strips follow design code standards. The strips are tied to the facing skin. The facings are commonly made out of modular concrete blocks. Steel sheet facings are also common. Different tying approaches can be chosen, depending on the type of reinforcement and facing skin used.

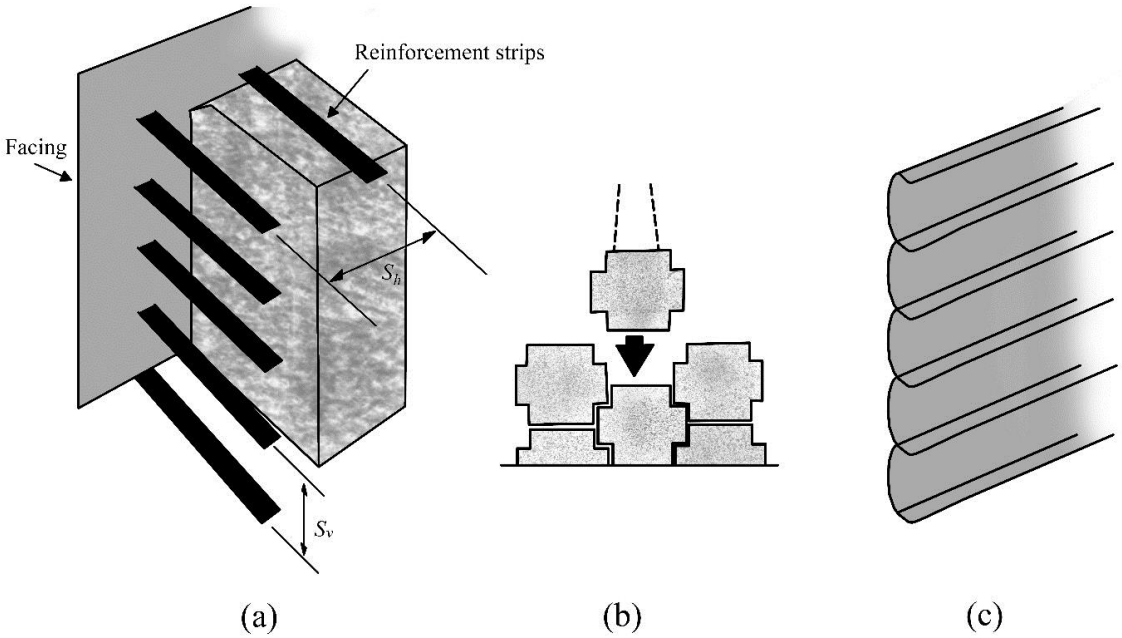

Figure 2.5 Simple schematic view of a reinforced earth wall (a) MSE wall; (b) cross -shaped modular facing; (c) steel sheet facing.

The most popular types of reinforcement used in MSE Wall construction are: steel strips, plastic strips, steel meshes, Geosynthetics (Geotextile and Geogrid), and locker and strip. Figure 2.6 shows the photograph of a MSE wall construction in which steel strips are used as reinforcement. The MSE wall in this figure shows a double face wall located in the corner of a construction site. As can be seen, strips from one face overlap those from the orthogonal face. Figure 2.7 shows steel meshes and their installation in MSE wall construction.

Figure 2.6 MSE wall reinforced by steel strips.[1]

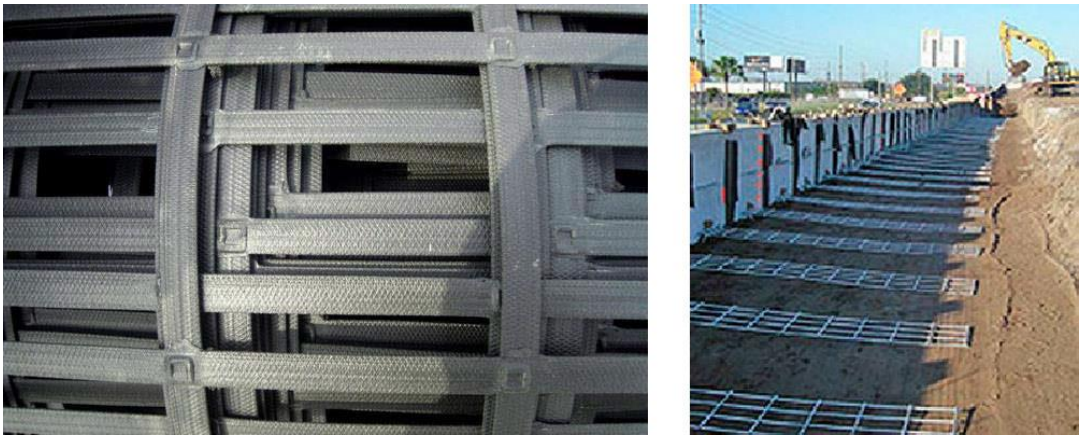

Figure 2.7 MSE wall (right) reinforced by steel meshes (left).

Figure 2.8 shows a MSE wall construction using polymeric strip reinforcement. The polymeric strip passes through hoops on the backside of the facing

[1] Figure 2.6 through 2-10 are adopted from Reinforced Soil Wall Seminar held in Iran, November, 17th, 2015.

blocks. The flexibility of these walls is relatively higher than that of metal strip reinforced walls.

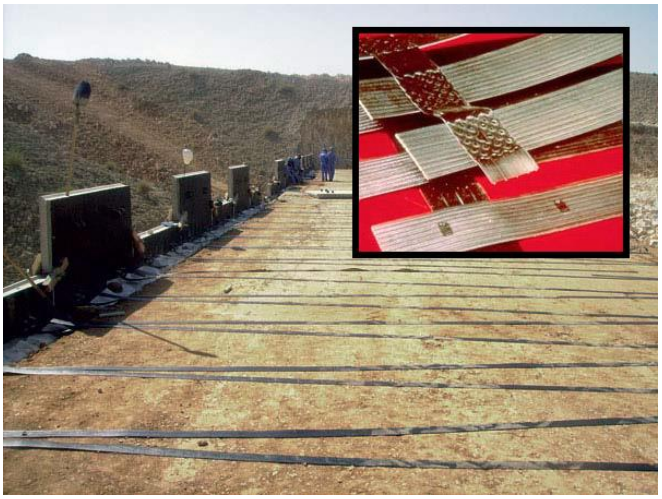

Figure 2.8 MSE wall reinforced by plastic strips.

Figure 2.9 shows the construction of a MSE wall reinforced using the locker and polymeric strips. The strips pass through hoops attached on the back of the facing blocks and around a concrete locker embedded within the backfill. The inclusion of locker systems enhances the pullout resistance of the reinforcement. Such construction method, even though not common, is useful when there are space limitations.

Figure 2.9 MSE wall reinforced by locker and plastic strips.

The most recent development in MSE walls is in the area of geosynthetic reinforcement. Geosynthetic fabrics are fabricated from woven polymers. Advancing the manufacturing and implementation aspects, and improving tensile strength of geosynthetic fabrics has been the focus of many research studies. Since their development, the application of geosynthetics has prevailed in several engineering fields, especially in Civil Engineering. Figure 2.10 shows the two most common forms of geosynthetic reinforcements (geogrid (a) and geotextile (b)) in the construction of MSE walls. From construction standpoint, it is a common practice to fold geosynthetic textile to the next layer and maintain continuity in confinement. A sequence of light concrete blocks have also been used in tiling the geotextile with the face of the wall.

(a) (b)

Figure 2.10 Geosynthetics in construction of MSE walls: (a) Geogrid; (b) Geotextile.

2.2.2 Considerations for the stabilized soil type and wall facing

The considerations for the construction of MSE walls and the material requirements have been described in more details in several codes such as the FHWA NHI-10-024 and ASTM D 2488 standards (Elias et al. (2001), and AASHTO (1996)). In the following chapters, the technical aspects of the design will be discussed thoroughly. Here, only some considerations for reinforced fill are discussed. Based on the Federal Highway Administration standard, the percentage passing from the U.S. sieve number 4 should be 100 percent, which means that gravel particles are not allowed in the reinforced fill zone. In addition, the percentage passing from sieve numbers 40 and 200 must be less than 60 and 15 percent, respectively. The maximum plasticity index of the soil and minimum acceptable internal friction angle for the stabilized soil are limited to 6 and 25 degrees, respectively. AASHTO T-104

emphasizes that the material shall be substantially free of shale or other soft, organic poor durability particles (AASHTO 1996). Also, there are some chemical and electrochemical considerations that need to be evaluated before using the fill soil. The reinforced soil, at each layer of geosynthetics, must be compacted using suitable compactors before adding the next layer of reinforcement.

Although facings are of least structural importance, the role they play in ensuring aesthetics is of paramount significance. A facing skin can be made from pre-cast concrete sections or steel sheets. A cross-shaped pre-cast concrete facing and horizontal steel sheet facings were shown in Figures 2.5 (b) and (c), respectively. These facings are conventional type of facings that have been in use since the engineered construction of MSE walls begun. The pursuit for better finishing and flexibility in landscaping, has led to the development of newer type of facings such as gabions, concrete modular panels, concrete planter boxes, and steel mesh facings.

The use of MSE walls reinforced with geosynthetics is expanding exponentially. In this study, geosynthetic-reinforced earth walls are selected for design and cost optimization purposes. In the rest of this chapter, a brief literature review of optimization techniques in geotechnical engineering is presented.

2.3 Optimization in Geotechnical Engineering Problems

Optimization has recently found its own place in civil engineering. Structural engineers try to reduce the weight of structures. For example, Lamberti (2008) presented an optimization algorithm, based on Simulated Annealing, that can be used

to optimize the design of truss structures. He examined the optimization algorithm on three different structural problems with the objective of minimizing the weight of bar trusses with 200 design variables and 3500 optimization constraints. Another example on the application of optimization techniques in structural engineering design is the work done by Serpik et al. (2016). In their work, Genetic algorithm was used to optimize the design of non-pre-stressed reinforced concrete structures of flat frames. (Serpik et al. 2016) considered the possibility of crack formation, nonlinear behavior of concrete and reinforcements, and minimized the cost of the concrete frame. A single-span reinforced concrete frames, similar to shown in Figure 2.11, were used to illustrate the performance of the proposed algorithm.

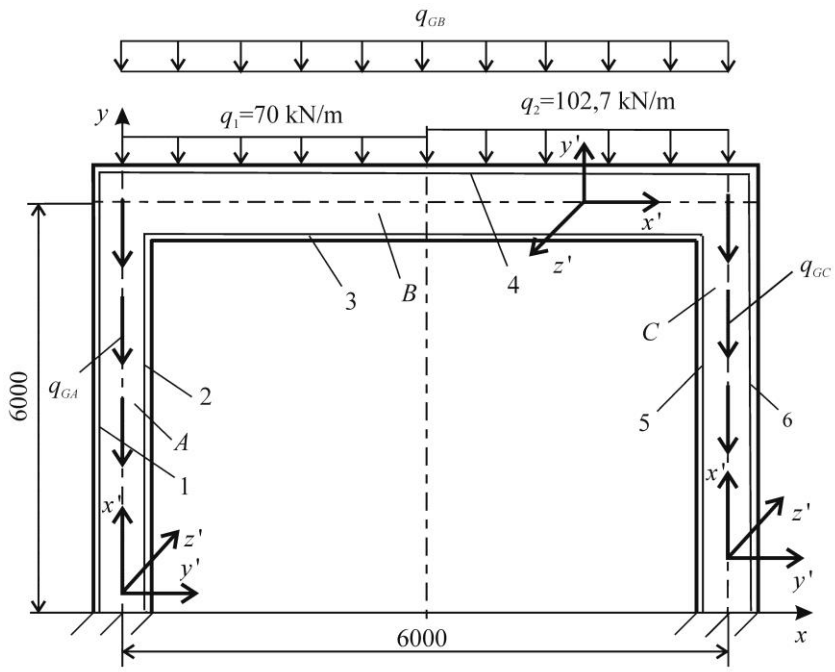

Figure 2.11 Single-span reinforced concrete frame used by Serpik et al. (2016).

Another application of optimization in civil engineering and mechanical engineering is in the area of heat transfer. Heat transfer optimization problem is a multi-objective problem in which the rate of heat transfer must be maximized while the pressure drop is minimized (Abdollahi and Shams (2015a), Abdollahi and Shams (2015b), Jamali Keisari and Shams (2016), Alimoradi and Shams (2017)).

The general advancements in optimization methods have reached the boundaries of geotechnical engineering for different practical problems such as retaining walls, seepage, back analysis in geotechnical constructions, pavement design, etc.

In the area of MSE walls, multiple ongoing state-of-the-art studies have been performed. For example, Basudhar et al. (2008) used Sequential Unconstrained Minimization Technique (SUMT) to optimize the cost of the construction for geosynthetic-reinforced earth walls. Basha and Babu (2012) used a reliability-based design optimization (RBDO) to evaluate the internal seismic stability of reinforced soil structures based on three dominant failure modes. Basha and Raviteja (2016) optimized the tensile strength of geomembrane liner for V-shaped anchor trenches. Ben (2014) performed a limit analysis optimization of design factors for MSE wall-supported footings. He conducted a parametric study to evaluate the effects of reinforcement strength, the location of footing, and failure mechanisms. Vahedifard et al. (2016) designed a constrained optimization approach to find the optimal facing profile for concave geosynthetic-reinforced soil structures (CGRSSs). They showed

that the use of concave facing results in higher stability and lower tensile pressure in reinforcement layers.

Seepage is also another geotechnical engineering problem where optimization techniques have been found to apply. For example, Shahrokhabadi and Toufigh (2013) used a Genetic Algorithm integrated with a mesh-free method, called NEM, to find a solution for the unconfined seepage problem. Shahrokhabadi et al. (2016) integrated Particle Swarm Optimization (PSO) algorithm with a couple of other techniques to estimate the location of the phreatic line in unconfined seepage problem. They found a strong agreement between their proposed solution and existing analytical solutions and experimental tests.

It has been shown that multi-objective problems can be defined in geotechnical engineering by borrowing concepts from other engineering fields. For example, Robinson et al. (2016) used a work optimization strategy to optimize traction control parameters for vehicles in loose dry sand. The interaction of vehicle tire and dry sand (see Figure 2.12) was their primary framework of optimization.

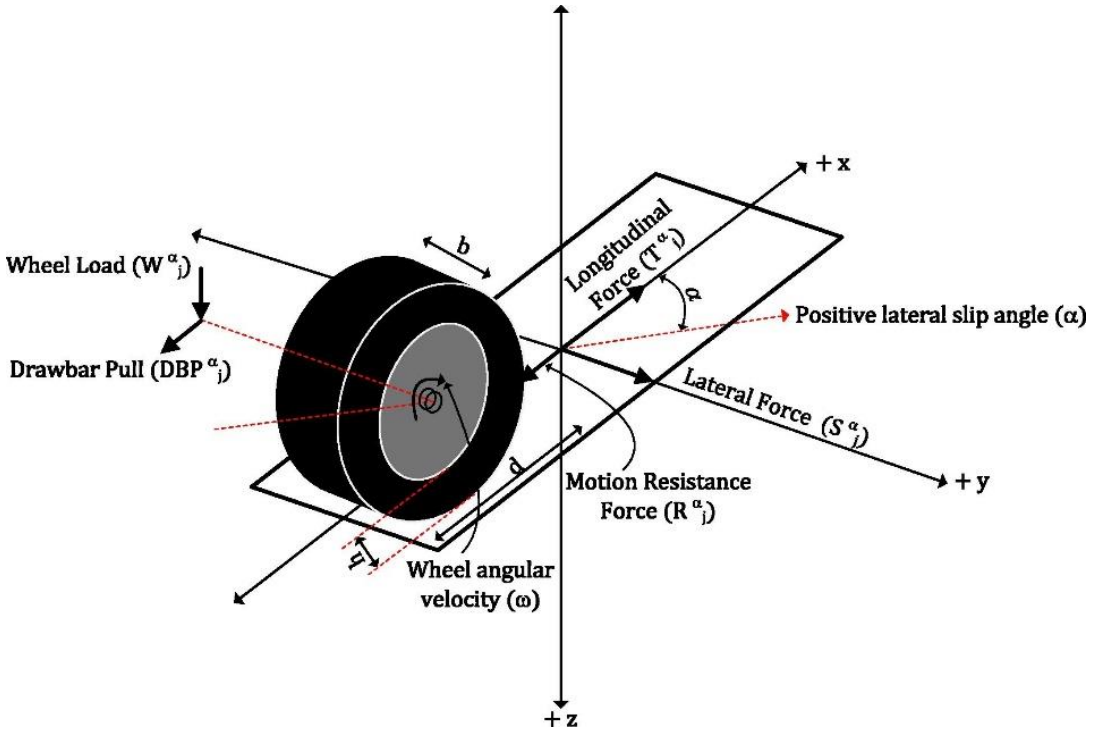

Figure 2.12 Interaction between tire and soil (Robinson et al. 2016)

Zentar et al. (2001) used optimization based back analysis for the identification of soil parameters for modified Cam-Clay model. They minimized the difference between experimental data and the results obtained from integrated general finite element and an optimization code. Mattsson et al. (2001) proposed an optimization routine for identification of model parameters in soil plasticity. The concepts of Rosenbrock (Rosenbrock 1963) and simplex (Murty 1983) methods are borrowed in their work to identify model parameters on the basis of different soil tests. Zhang et al. (2009) used parallel hybrid moving boundary particle swarm optimization, for simulation-based calibration of geotechnical parameters. Their proposed model

showed a good performance for the calibration of the geotechnical models from laboratory of field measurements.

Using an Iterative procedure unsaturated hydraulic properties of vertically heterogeneous soils have been estimated by Kosugi and Nakayama (1997), from transient capillary pressure profiles. Simunek et al. (1998) used Levenberg-Marquardt (Levenberg (1944), and Marquardt (1963)) optimization algorithm to estimate the unsaturated soil hydraulic properties from transient flow processes.

Pucker and Grabe (2011) discussed the basics and applications of structural optimization in geotechnical engineering. The limitations and potentials of topology optimization were described in their work. They presented an example of a gravity wall, single anchored wall and grouted anchored wall for design optimization using topology approach. In addition, the application of design optimization was extended to foundations where the topology optimization is integrated with finite element model of strip foundation. Zhang et al. (2011) discussed reliability-based optimization for geotechnical systems and illustrated its application in shallow foundation design and retaining wall designs. In order to optimize the cost of construction they suggest a simplified reliability analysis by using mean first order method.

In this study, a metaheuristic method, called Harmony Search Algorithm (HSA) has been utilized to optimize the cost of construction for MSE Walls reinforced with geosynthetics. A brief history and introduction to HSA is presented in the subsequent section.

2.4 Harmony Search Algorithm

First proposed by Geem et al. (2001), Harmony Search Algorithm (HSA) is one of the newly developed metaheuristic optimization algorithms. It has gotten a lot of attention because of its fewer mathematical requirements and insensitivity to initial value of the variable vectors. HSA uses stochastic approaches to generate new variables and independent of derivative information. HSA also allows modification on each variable of the solution vector, which is not the case for other metaheuristic approaches. With such flexibility, HSA has shown successful performance in a wide variety of optimization problems (Lee and Geem (2004), Mahdavi et al. (2007), Kim et al. (2001), Geem et al. (2001), and Geem et al. (2002)). The detailed discussion of HSA will be presented later in subsequent chapters.

2.4.1 The idea behind the Harmony Search Algorithms

The idea behind the HSA algorithm is to create the best musical harmony by using a fixed number of musical notes where each note can choose any music pitch. Different combinations of the music pitches result in different harmonies, some are ear-catching while some are annoying. The most beautiful harmony that can be composed and performed by professional musicians is the optimal harmony. Professional musicians first choose a pitch for each note in the harmony and then, based on their experience, pitch-adjust each note to improve the song. This is the exact logic behind the harmony search optimization algorithm. A vector of variables, called

the solution vector, is defined for a given problem. Several vectors of the same type are saved in a memory matrix. The variables for each solution vector are pitch-adjusted by both random and stochastic approaches. Finally, the vectors are sorted based on the resulting solution. Following an iterative procedure, a new vector is produced in each step. If the new vector produces a better solution. The worst solution in the memory matrix will be substituted by the new solution vector. If the solution did not improve in the new vector, the memory matrix remains unchanged.

2.4.2 Parameters of Harmony Search Algorithms

The probability of generating new value for each variable inside a solution vector is called Harmony Memory Consideration Rate (HMCR), and the probability of pitch-adjustment is called Pitch Adjustment Rate (PAR). The value of pitch-adjustment is called Bandwidth (BW). These three parameters play a pivotal role in the quick convergence of the HSA algorithm, and their value needs to be defined based on the specifications of a given optimization problem.

2.4.3 Some of the popular modified Harmony Search Algorithms

The initial HSA assumes that the parameters listed in section 2.4.2 do not change during the iteration process. From the advent of the HSA, several researchers have tried to improve the performance of the algorithm by defining mathematical expressions for HSA parameters or including derivative variables. Some of the popular modified HSA algorithms are discussed here.

Geem (2008) proposed a novel derivative-based HSA algorithm that can be applied for problems with discrete design variables. He formulated a stochastic derivative for variables as a function of HSA parameter. Mahdavi et al. (2007) proposed an improved HSA algorithm where a logarithmic function is adapted to decrease the BW for each iteration. BW in the modified method changes between a minimum and maximum user-defined values. In addition, their proposed method follows a linear equation that increases the pitch adjustment rate with increase in iteration. It is worth mentioning that this Improved Harmony Search Algorithm (IHSA) will be discussed and applied in Chapter 4 of this study. Omran and Mahdavi (2008) borrowed concepts of swarm intelligence to create Global-best harmony search algorithm (GHS). In this method, BW is not involved in any of the steps. Instead, the best solution lend one of its variable to the new solution. Hasancebi (2008) and Hasancebi et al. (2009) attempted an adaptive HS which takes advantage of two varying control parameters, η and ρ, to generate new harmony vectors. Both of these parameters are selected from the average values that are observed within the current harmony memory matrix using a given probability density function.

In all of the methods mentioned above the parameters of HSA are case dependent and should be defined by the operator. A number of studies tried to avoid the definition of initial parameters. For example, Wang and Huang (2010) proposed a new self-adaptive HS technique that is almost parameter-free and uses the minimum and maximum of the current HM members, to automatically control the pitch adjustment step. Geem and Sim (2010) defined PHF-HS algorithm that stands for

Parameter-Setting-Free Harmony Search. They added a new step to the original HSA, called Rehearsal, in which a few first steps of the iteration are used to adjust random initial values for PAR and HMCR. Then, the new values are set for the rest of the iterations. A thorough history of harmony search method can be found in Gao et al. (2015).

Chapter 3

MANUSCRIPT 1. OPTIMIZATION OF DESIGN PARAMETERS AND COST OF GEOSYNTHETIC-REINFORCED EARTH WALLS USING HARMONY SEARCH ALGORITHM

Mohammad Motalleb Nejad

Kalehiwot Nega Manahiloh

Mohammad Sadegh Momeni

Published in:

International Journal of Geosynthetics and Ground Engineering (2015) 1:15

DOI 10.1007/s40891-015-0017-3

3.1 Abstract:

This paper proposes a new approach to optimize the design of geosynthetic-reinforced retaining walls. Minimizing the cost of construction is considered as the optimization criterion. A metaheuristic technique, named Harmony Search Algorithm (HSA), is applied in optimizing the design of geosynthetic-reinforced earth walls. The involved optimization procedures are discussed in a step-wise approach and their applicability is demonstrated on geosynthetic-reinforced walls of height 5, 7 and 9 meters. The effect of static and dynamic load are considered. Results are compared

between this study and studies that used Sequential Unconstrained Minimization Technique (SUMT). It is found that the construction cost, for a geosynthetic-reinforced walls optimized by HSA, showed as high as 9.2 % reduction from that of SUMT.

3.2 Introduction

Retaining walls are among the most extensively used structural elements in the construction industry. The abundance of construction materials and the simplicity in analysis, design, and construction had given rise to the early popularity of non-reinforced retaining walls. It is known that the range of application of non-reinforced walls is limited to shorter heights. The need to enhance structural capacity by introducing a tension-resisting elements led to the introduction of reinforced wall systems. One of such developments was the geosynthetic-reinforced wall system. Geosynthetic reinforcement plays the superposed roles of isolation, tensile resistance and improved drainage in the reinforced system. These overlapping benefits have made geosynthetic-reinforced walls favorable and their design and implementation is expanding. Over the past five decades the production and use of polymer-based reinforcement has shown a sustained upsurge (Mouritz and Gibson 2006). Geosynthetic reinforced soil walls, compared to concrete or gravity walls, have superior flexibility that makes them better in withstanding natural disasters such as earthquake and landslides.

Construction cost is one of the decisive factors in engineering projects. Koerner and Soong (2001) have indicated that the cost of construction for geosynthetic-reinforced soil walls is the lowest as compared to gravity, steel-reinforced Mechanically Stabilized Earth (MSE), and crib walls (see Figure 3.1). In addition to the benefits discussed above, their affordability have played a role in the increased use of geosynthetic reinforcement in weak and collapsible soils, soils in earthquake-prone areas, and projects involving the construction of large embankments.

In recent studies, Harmony Search Algorithm (HSA) has been applied in various engineering optimization problems. A river flood model (Kim et al. 2001), an optimal design of dam drainage pipes (Paik et al. 2005), a design of water distribution networks (Geem 2006), a simultaneous determination of aquifer parameters and zone structures (Ayvaz 2007) are some applications of HSA in the Civil Engineering discipline. HSA has also been applied in space science studies towards the optimal design of planar and space trusses (Lee et al. (2005), Lee and Geem (2004))and the optimal mass and conductivity design of a satellite heat pipe (Geem and Hwangbo 2006). Other studies that make use of HSA include: optimum design of steel frames (Degertekin (2008)), transport energy modeling problem (Ceylan et al. 2008), solving machining optimization problems such as water-water energetic reactor core pattern enhancement (Zarei et al. 2008), selecting and scaling real ground motion records (Kayhan et al. 2011), pressurized water reactor core optimization (Nazari et al. (2013 (a)), and Nazari et al. (2013 (b))).

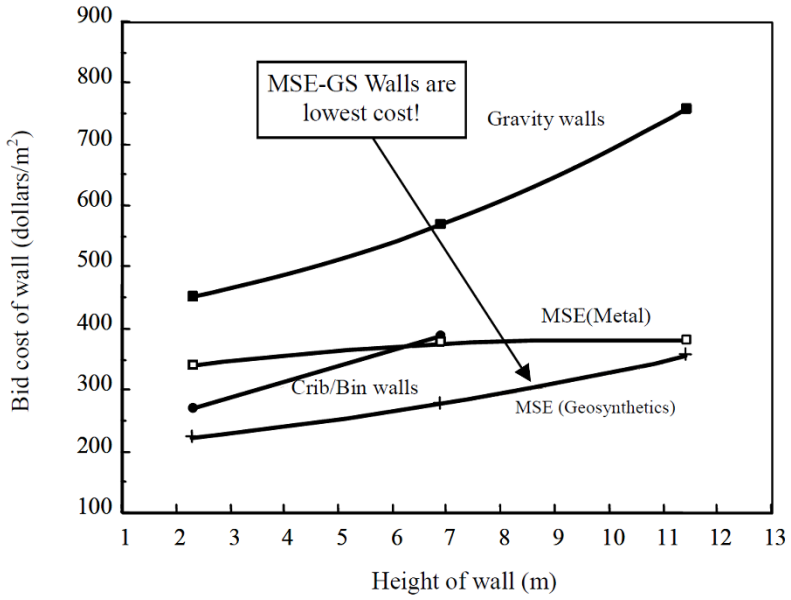

Figure 3.1 Cost of construction for various wall types (after Koerner and Soong (2001))

Using Sequential Unconstrained Minimization Technique (SUMT), assuming the length and strength of reinforcements as variables and construction cost as the objective function, Basudhar et al. (2008) optimized design of geosynthetic-reinforced walls. In this paper the cost of construction of geosynthetic-reinforced soil walls is optimized by using HSA. Optimization variables are the length of geosynthetic in each layer and the spacing between adjacent geosynthetic layers. Every optimization technique requires the definition of constraints that control the design process. Once the governing boundary conditions are formulated, they are imposed on objective functions so that results converge. In optimizer systems constraints may be set in terms of factors of safety. Cost is a good example for objective functions that may be used in construction projects.

3.3 Analysis of Geosynthetic-Reinforced Earth Wall

Stability analyses, for Geosynthetic-reinforced walls with a vertical face, are made assuming a rigid body behavior. Lateral earth pressures are computed on a vertical pressure surface located at the end of the reinforced zone. Rankine's theory is followed as discussed in the FHWA (Elias et al. 2001). Parameters used in the design process are presented in Figure. 3.2.

For horizontal and inclined backfill (angle β from horizontal) retained by a smooth veritcal wall, the coefficient of active lateral earth pressure may be calculated from Equations (3.1) and (3.2) respectively.

$$K_a = \tan^2\left(45 - \frac{\emptyset}{2}\right) \tag{3.1}$$

$$K_a = \cos\beta \left[\frac{\cos\beta - \sqrt{\cos^2\beta - \cos^2\emptyset}}{\cos\beta + \sqrt{\cos^2\beta - \cos^2\emptyset}}\right] \tag{3.2}$$

In this paper the active earth pressure coefficient (K_a) for the backfill is designated with K_{ae}. $\emptyset$ is defined as $\emptyset_b$ and $\emptyset_f$, for the soil in reinforced zone and the backfill (i.e. soil behind and on the top of the reinforced mass) respectively.

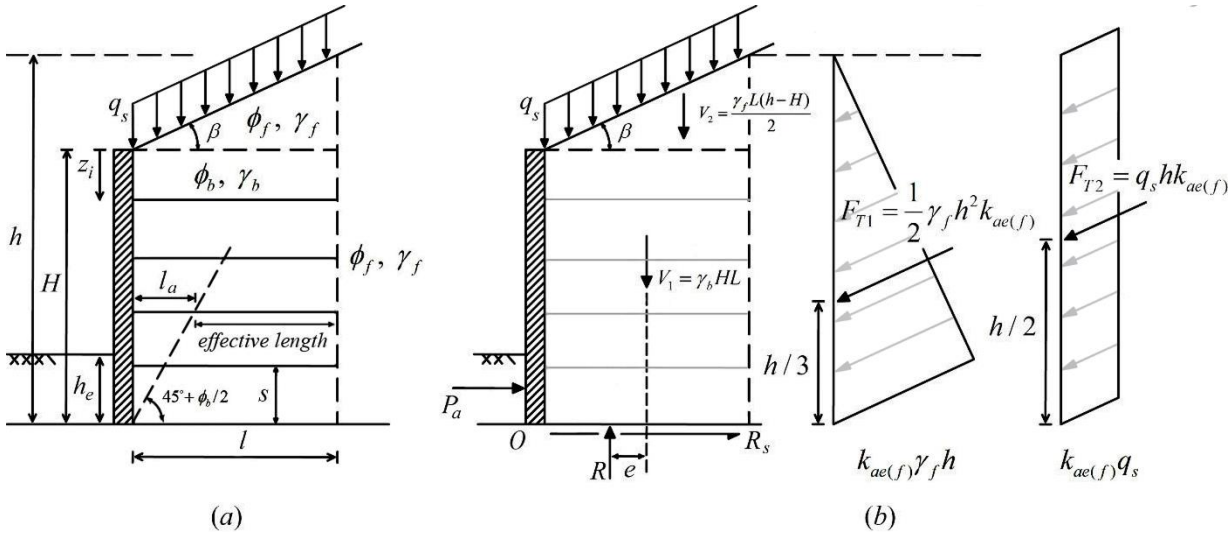

Figure 3.2 (a) Parameters used in different steps of the design; (b) external forces considered for the Geosynthetic reinforced retaining wall system.

3.3.1 Evaluation of external stability

Commonly, soil walls are classified as externally stable after three failure mechanisms are satisfied. They must be safe against sliding, bearing and overturning failures. Figure 3.2 (b) shows the external forces in a geosynthetic-reinforced wall system. Considering the reinforced system as a plain strain problem, the weight, V_1, of the soil within the area defined by the height H and width l is considered to act as a block. Since the wall embedment depth is small, the stabilizing effect of the passive pressure (moment) has been neglected in the analysis. The factors of safety against the above failure mechanisms are presented below.

3.3.1.1 Safety factor against overturning

Referring to Figure 3.2 (b), the safety factor against overturning is evaluated by considering moment equilibrium about point O. It can be calculated from:

$$FS_{overturning} = \frac{\sum M_{Ro}}{\sum M_o} = \frac{l^2\left(3(\gamma_b H + q_s) + 4\gamma_f(h-H)\right)}{K_{ae(f)}H^2\left(\left(\gamma_f H + 3q_s\right) + 3\gamma_f(h-H)\right)} \qquad 3.3$$

Where $\sum M_{Ro}$ and $\sum M_o$ are resisting and overturning moments respectively.

Safety factor against sliding: sliding resistance is directly related to the interface friction angle (δ) between soil and the geosynthetic fabric. In this paper, the interface angle is taken to be $(2/3)\emptyset$. Sliding resistance can be evaluated from $\sum P_R = [V_1 + V_2 + (F_{T1} + F_{T2})\sin\beta]\tan\delta$. It can be shown, from Figure 3.2 that the forces causing sliding are given by $\sum P_d = [F_{T1} + F_{T2}]\cos\beta$. With these two forces, the factor of safety against overturning can be defined as:

$$FS_{sliding} = \frac{\sum horizontal\ resisting\ forces}{\sum horizontal\ driving\ forces} = \frac{\sum P_R}{\sum P_d} \qquad 3.4$$

3.3.1.2 Safety factor for bearing capacity

The overturning moment, because of the lateral pressure in the backfill results in an eccentric base reaction. The reaction's eccentricity, e, from the centerline of the reinforced earth block, can be evaluated from moment equilibrium about point O.

Considering a unit length of the wall one can obtain:

$$e = \frac{(F_{T1}/3 + F_{T2}/2)(h.\cos\beta)(F_{T1} + F_{T2})(h.\sin\beta)(l/2) - V_2(l/6)}{V_1 + V_2 + (F_{T1} + F_{T2})\sin\beta} \qquad 3.5$$

Two different pressure distribution namely "Trapezoidal" (Elias 2001) and "Meyerhof's rectangular" (Prakash and Saran 1971) are usually used to calculate bearing capacity of foundations under eccentric loads (Meyerhof 1953). These two distributions are illustrated in Figure 3.3.

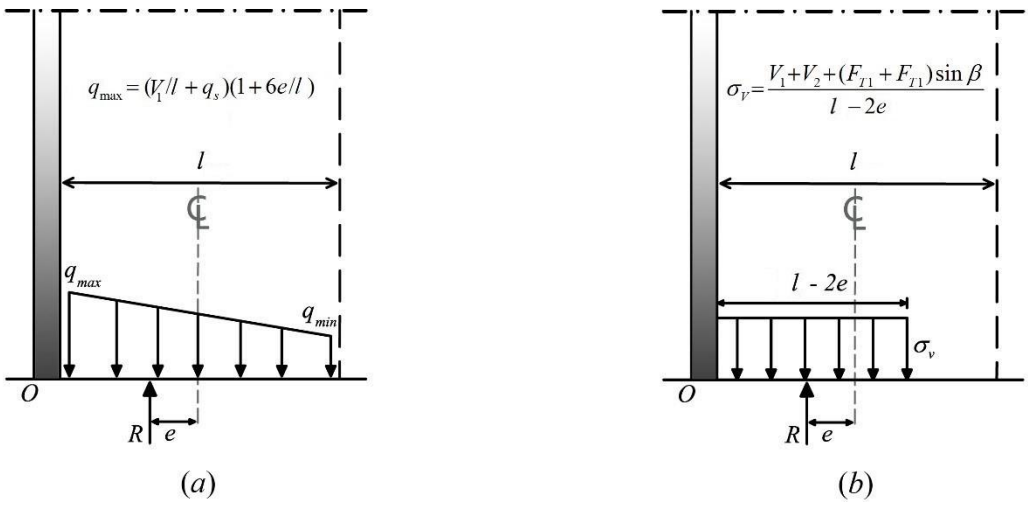

Figure 3.3 (a) Trapezoidal distribution of reaction (Elias 2001); (b) Rectangular distribution based on Meyerhof's theory (Prakash and Saran 1971).

Based on the selected distribution σ_v or q_{max} can be used to calculate the factor of safety for bearing capacity. In this study trapezoidal reaction pressure has been considered. Referring to Figure 3.3, for mild natural ground slope (i.e. small values of the angel β) the maximum stress in trapezoidal pressure can be calculated using the following equation:

$$q_{max} = (V_1/l + q_s) + (1 + 6e/l) \quad 3.6$$

Using the equation proposed by Terzaghi (1943) for a strip footing on a cohesion-less soil, and assuming q as the surcharge associated with the soil to the left of the wall that prevents failure, the ultimate bearing capacity can be calculated as:

$$q_{ult} = qN_q + 0.5\gamma_f N_f l \quad 3.7$$

1.7

The safety factor for bearing capacity can be calculated from:

$$FS_{bearing\ capacity} = \frac{q_{ult}}{q_{max_q}} \quad 3.8$$

3.3.2 Evaluation of internal stability

A geosynthetic reinforced soil system must withstand internal soil fracture and there should be no slippage along the soil-geosynthetic interface. The tensile strength of the geosynthetic reinforcement, in conjunction with the shear strength of the soil,

ensure internal stability of the soil mass. In line with this, internal stability may be defined as the ability of this composite system to resist pullout, grid rupture and bulging. Factors of safety for grid rupture and bulging are not explicitly sought as these failure phenomena are prevented by providing code-specified minimum spacing between layers.

3.3.2.1 Safety factor against pullout

To calculate the factor of safety against pullout, information regarding the pullout resistance and tensile strength of the geosynthetic material is needed. The pullout resistance of the reinforcement, as given in Equation (3.9), is defined by the ultimate tensile load required to generate outward sliding of the reinforcement through the reinforced soil mass (Basudhar et al. 2008).

$$P_r = \alpha \sigma_v' l_{ei} C \tan \delta \qquad 3.9$$

Where α is the scale effect correction factor with a value of 1.0 for metallic and 0.6 to 1.0 for geosynthetic reinforcements. Here, α is assumed to be 1.0. C is the reinforcement effective unit perimeter and recommended to have a value of 2 for strips, grids and sheets. σ_v' is the effective vertical stress at the soil-reinforcement interfaces. δ is interface friction angle between the soil and the geosynthetic. Although this angle should be determined in the laboratory, here it has been taken to be $(2/3)\emptyset$ for the purposes of comparing our results with previous work. l_e is the

embedment length in the resisting zone behind the failure surface and can be written as:

$$l_{ei} = l_i - (H - z_i)\tan(45 - \emptyset_b/2) \quad 3.10$$

Incorporating the assumptions described above and considering mild ground slope, the expression for pullout resistance can be written as:

$$P_{ri} = 2(\gamma_b z_i + q_s)\tan\delta\, l_{ei} \quad 3.11$$

Assume S_i and σ_h as the spacing between consecutive geosynthetic layers and the horizontal stress at the middle of each layer respectively. The maximum lateral force allowed to be carried by each geosynthetic layer is equal to the tensile strength, T_i, of the geosynthetic material. In addition to serving as a means to check resistance against pullout, this constraint ensures prevention of geosynthetic rupture intrinsically.

$$T_i = s_i \times \sigma_h \quad 3.12$$

Considering equation 3.12, the required strength of reinforcement varies from layer to layer and increases with depth. Correspondingly, the factor of safety against pullout should be calculated and controlled for each geosynthetic layer. For design layer located at depth z_i, safety factor against pullout is given by:

$$FS_{pullout} = \frac{P_{ri}}{T_i} \quad 3.13$$

3.3.2.2 Spacing between Geosynthetic layers:

The spacing between geosynthetic layers, kept greater than the minimum specified by codes, is allowed to vary until the design is optimized.

3.3.3 Considerations for dynamic loads

The dynamic response of the retaining walls can be estimated from quasi-static design approaches. In quasi-static methods, pseudo-static loads are imposed on the retaining wall to simulate dynamic response. The pseudo-static load is composed of the dynamic soil thrust (P_{AE}) and the inertial force form the reinforced zone (P_{IR}). For illustration, a system with horizontal backfill has been selected and the dynamic forces acting on such a system have been shown in Figure 3.4.

In the evaluation of external stability for a wall under dynamic conditions, in addition to the static force, the inertial force (P_{IR}) and half of the dynamic soil thrust (P_{AE}) are assumed to act on the wall (Basudhar et al. 2008). The reduced P_{AE} is used because the two dynamic forces are unlikely to peak simultaneously. Referring to Figure 3.4, P_{AE} and P_{IR} can be obtained using the following expressions.

$$P_{AE} = 0.375 A_m \gamma_b H^2 \quad 3.14$$

$$P_{IR} = A_m \gamma_f H (H/2)^2 = 0.5 A_m \gamma_f H^2 \quad 3.15$$

Where A_m is the maximum acceleration at the center of the reinforced zone that can be estimated from:

$$A_m = (1.45 - A)A \quad 3.16$$

Where A is the given value of the peak horizontal ground acceleration based on the design earthquake. A_m and A are defined in AASHTO Division I-A as acceleration coefficients (AASHTO 1996).

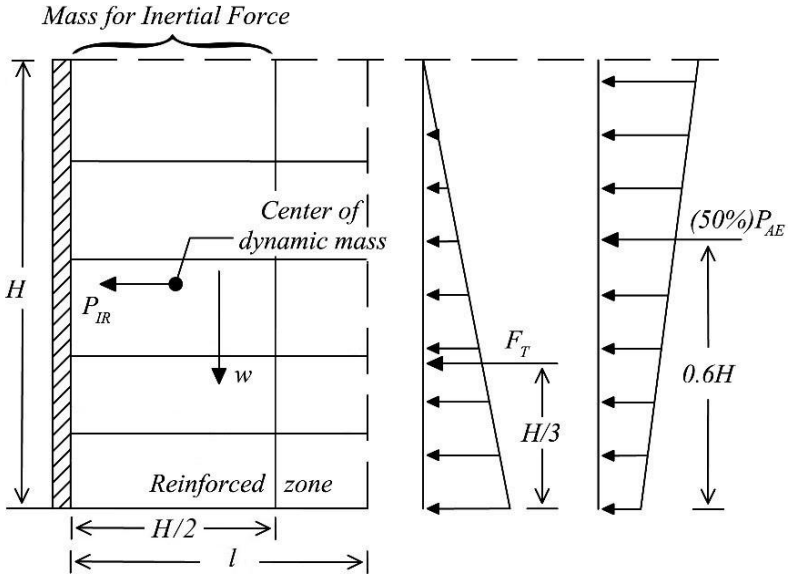

Figure 3.4 Static and pseudo-static forces acting on a reinforced zone (Basudhar et al. 2008).

To evaluate internal stability under dynamic loading conditions, the pseudo-static internal force acting on the failure zone is determined by:

$$P_{IR} = A_m W \qquad 3.17$$

Where W is the weight of the soil block within Rankine's failure zone. This force is distributed to each layer in proportion to the length of reinforcement that extends beyond the potential failure surface (i.e. the "effective length" as shown in Figure 3.2). A dynamic component of the tensile force for each layer is calculated following the approach discussed above. Having added this force to the static forces, safety factor against pullout is calculated for each layer.

3.4 Design Constraints

Design constraints, in terms of safety factors, hold information on the limits inside which all considerations that prevent failure are satisfied. Recommended design safety factors for each mechanism are shown in Table 3.1.

Table 3.1 Minimum recommended safety factors (Basudhar et al. 2008)

Safety factor	$FS_{overturning}$	$FS_{sliding}$	FS_{bear}	$FS_{reinforcement\ strength}$	$FS_{pullout}$
Value	2.0	1.5	2.0	1.5	2.0

Design constraints (g_1 to g_6) relevant to the safety factors discussed above are as presented below (Basudhar et al. 2008).

3.4.1 Constraint related to overturning

The factor of safety for overturning, calculated from Equation 3.3 must be greater than the design factor of safety or:

$$g_1 = FS_{design(overturning)} - FS_{overturning} \leq 0 \quad 3.18$$

3.4.2 Constraint related to sliding:

The factor of safety for sliding, calculated from Equation 3.4 must be greater than that of the design or:

$$g_2 = FS_{design(sliding)} - FS_{sliding} \leq 0 \quad 3.19$$

3.4.3 Constraint related to bearing capacity

The factor of safety for bearing capacity, calculated from Equation 3.8 must be greater than the corresponding design factor of safety or:

$$g_3 = FS_{design(bearing\ capacity)} - FS_{bearing\ capacity} \leq 0 \quad 3.20$$

3.4.4 Constraint related to geosynthetic pullout

The factor of safety for pullout, calculated from Equation 3.13 must be greater than the corresponding design factor of safety or:

$$g_4 = FS_{design(pullout)} - FS_{pullout} \leq 0 \quad 3.21$$

3.4.5 Constraint related to spacing between geosynthetic layers

The spacing between geosynthetic must be greater than the proposed minimum spacing:

$$g_5 = s_{min} - s \leq 0 \quad 3.22$$

3.4.6 Constraint related to allowable tensile strength of geosynthetic

The greater the allowable tensile strength ($T_{(u)_i}$), the higher the cost of geosynthetic. Accordingly, the tensile strength of geosynthetic was set to comply with:

$$g_6 = T_{(u)_i} - 60\ (kN\ /\ m) \leq 0 \qquad 3.23$$

3.4.7 Constraint related to length of geosynthetic

The effective length of geosynthetic must be greater than the assumed minimum effective length:

$$g_7 = l_{e-min} - l_e \leq 0 \qquad 3.24$$

The methods used to apply these constraints to objective function will be discussed in next section.

3.5 Objective Function

3.5.1 Mathematical formulation

Objective function, in optimization problems, is a function that the optimizer utilizes to maximize or minimize something based on the problem requirements. For the geosynthetic reinforced retaining walls considered in this study, construction cost has been selected as the objective function and parameters, set to constraints, have been optimized such that the cost of construction is minimized. The rates associated with various items (i.e. the cost factors) are presented in Table 3.2. For comparison

purposes, the same cost parameters, to that of Basudhar et al. (2008), have been adopted.

Table 3.2 Assumed cost factors (after Basudhar et al. (2008))

Item cost						**Engineering and testing cost**		
Symbol:	c_1	c_2	$c_{3(gt)}$	$c_{3(gg)}$	c_4	$c_{5(gt)}$	$c_{5(gg)}$	c_6
Value:	\$10	\$3	\$[Ta(0.03)+2.6]	\$ [Ta(0.03)+2.0]	\$60	\$30	\$10	\$50
Unit:	m	1000kg	m^2	m^2	m^2	m^2	m^2	m^2

The costs, applied per unit length of the wall, are as follows:

Cost of leveling pad = c_1

Cost of the wall fill = $c_2 \times \gamma_b / g \times H \times l$

Cost of the geosynthetic used = $c_3 \times n_i \times l$

Modular Concrete face unit (MCU) cost = $c_4 \times H$

Engineering and testing cost = $c_5 \times H$

Installation cost = $c_6 \times H$

The value attained by the objective function, in terms of the length and spacing between the geosynthetic reinforcements (i.e. the design variables), is obtained by summing all the costs listed above.

3.5.2 Applying design constraints to the objective function

The gamut of approaches proposed to incorporate the effect of constraints into random optimization problems may be categorized into two major classes. The first category operates based on concepts that search for the variables from acceptable ranges of design. Methods in this category were mostly used for simple problems with few number of variables. For problems that are complicated in their very nature and that involve numerous design constrains, the second category namely Penalty Function Method has been more useful. Methods in this category use approaches that change a constrained problems into an unconstrained one by constructing a new function (Coello 2002). For the second class, the mathematical formulation for an objective function subject to m constraints can expressed as follows:

$$\begin{aligned} &minimize\ f(x) subject\ to: \\ &\quad g_j \leq 0;\ \ j = 1,2,\dots,m \end{aligned} \tag{3.25}$$

The modified objective function $\emptyset(R)$ can then be represented by:

$$\emptyset(x) = f(x)[1 + K \times C] \tag{3.26}$$

Where *K* and *C* are penalty parameters in which *K* is a constant coefficient and for most engineering problems *K* =10 is assumed appropriate. *C* is a violation coefficient defined as:

$$\mathrm{C} = \sum_{j=1}^{m} C_j \quad \leftarrow \begin{cases} C_j = g_j & \text{if } \; g_j > 0 \\ C_j = 0 & \text{if } \; g_j \leq 0 \end{cases} \tag{3.27}$$

3.6 Harmony Search Algorithm (HSA)

Natural and artificial phenomena are attributed as to have inspired the development of some of the recent metaheuristic algorithms including Tabu Search, Simulated Annealing, Evolutionary Algorithm, and HSA. For example music is a relaxing phenomenon which is produced artificially by human beings and naturally by nature. Harmony in human-made music is achieved by playing different overlapping notes simultaneously such that the sound of multiple instruments eventually evolve into an audibly rhythmic and beautiful song. HSA is introduced as one of the new metaheuristic optimization methods that were inspired by music and the improvisation ability of musicians (Geem 2000). The fundamental concepts of HSA were introduced by the famous ancient Greek philosopher and mathematician Pythagoras. Since the pioneering work by Pythagoras, many researchers have investigated HSA. French composer and musician Jean Philippe, who lived in the years 1764-1683, has proved the classical harmonic theory (Parncutt 1989). The complete structure of the algorithm was then presented by Geem (2000).

Figure 3.5 shows a flowchart of the HSA idealized as a five step process. The optimization program is initiated with a set of individuals (solution vectors that

contain sets of decision variables) stored in an augmented matrix called harmony memory (HM). These processes are indicated as steps 1 and 2 in Figure 3.5. The word "individuals" in this paper refers to solution vectors that contain sets of decision variables. HM is a centralized algorithm where, at each breeding step, new individuals are generated by interacting with the stored individuals. HS follows three rules in the breeding step (shown as step 3 in Figure 3.5) to generate a new individual: memory consideration, random choosing, and pitch adjustment. In the fourth step, the algorithm tests if the new individual is better than the stored individuals in the HM. If "yes", a replacement process is triggered. This process continues iteratively until the HS has stagnated and all criteria are satisfied in the termination step (i.e. step 5). The description for each step is presented below for a geogrid wall with the height equal to 7 m, length of 200 m, A_m = 0 and q_s = 10.

3.6.1 *Step 1:* Introducing optimization program and parameters for the algorithm.

In this step, a set of specific parameters in HSA is introduced including:

1. The harmony memory size (HMS) which determines the number of individuals (solution vectors) in HM. For the given wall, 10 solution vectors are introduced to build the harmony memory.
2. The harmony memory consideration rate (HMCR), which is used to decide about choosing new variables from HM or assign new arbitrary values.

3. The pitch adjustment rate (PAR), which is used to decide the adjustments of some decision variables selected from memory.

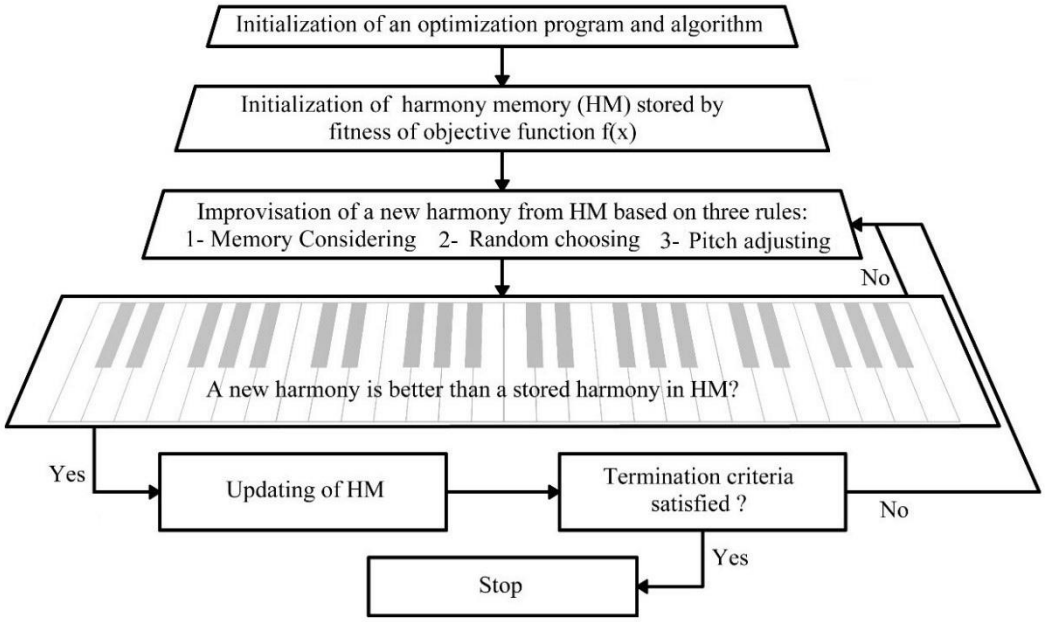

Figure 3.5 Harmony Search Algorithm flowchart.

4. The distance bandwidth (BW), which determines the distance of the adjustment that occurs to the individual in the pitch adjustment operator.
5. The maximum number of improvisations (NI) which is also called stopping criteria and is similar to the number of generations.

The values of the parameters HMCR, BW, PAR and HMS are different from one problem to another. The value of these parameters can affect the convergence of the HSA. Therefore, sensitivity analysis is necessary for evaluation of these

parameters. Generally, HMCR is considered to have values in the range of 0.70 to 0.99. For most problems, 0.95 is used as the optimum value for HMCR. The harmony memory size is dependent on the number of decision variables. The bigger the harmony memory size, the bigger the dimension of the problem and the more computational time and cost needed. Therefore, it is better to select a small value for this parameter. Generally, a value between 5 and 50 for HMS is reasonable. The pitch adjustment rate (PAR), is considered to have a value between 0.3 and 0.99. However, depending on the conditions of the problem, smaller values may be considered (Mahdavi et al. 2007). Lee et al. (2005) proposed a value between 0.7 and 0.95 for HMCR; 0.2 and 0.5 for PAR; and 10 to 50 for HMS to achieve a good HSA performance. In this study, based on trial and error approach and sensitivity analysis, the values for HMCR, PAR and HMS are chosen to be 0.7, 0.5 and 10, respectively.

The optimization problem is initially represented as minimizing or maximizing $\{F(R)|R \in R(t)\}$, where $F(R)$is the objective function, and $R = \{R_i|i = 1, \dots, N\}$ is the set of decision variables where N represents the number of decision variables which in this particular problem is equal to 2 (i.e. i=1 and i=2 that indicate length and number of reinforcements (NoG), respectively). $R(t) = \{R(t)_i|i = 1, \dots, N\}$ is the possible value range for each decision variable. The lower and upper bounds for the decision variable $R(t)_i$ is L_i and U_i (i.e. $R(t)_i \in [L_i, U_i]$). In this paper the lower and upper values of $R(t)$ are 1m and 10 m for reinforcement's length. The second variable is the number of geosynthetic (NoG). NoG is obtained from possible values corresponding to minimum and maximum spacing (0.5 m and 1.5 m respectively) and

the height of the wall. As the variables are assigned, objective function is optimized by minimizing its value. Upon the process of optimization, to minimize the objective function, individuals are arranged from smallest to largest values.

3.6.2 *Step 2:* Initialization of initial Harmony Memory (HM).

In this step, the initial HM matrix is populated with as many randomly generated individuals as the HMS and the corresponding objective function value of each set of random individual $F(R)$. Each individual is generated from the possible value range $R(t)$. The initial harmony memory is formed as follows:

$$HM = \left[\begin{array}{cccc|c} R_1^1 & R_2^1 & \cdots & R_N^1 & F(R^1) \\ \vdots & \vdots & \cdots & \vdots & \vdots \\ R_1^{HMS-1} & R_2^{HMS-1} & \cdots & R_N^{HMS-1} & F(R^{HMS-1}) \\ R_1^{HMS} & R_2^{HMS} & \cdots & R_N^{HMS} & F(R^{HMS}) \end{array}\right] \quad 3.28$$

The initial HM matrix for the given wall and corresponding worst harmony (i.e. column 7) are presented in Table 3.3. It is inferred, from Table 3.3, that HMS and the number of decision variables (N) for the given wall are equal to 10 and 2, respectively.

Table 3.3 Randomly generated initial variables for HM matrix for Geogrid wall A_m = 0, q_s = 10

Harmony Number	1	2	3	4	5	6	7	8	9	10
Length	4.54	4.53	5.44	5.11	6.12	4.9	4.3	5.59	6.465	5.77
NoG	6	7	8	11	6	14	11	11	7	11

Cost ($)	236763.1	238523.3	252407	254272	256233	257402	1192619	261242	263200	263830

3.6.3 *Step 3:* Improvisation for a new individual.

In this step, a New Harmony vector $R' = \{R'_i | i = 1, \dots, N\}$, is improved based on three mechanisms:

1- memory consideration

2- Random selection

3- Pitch adjustment.

Memory consideration and random choosing are mechanisms that allow the algorithm to produce New Harmony vector to be compared with existent harmony vectors in HM. In this step, the value of each decision variable in the new harmony vector (R'_i), is randomly selected from previously stored values, in the HM individuals $\{R_i^1, R_i^2, \dots, R_i^{HMS}\}$, with a probability of $HMCR \in (0,1)$. The *HMCR* is the rate of choosing one value from the historical values stored in HM. Then, decision variables that are not assigned with values according to the memory consideration are randomly chosen according to their range of $R(t)$ with a probability of 1-*HMCR*. 1-*HMCR* is the rate of randomly selecting one value from the possible range of values:

$$R'_i \leftarrow \begin{cases} R'_i \in \{R_1^1,\ R_1^2, \dots, R_1^{HMS}\} & \text{with probability } HMCR \\ R'_i \in R(t) & \text{with probability } (1 - HMCR) \end{cases} \quad 3.29$$

For instance, assuming HMCR equal to 0.85, HSA selects the new variables from values stored in HM with a probability of 85%.

In pitch adjustment, each decision variable $R_i^{'}$ of the new individual, $\{R_1', R_2', \dots, R_N'\}$, that has been assigned a value by the memory consideration is pitch adjusted with the probability of PAR, where $PAR \in (0,1)$ as follows:

$$\text{Pitch adjusdting decision for } R_i' \leftarrow \begin{cases} Yes & \text{with probability } PAR \\ \text{No} & \text{with probability } (1 - PAR) \end{cases} \qquad 3.30$$

In pitch adjustment, if the decision for R'_i ends with a "Yes", the value of R'_i is modified to its neighboring values. For the Given problem pitch adjustment is applied for length (L) as described with the following expression:

$$L_i' \leftarrow= L_i' \pm (a\ normal\ random\ value) \times BW;\ B = 0.02(L_{max} - L_{min}) \qquad 3.31$$

The random value in equation 3.31 can be determined using a possibility membership function or it can randomly be chosen from a specific range. A Gaussian Membership Function is used in order to find this value. If the random value is chosen simply from a solid specified range, the values outside this range do not have any chance to be chosen. Gaussian Membership Function covers a higher range for the random value and gives a small possibility to higher values to be chosen.

Pitch adjustment is also applied for the number of reinforcements (NoG) as follows:

$$NoG_i' \leftarrow= NoG_i' \pm (rand(1\ or\ 2)) \quad 3.32$$

It should be noted that, if pitch adjustment causes a variable to fall outside the given range for variable, an alternative value must be replaced with outlier. This alternative value can be the minimum or maximum of the range assigned to the variable.

3.6.4 *Step 4:* Updating the harmony memory

If the newly generated harmony vector is better than the any of the stored harmony vectors in the HM (i.e. has better objective function value than that of a stored individual) it will replace the old stored vector in the HM. Otherwise, the algorithm enters the next loop (iterating between steps 3 and 4) without any replacement. Table 3.4 shows the HM generated after one iteration in this study. The 7th vector (solution) in the initial harmony memory (i.e. Table 3.3) which had the worst cost function value is replaced by new one which is highlighted in Table 3.4.

Table 3.4 HM matrix after first iteration for Geogrid wall A_m = 0, q_s = 10

Harmony Number	1	2	3	4	5	6	7	8	9	10
Length	4.54	4.53	5.44	5.11	6.12	4.9	5.11	5.59	6.465	5.77
NoG	6	7	8	11	6	14	7	11	7	11
Cost ($)	236763.1	238523.3	252407	254272	256233	257402	245897	261242	263200	263830

3.6.5 *Step 5:* Evaluation of termination rule.

Steps 3 and 4 continue to repeat until the termination rule is satisfied. The last solution vector that meets the requirements of the termination rule is reported as the optimized solution for the problem under consideration. Undoubtedly, the maximum number of generations could be different from problem to problem depending on the desired accuracy. Here, the termination rule is considered to be satisfied, when for 50 consecutive iterations the values of cost function, $F(R)$, are equal up to ten decimal places. Figure 3.6 shows the reduction in cost with progressive iterations. In order to reduce the iterations, 10 new harmonies are produced in each iteration based on mentioned rules. It is shown that Mean Cost Values in HM converge to the best cost, after 120 iterations. Further iteration causes slight changes in variables, however, the change in cost function will be insignificant.

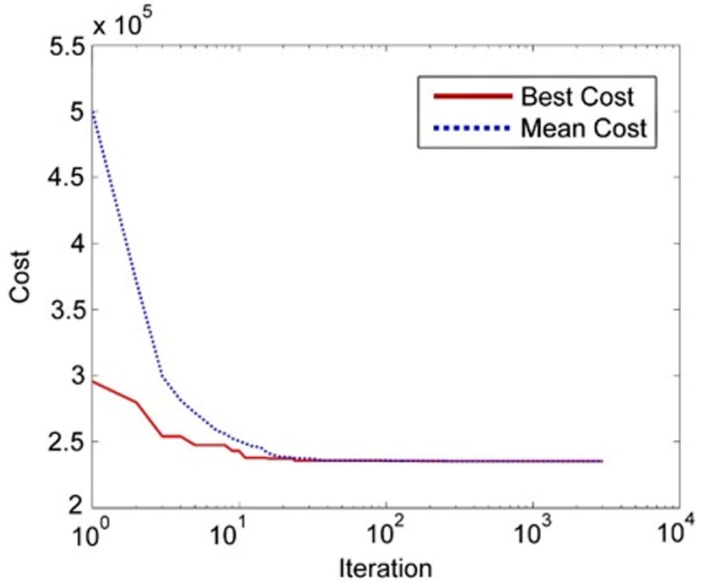

Figure 3.6 Reduction in cost with progressive iterations for Geogrid wall $A_m=0$, $q_s=10$.

3.7 Results and Discussions

To compare results and illustrate the effectiveness of the proposed method, an example has been described in this section. Since the following analyses and associated results are compared to the results of Basudhar et al. (2008), similar parameters and geometry are considered. HSA is used to run the optimization problem for walls of height 5, 7 and 9 meters. The input parameters used to define the problem are presented in Table 3.5.

Table 3.5 Input design parameters

Parameter	**Value**
Height of Wall (H)	5-9 m
Minimum embankment of the fill (h_e)	0.45
Angle of internal friction of the backfill (ϕ_f)	30°
Unit weight of the backfill (γ_f)	18 kN/m^3
Angle of internal friction of the fill (ϕ_b)	35°
Unit weight of the fill in the reinforced zone (γ_b)	20 kN/m^3
Ultimate tensile strength of the geosynthetic (T_u)	<60 kN/m
Allowable tensile strength of the geosynthetic (T_a)	$T_a = T_u/1.5$ kN/m
Surcharge slope angle (β)	0°
Minimum length of the reinforcement ($l_{\text{e min}}$)	1.0 m
Length of the wall	200 m

Table 3.6 shows the summary of results, obtained by SUMT method, that has been referred to compare the results of this study with that of Basudhar et al. (2008). The values for the total cost in Table 3.6 were obtained by applying the cost factors

given in Table 3.2 and the spacing and length that were obtained by Basudhar et al. (2008). An example calculation, for a geogrid-reinforced wall, on how the values in Table 3.6 were obtained is presented here.

Example:

For 5 m geogrid reinforced wall (No surcharge; No earthquake load)
Wall embedment = 0.45 ➔ H_d = 5 m + 0.45 m = 5.45 m
Parameters from Table 3.5 (Basudhar et al. 2008): Number of layers, n_l = 4; Length of each layer, l = 3.73; Length of wall, L = 200m; Ultimate tensile strength of geogrid, T_u = 40.24 kN/m; Allowable tensile strength of geogrid, T_a = 26.83 kN/m (Using expression, for geogrid, from Table 3.1)
Cost of leveling pad: (200 m)($10/m) = $2000
Cost of the reinforced wall fill: (200 m)(5.45 m)(3.73 m)[(20 kN/m^3)/(9.81)]($3/1000kg) = $24866.67
Cost of geogrid reinforcement: (4 layers)(3.73 m)(200 m)[(26.83 kN/m)(0.03)+2.0]($/m^2) = $8369.82
Cost of the MCU face units: (200 m)(5.45 m)($60/m^2) = $65400
Cost of Engineering and testing: (200 m)(5.45 m)($10/m^2) = $10900
Installation cost: (200 m)(5.45 m)($50/m^2) = $54500

Adding all the costs, **Total cost = $166036.49**. This is value is indicated in bold in Table 3.6. Similarly calculated cost values are populated in the same table.

Table 3.7 and Table 3.10 present the result of static analysis, in the absence of overburden, for Geotextile and Geogrid respectively. As can be inferred from the tables, the total cost of construction for 5m high reinforced retaining walls with Geotextile and Geogrid was reduced by about 4.42% and 4.08% respectively, compared to SUMT results. Under the same loading conditions the cost savings for 7 m and 9 m walls reinforced with geosynthetic wrap and geogrid were 4.27% and

3.72% respectively. For this loading condition no significant cost changes were observed for the 9 m wall.

Table 3.8 and Table 3.11 present the results for the case where there is an assumed overburden of 10 kN/m^2. A relatively higher cost reduction (6%) was obtained for the wall with height of 5m. Here also, the cost savings for the 9 m wall were small (i.e. 0.32% and 1% for Geotextile-wrap and geogrid respectively).

Table 3.9 and Table 3.12 show the results of analysis when the seismic loading is considered. It was found that the cost of construction for a 5m wall reduced by 7.62% and 6.36% respectively for geotextile and geogrid reinforcement. For 7 m high wall, the cost reduction were of 9.18% and 7.54% respectively for geotextile and geogrid. A reduction equal to 6.32% and 6.0% were obtained for 9m wall reinforced with geotextile and geogrid respectively. It is undeniable that, in big scale construction projects that involve mechanically stabilized walls, a small percentile decrease in cost is a big save. It can also be observed that, compared to geotextile reinforced walls, the cost of construction for geogrid reinforced walls is considerably higher. This could be related to the additional cost of modular concrete blocks and leveling pad in geogrid-reinforced walls.

Table 3.6 Summary of results from SUMT method (modified from Basudhar et al. (2008))

Geotextile-Wrap wall												
A_m = 0 , q_s = 0					**A_m = 0 , q_s = 10**				**A_m = 0.05 , q_s = 0**			
H_t (m)	**NoG**	**L(m)**	**T_u (kN/m)**	**Cost ($)[1]**	**NoG**	**L(m)**	**T_u (kN/m)**	**Cost ($)[1]**	**NoG**	**L(m)**	**T_u (kN/m)**	**Cost ($)[1]**
5	4	3.73	40.24	122226.59	5	3.73	35.72	124429.38	4	4.55	45.66	130321.38
7	6	4.78	45.12	182850.62	7	4.96	42.65	188378.86	6	6.23	51.19	203066.45
9	9	5.84	45.38	255580.15	10	5.82	44.6	259123.94	8	7.9	58.83	290257.32
Geogrid wall												
A_m = 0 , q_s = 0					**A_m = 0 , q_s = 10**				**A_m = 0.05 , q_s = 0**			
H_t (m)	**NoG**	**L(m)**	**T_u (kN/m)**	**Cost ($)[1]**	**NoG**	**L(m)**	**T_u (kN/m)**	**Cost ($)[1]**	**NoG**	**L(m)**	**T_u (kN/m)**	**Cost ($)[1]**
5	4	3.73	40.24	**166036.19**	5	3.73	35.72	167791.38	4	4.55	45.66	173737.38
7	6	4.78	45.12	241009.02	7	4.96	42.65	245812.46	6	6.23	51.19	260180.85
9	9	5.84	45.38	326872.95	10	5.82	44.6	329739.94	8	7.9	58.83	360273.32

Bold value signifies the result obtained from the demonstrated cost calculation before the table

[1]Total values indicated as Cost ($) are calculated using the cost functions (Table 1 of Basudhar et al. (2008)) by following the illustration provided in section 4.1 of the same reference.

Table 3.7 Optimum cost for Geotextile-Wrap wall $A_m = 0$, $q_s = 0$

H_t (m)	L(m)	Ta-max (kN/m)	NoG	Spacing (m)	Cost ($/m^2)	Saving w.r.t. SUMT (%)
5	3.23	26.5	3	1.25	116826.20	4.42
7	4.34	38.5	5	1.17	175045.20	4.27
9	5.59	37.8	10	0.82	253864.80	0.67

Table 3.8 Optimum cost for Geotextile-Wrap wall $A_m = 0$, $q_s = 10$

H_t (m)	L(m)	Ta-max (kN/m)	NoG	Spacing (m)	Cost ($/m^2)	Saving w.r.t. SUMT (%)
5	3.24	30	3	1.25	117066.00	5.92
7	4.43	36.75	6	1	178993.70	4.98
9	5.62	37.1	11	0.75	258287.40	0.32

Table 3.9 Optimum cost for Geotextile-Wrap wall $A_m = 0.05$, $q_s = 0$

H_t (m)	L(m)	Ta-max (kN/m)	NoG	Spacing (m)	Cost ($/m^2)	Saving w.r.t. SUMT (%)
5	3.62	32	3	1.25	120390.50	7.62
7	4.83	40	6	1	184432.20	9.18
9	6.15	37.84	12	0.692	271914.30	6.32

Table 3.10 Optimum cost for Geogrid-Wrap wall $A_m = 0$, $q_s = 0$

H_t (m)	L(m)	Ta-max (KN/m)	NoG	Spacing (m)	Cost ($/m^2)	Saving w.r.t. SUMT (%)
5	3.233	26.5	3	1.25	159262.70	4.08
7	4.341	38.5	5	1.17	232052.60	3.72
9	5.59	37.8	10	0.82	322755.30	1.26

Table 3.11 Optimum cost for Geogrid wall $A_m = 0$, $q_s = 10$

H_t (m)	L(m)	Ta-max (kN/m)	NoG	Spacing (m)	Cost ($/m^2)	Saving w.r.t. SUMT (%)
5	3.238	30	3	1.25	159510.60	4.94
7	4.43	36.75	6	1	235405.10	4.23
9	5.626	37.1	11	0.75	326459.70	1.0

Table 3.12 Optimum cost for Geogrid wall $A_m = 0.05$, $q_s = 0$

H_t (m)	L(m)	Ta-max (kN/m)	NoG	Spacing (m)	Cost ($/m^2)	Saving w.r.t. SUMT (%)
5	3.62	32	3	1.25	162693.40	6.36
7	4.83	40	6	1	240560.50	7.54
9	6.15	37.84	12	0.692	338650.20	6.00

Table 3.9 and Table 3.12 show the results of analysis when the seismic loading is considered. It was found that the cost of construction for a 5m wall reduced by 7.62% and 6.36% respectively for geotextile and geogrid reinforcement. For 7 m high wall, the cost reduction were of 9.18% and 7.54% respectively for geotextile and geogrid. A reduction equal to 6.32% and 6.0% were obtained for 9m wall reinforced with geotextile and geogrid respectively. It is undeniable that, in big scale construction projects that involve mechanically stabilized walls, a small percentile decrease in cost is a big save. It can also be observed that, compared to geotextile reinforced walls, the cost of construction for geogrid reinforced walls is considerably higher. This could be related to the additional cost of modular concrete blocks and leveling pad in geogrid-reinforced walls.

3.8 Conclusions

In this study different cost optimization methods were highlighted. The application of one of the metaheuristic optimization techniques, namely Harmony Search Algorithm, was shown on designing geosynthetic reinforced walls. The iterative design optimization was coded with MATLAB. Optimization using HSA resulted in reduced cost of construction. Geosynthetic-wrap and geogrid reinforcement options were optimized with HSA. Static and dynamic loading conditions were considered under the existence and absence of overburden. Compared to results obtained with the SUMT optimization technique (Basudhar et al. 2008), the cost of construction -for a 5, 7, and 9 meter geotextile-reinforced walls- were reduced by

4.42%, 4.27%, and 0.67% respectively. These savings were obtained under static load assumptions. The reductions under dynamic loading conditions were 7.62%, 9.18%, and 6.32% respectively. For geogrid-reinforced walls the cost savings for the 5, 7 and 9 meter walls were 4.08%, 3.72% and 1.26% for static analysis and 6.36%, 7.54%, and 6.0% for dynamic analysis respectively. It was also found that the HSA program has a very fast rate of convergence towards the most optimum design.

Chapter 4

MANUSCRIPT 2. A MODIFIED HARMONY SEARCH ALGORITHM FOR THE OPTIMUM DESIGN OF EARTH WALLS REINFORCED WITH NON-UNIFORM GEOSYNTHETIC LAYERS

Mohammad Motalleb Nejad

Kalehiwot Nega Manahiloh

Published in:

International. Journal of Geosynthetics and Ground Engineering (2015) 1:36

DOI 10.1007/s40891-015-0039-x

4.1 Abstract

Traditional Design and Construction of Reinforced Earth Walls assumes uniform length and spacing of reinforcements. Even though the assumption simplifies the design and construction efforts, the inherently conservative approaches followed in picking the final values for the reinforcement length and spacing result in unnecessarily big construction costs. This paper presents an Improved Harmony Search (*IHS*)-based approach that can be adopted to optimize the design of Geosynthetic-Reinforced Earth Walls. An existing Improved Harmony Search Algorithm is modified into a New Harmony Search Algorithm by extending its

capabilities to consider permutation-based operations for inter-dependent variables. The involved optimization procedures are discussed in a step-wise approach. This novel approach allows the consideration of non-uniform length and spacing for the reinforcement layers. As such, Length of the Geosynthetic Reinforcement and the Spacing between adjacent Geosynthetic layers are taken as the design variables to be manipulated until the cost of construction is optimized. Static and Dynamic loads are considered. The application of the proposed optimization technique is demonstrated on Geosynthetic-Reinforced Earth Walls of height 5, 7 and 9 meters. The extent of cost saving is assessed by comparing the results of this work and previous work. The previous work selected for comparison uses Harmony Search Algorithm (*HSA*) to optimize the design and construction of Earth Walls reinforced with uniform length- and spacing-Geosynthetic layers. The *IHS*-based optimization resulted in Cost reduction of up to 11%.

4.2 Introduction

Retaining walls are among the most extensively used structural elements in the construction industry (Manahiloh et al. 2015). In spite of their ubiquitousness, applicability of non-reinforced retaining walls is confined to lower heights (Pourbaba et al. 2013). To overcome this limitation and enhance the performance of walls at higher heights, different types of reinforcing material are introduced. The tension-resisting element (i.e. the reinforcement) in reinforced earth wall systems works as a unit with surrounding soil to augment its strength and sustainability. One group of

such reinforcements consists of different types of Geosynthetics. Geosynthetic reinforcements are fabricated from polymeric material. In reinforced earth systems, the Geosynthetic element plays the combined pivotal roles of isolation, increased tensile resistance and improved drainage. Use of Geosynthetics as reinforcement provides additional strength against various failure mechanisms. This in turn allows increasing the reinforced-wall height without the need for external lateral support (e.g. heavy gravity walls constructed by substantial concrete material (Yoo et al. 2007). The decent endurance of the polymeric material against erosion has made it a better choice in reinforcing earth structures (Lawrence 2014). These overlapping benefits have made Geosynthetic-reinforced walls favorable and their design and implementation is expanding. Over the past five decades the production and use of polymer-based reinforcement has shown a sustained upsurge. Geosynthetic reinforced soil walls, compared to the classic rigid-walls, have superior flexibility which makes them better in withstanding natural disasters such as earthquakes and landslides (Yoo et al. 2007).

In addition to aforementioned benefits, in Geosynthetic-reinforced soil walls, the cost of the construction is significantly lower than other earth retaining systems (Zhang et al. 2006). Construction cost is one of the decisive factors in the execution of engineering projects. (Koerner and Soong 2001) compared the cost of construction for different types of retaining walls and showed that the cost of construction for Geosynthetic-reinforced soil walls is by far lower than its classic competitors.

In recent studies, Harmony Search Algorithm (*HSA*) has been applied in various engineering optimization problems. River flood models (Kim et al. (2001) and

Karahan et al. (2013)), optimal rainfall-runoff models (Paik et al. 2005), a design of water distribution networks (Geem 2006), a simultaneous determination of aquifer parameters and zone structures (Ayvaz 2007) are some applications of *HSA* in the Civil Engineering discipline. *HSA* has also been applied in scheduling problems (Wang et al. 2011), steel frame designs (Degertekin 2008), reliability optimizations (Zou et al. 2010), optimal design of planar and space trusses and the optimal mass and conductivity design of a satellite heat pipe (Lee et al. (2005), Lee and Geem (2004)). Other studies that make use of *HSA* include: transport energy modeling problem (Ceylan et al. 2008), selecting and scaling real ground motion records (Kayhan et al. 2011), a water-water energetic reactor core pattern enhancement (Nazari et al. 2013 (a)), solving machining optimization problems (Zarei et al. 2008), pressurized water reactor core optimization (Nazari et al. 2013 (b)).

Compared to other metaheuristic methods *HSA* possesses unique features in that it: considers all the solution harmonies during new iterations; and utilizes stochastic random searches. These features enable *HSA* to, systematically, handle huge optimization problems with less mathematical requirements (Mahdavi et al. 2007) and make it a preferable tool in optimization-related research.

Recently, different methods (i.e. Particle Swarm Optimization (PSO), Ant Colony etc.) have been combined with *HSA* in pursuit of improved hybrid-algorithms (Wu et al. (2012), and Shi et al. (2013)). Several other studies have also tried to further improve the performance of *HSA*. Wang and Li (2013) proposed a differential harmony search algorithm in solving non-convex economic load dispatch problems.

An improved harmony search (*IHS*) (Mahdavi et al. 2007) and a global-best harmony search (*GHS*) (Omran and Mahdavi 2008) algorithms have been implemented to enhance the searching power of the *HSA*.

Basudhar et al. (2008) optimized Geosynthetic-reinforced walls using Sequential Unconstrained Minimization Technique (SUMT algorithm). Using *HSA*, and assuming the constant-length and number of Geosynthetic layers as design variables and construction cost as the objective function, Manahiloh et al. (2015) optimized the design of Geosynthetic-reinforced walls. In both studies the length of reinforcement and the spacing between adjacent layers were set to be constant.

In this study the applicability of *IHS* is discussed and its utilization is demonstrated by optimizing the design and construction of Geosynthetic-reinforced Earth Walls. The algorithm associated with *IHS* is modified and expanded to account for non-uniform length of Geosynthetic reinforcement layers and non-constant spacing between adjacent layers. The optimization variables are: the independent lengths of Geosynthetic in each layer; and a vector that contains distance information between two adjacent Geosynthetic layers.

4.3 Analysis of Geosynthetic-Reinforced Earth Wall

Stability analysis for Geosynthetic-reinforced walls introduced in FHWA code (Elias et al. 2001) uses Rankine's theory. The same theory is adopted in this study to analyze walls while non-uniform variation in spacing and length of geosynthetic reinforcement is permitted. The non-uniform length and spacing values are set to be

picked with a random selection process pre-defined in the *HSA*. The feasibility of construction is accounted for by constraining the variation in length of geosynthetics in such a way that it shows a consistent trend. Moreover, the length of geosynthetics in each layer is kept lower than the smaller of: the maximum limit of the range for length; and the length of geosynthetic in the layer above. Stability analyses, for Geosynthetic-reinforced walls with a vertical face, are made assuming a rigid body behavior for the reinforced zone as shown in Figure 4.1. Lateral earth pressures are computed on a vertical surface located at the end of the reinforced zone. The reinforced zone is further divided into multiple sub-zones. The first zone related to shortest length of the reinforcement which is associated with the bottom layer of geosynthetics. The other zones are fractions of an assumed rigid body that exceed the area corresponding to the least length. Parameters used in the design process are presented in Figure. 4.1.

For horizontal and inclined backfill (angle β from horizontal) retained by a smooth veritcal wall, the coefficient of active lateral earth pressure may be calculated from Equations (4.1) and (4.2) respectively.

$$K_a = \tan^2\left(45 - \frac{\emptyset}{2}\right) \tag{4.1}$$

$$K_a = \cos\beta \left[\frac{\cos\beta - \sqrt{\cos^2\beta - \cos^2\emptyset}}{\cos\beta + \sqrt{\cos^2\beta - \cos^2\emptyset}}\right] \tag{4.2}$$

In this study the active earth pressure coefficient (K_a) for the backfill is designated with K_{ae}. $\emptyset$ is defined as $\emptyset_b$ and $\emptyset_f$, for the soil in reinforced zone and the retained soil (i.e. soil behind and on the top of the reinforced mass) respectively.

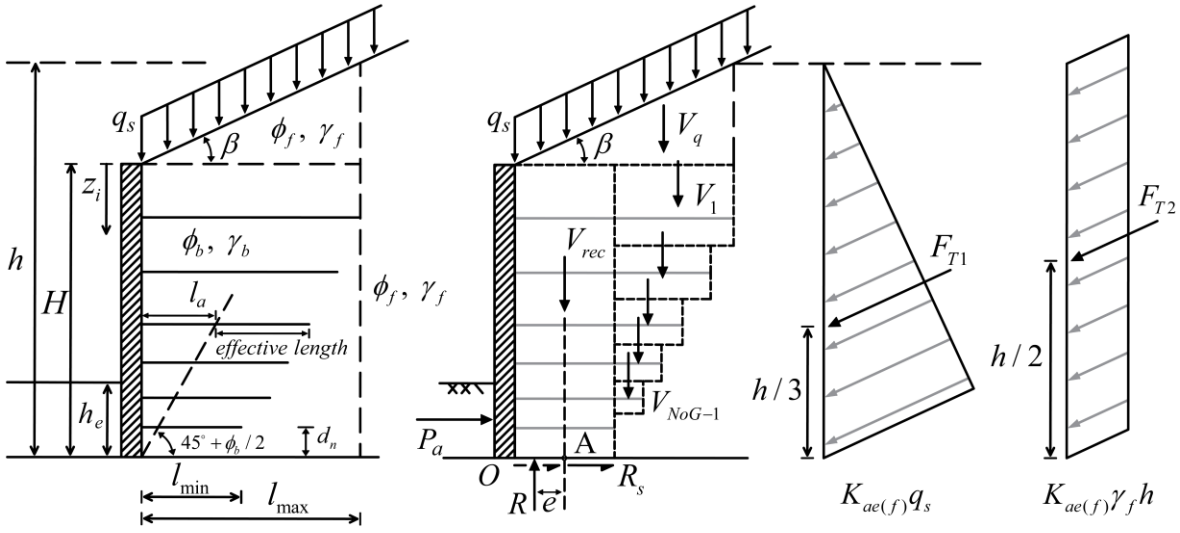

Figure 4.1 Parameters used in different steps of the design and external forces considered for the Geosynthetic reinforced retaining wall system.

4.3.1 Stability Analysis

Regardless of type of reinforcement, any reinforced system should be checked for internal and external stability. The internal stability deals with interactions between reinforcements and the material in contact with them and mechanisms that lead to soil fracture and the associated rupture of the reinforcements. The external stability, on the other hand, deals with the behavior of the rigid body of reinforced-soil zone interacting with neighboring soil and the mechanisms that disturb its stability. The

design of geosynthetic-reinforced soil walls is not considered safe until the safety factors against internal and external failure mechanisms are above the corresponding minimum values specified by codes.

Internal stability analysis of non-uniform lengths and spacing is exactly the same as that of uniform lengths and spacing. Details regarding this have been covered in other literature (e.g. Manahiloh et al. (2015), and Elias et al. (2001)).

Generally, three failure mechanisms are assessed in examining the external stability of retaining structures. In geosynthetic-reinforced earth wall systems, the sliding of the rigid body of reinforced-soil system, bearing capacity of the foundation soil below the reinforced zone and overturning of the reinforced-soil zone are considered to be these three failure mechanisms. Figure 4.1 shows the external forces in a geosynthetic-reinforced wall system. In the figure, V_i refers to the weight of the soil enclosed by the associated geometric shapes. The summation of the weights $V_{rec,}$ V_q and V_1 through V_{NoG-1}, is the total weight of the soil within the reinforced zone where *NoG* refers to the number of geosynthetic layers. Considering the reinforced system as a plane-strain problem, this weight is considered to act as a block. Since the wall embedment depth is small, the stabilizing effect of the passive pressure (moment) has been neglected in the analysis. The factors of safety against the above failure mechanisms are presented below.

4.3.1.1 Safety factor against overturning:

It is assumed that, if overturning takes place, the whole reinforced zone will behave as a rigid body. Referring to Figure 4.1, the safety factor against overturning is evaluated by considering moment equilibrium about point O. It can be calculated from:

$$FS_{overturning} = \frac{\sum M_{Ro}}{\sum M_o} = \frac{\left(F_{T1} \times (h/3) + F_{T2} \times (h/2)\right)\cos\beta}{V_{rec} \times (l_{min}/2) + V_q \times (2l_{max}/3) + \sum_{i=1}^{NoG-1}\left(V_i \times \frac{l_i + l_{min}}{2}\right) + q_s \times (l_{max}^2/2)} \quad 4.3$$

Where $\sum M_{Ro}$ and $\sum M_o$ are the resisting and overturning moments respectively. The other parameters in Eq. 3 are as defined and indicted in Figure 4.1.

4.3.1.2 Safety factor against sliding

Three relevant components are accounted for during the evaluation of safety against sliding. The first consists of the weight of the reinforced zone and all vertical forces acting above this zone. Interface friction angle between the soil and fabric(δ)is the second component that needs consideration. The third components refers to all the driving lateral forces that try to cause sliding. The factor of safety against sliding can be expressed as:

$$FS_{sliding} = \frac{\sum horizontal\ resisting\ forces}{\sum horizontal\ driving\ forces} = \frac{\sum P_R}{\sum P_d}$$
$$= \frac{\left(V_{rec} + V_q + \sum_{i=1}^{NoG-1} V_i + q_s \times l_{max}\right) \times \tan\delta}{(F_{T1} + F_{T2})\cos\beta} \qquad 4.4$$

Where $\sum P_R$ and $\sum P_d$ are resisting and driving forces respectively.

4.3.1.3 Safety factor for bearing capacity

The reaction's eccentricity, *e*, from the centerline of the reinforced earth block, can be evaluated from moment equilibrium about point *A*:

$$e = \frac{\sum M_d - \sum M_R}{\sum V} \qquad 4.5$$

In this study Meyerhof's equivalent-rectangular pressure distribution (Meyerhof (1953), and Das (2007)) is used to calculate the bearing capacity of the foundation soil under eccentric load conditions. To stay in the conservative side of design, l_{min} is used in calculating the vertical stress acting on the foundation. For mild natural ground slopes (i.e. small angels of β in Figure 4.1), the vertical pressure σ_v can be calculated using the following equation:

$$\sigma_v = \left(V_{rec} + V_q + \sum_{i=1}^{NoG-1} V_i \right) \Big/ (l_{min} - 2e) \quad 4.6$$

Using the Terzaghi's equation (Terzaghi 1943) for a strip footing on a cohesion-less soil and assuming q as the surcharge associated with the soil to the left of the reinforced-soil, the ultimate bearing capacity can be calculated as:

$$q_{alt} = qN_q + 0.5\gamma_f N_f l_{min} \quad 4.7$$

$$FS_{bearing\ capacity} = \frac{q_{ult}}{\sigma_v} \quad 4.8$$

The safety factor for bearing capacity is then obtained from:

In the evaluation of external stability for a wall under dynamic conditions, in addition to the static forces, the inertial force and half of the dynamic soil thrust are assumed to act on the wall (Elias et al. 2001). The details for dynamic considerations can be referred from earlier works (e.g. Manahiloh et al. (2015), and AASHTO (1996)).

4.4 Objective Function

4.4.1 Mathematical Formulation

In this study the cost of construction is taken as the objective function and is minimized by searching for a set of optimum design variables. The rates associated with various items (i.e. the cost factors) are presented in Table 4.1. For comparison purposes, the same cost parameters, to that of Manahiloh et al. (2015) have been adopted.

Table 4.1 Assumed cost factors (after Manahiloh et al. (2015))

Item	Assumed cost factor			Cost applied per unit length of the wall
	Symbol	Value		
		Geogrid	Geotextile	
Leveling pad	C_1	\$10/m	\$10/m	C_1
Wall fill	C_2	\$3/1000kg	\$3/1000kg	$c_2 \times \frac{\gamma_f}{g} \times (Vol_{reinforced\ zone})$
Geosynthetic	C_3	\$[Ta(0.03)+2.0]m^2	\$[Ta(0.03)+2.6]m^2	$\sum_{i=1}^{NoG} c_3 \times l_i$
MCU face unit*	C_4	\$60/m2	0	$c_4 \times H$
Engineering tests	C_5	\$10/m2	\$30/m2	$c_5 \times H$
Installation	C_6	\$50/m2	\$50/m2	$c_6 \times H$

* The Modular Concrete Facing Units (MCU) are only applied for Geogrid type walls.

The total amount attained by the objective function, in terms of the length and spacing between the geosynthetic reinforcements (i.e. the design variables), is obtained by summing all the costs listed above.

4.4.2 Design Constraints

The design constraints, applied to check the stability of the reinforced earth-wall and corresponding minimum recommended safety factors, have been presented by Manahiloh et al. (2015). In addition to six constraints applied for the case of uniform lengths and spacing described by Manahiloh et al. (2015), a new constraint is needed to consider the feasibility of construction. Accounting for the process of excavation which imposes a restriction that confine the length of each geosynthetic to be lower than that of the adjacent upper layer, we can introduce the following constraint:

$$g_7 = l_{n+1} - l_n < 0 \quad \text{for } n = \{1,2,\dots,NoG-1\} \tag{4.9}$$

4.4.3 Applying Design Constraints to the Objective Function

For the sake of simplicity, a linear penalty function has been used in this study. The mathematical formulation for an objective function subject to seven constraints can be expressed as follows:

$$minimize\ f(x) subject\ to:\\ g_j \leq 0;\quad j = 1,2,\dots,7 \tag{4.10}$$

The modified objective function $\emptyset(x)$ can then be represented by:

$$\emptyset(x) = f(x)[1 + K \times C] \tag{4.11}$$

Where K and C are penalty parameters in which K is a constant coefficient which increases the rate of penalty applied to the function and for most engineering problems K =10 is assumed appropriate. C is a measure of violation defined as:

$$\mathrm{C} = \sum_{j=1}^{m} C_j \quad \leftarrow \begin{cases} C_j = g_j & \text{if } g_j > 0 \\ C_j = 0 & \text{if } g_j \leq 0 \end{cases} \tag{4.12}$$

4.5 Design Variables

In traditional HSA, the variables are independent. Using each spacing, as an individual variable, results in a conflict during algorithm execution. Noting that the summation of all spacing values must be equal to the height of the wall, the algorithm conflict can systematically be avoided by introducing an additional constraint that restricts the summation of all spacing values to be equal to the height of the wall. However, it has been discovered that this method introduces additional computational effort. To overcome this difficulty, a vector that contains all the distances (d_n)

between consecutive geosynthetic layers is considered in each harmony as a single variable (**S**) as shown in Equation 4.13.

$$\mathbf{S} = [d_1, d_2, \dots, d_{NoG}, d_{NoG+1}] \quad 4.13$$

The allocation of each value in this vector depends on the discretization of the acceptable range for spacing. It is also dependent on the algorithm's capability to search for combinations of spacing values whose summation equals to the height of the wall. The details are provided in the next sections.

The other variables are the lengths of geosynthetic in each layer staring from top of the wall. Each harmony, therefore, consists of a vector of dependent variables for spacing and lengths of each layer as independent variables as shown in Equation 4.14.

$$H = [\mathbf{S},\ l_1, l_2, \dots, d_{n-1}, d_n | C] \quad 4.14$$

In the calculation for spacing values between adjacent layers of geosynthetic layers, the spacing associated with each layer is assumed as the average of distances above and below each layer. This assumption is indicated in Equation 4.15.

$$S_n = \frac{d_n + d_{n+1}}{2} \quad 4.15$$

This value is modified for the first and last layers of geosynthetics to account for absence of adjacent layer of geosynthetics above and below those layers respectively.

4.6 Implementation of Harmony Search Algorithm

The process of finding a pleasing and ear-catching harmony in music is analogous to finding the optimality in an optimization process (Yang 2009). HSA is known as one of the powerful metaheuristic optimization methods inspired by improvisation ability of musicians that involves less mathematical efforts and highly accurate results. The base structure of this algorithm has been presented by Geem (2000). Since then, efforts have been made to modify the functionality of the base algorithm. In this study an improved harmony search, proposed by Mahdavi et al. (2007), is extended and implemented to the optimization of the cost associated with the construction of geosynthetic-reinforced earth walls.

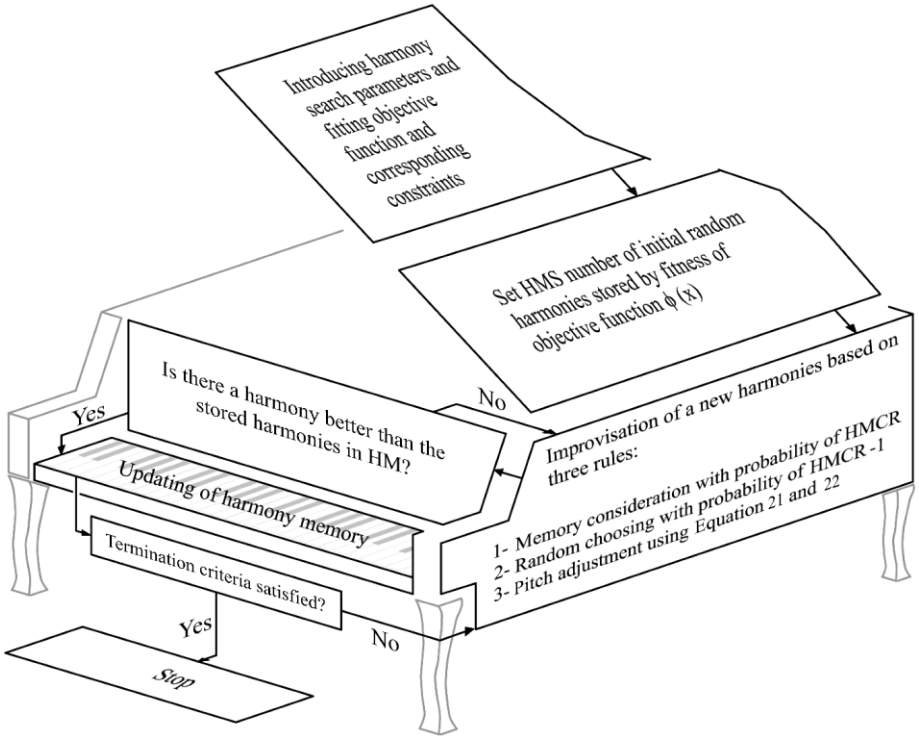

Figure 4.2 *IHS* Algorithm flowchart.

The steps involved in the IHS are presented in the flowchart shown in Figure 4.2. As indicated in the flowchart, the optimization program is initiated with a set of random harmonies (also called solution vectors or individuals) stored in a matrix called Harmony Memory (HM). The term "harmony" refers to solution vectors that contain sets of decision variables. HS algorithms use three mechanisms to produce a new harmony: memory consideration, random choosing, and pitch adjustment. The basic HS algorithm uses a constant probability and a fixed value to pitch-adjust the variables inside the new harmonies. IHS, on the other hand, employs interactive functions to improve the convergence of the harmonies to the optimized solution. In

each step, every new solution that is better than any of the stored harmonies from previous steps takes the place of the worst solution in the HM until termination criteria is satisfied. In order to fit the dependent variables into the HM and assign a random neighborhood for them, a new procedure is developed as discussed below.

4.6.1 Step 1: Introduction of the optimization program and parameters for the algorithm.

In this step, a set of specific parameters is introduced to the $IHSA$. Some of the parameters are:

1- The Harmony Memory Size (HMS). This determines the number of individuals (solution vectors) in the HM. For a given wall, in this work, 10 solution vectors are introduced to build the harmony memory.

2- The Harmony Memory Consideration Rate ($HMCR$). This parameter is utilized while decision is made to choose new variables from the HM or to assign new arbitrary values.

3- The Pitch Adjustment Rate (PAR). PAR, increasing functionally with iteration, is used to decide the adjustments of some decision variables selected from memory. The $IHSA$ expects the definition of minimum and maximum PAR values to this function.

4- The Bandwidth function (BW). This function determines the range of the adjustment that occurs to the variables in each iteration. A set of minimum

and maximum bandwidth values (BW_{min} and BW_{max}) must be introduced to this function. The value of this function decreases from BW_{max} in first iteration to BW_{min} in last iteration.

5- The maximum Number of Iteration (*NI*) which is also called Stopping or Termination Criteria.

6- The Permutation Evaluation Rate (*PER*). This parameter is useful in deciding whether different permutations of the solution vector, holding information about the non-uniform geosynthetic spacing values, are considered or not. This parameter is not included in the traditional *HSA* and *HIS*. It is proposed, by this work, in order to increase the probability of considering rare occurrences for vector **S** and to evaluate its different permutations.

The values attained by the parameters $HMCR$, PAR_{min}, PAR_{max}, BW_{min}, BW_{max} and HMS differ from one problem to another and can affect the convergence of the HSA to the optimum solution. Lower values attained by the PAR indicate an increased chance of adjusting one parameter without changing the others. However, BW must take bigger values for the first few iterations in order to ensure the creation of diversified solution vectors by the algorithm (Mahdavi et al. 2007). Setting appropriate values for these parameters will also enable the algorithm to avoid getting trapped in a local optimum. Lee et al. (2005) proposed a value between 0.7 and 0.95 for $HMCR$; 0.2 and 0.5 for PAR; and 10 and 50 for HMS to achieve a good

performance in the traditional HSA. In IHS Algorithm the value of PAR and BW varies with progressive iterations (Mahdavi et al. 2007).

The optimization problem is initially presented as minimizing $F(\mathbf{S}, l_1, l_2, \dots, l_N)$ which is the objective function. The vector S and geosynthetic lengths are the decision variables where $\mathbf{S} = [d_1, d_2, \dots, d_2, d_{NoG+1}]$ and $l = \{l_N | N = 1,2, \dots, NoG\}$. Therefore, the number of decision variables (NoV) is equal to the number of geosynthetic layers plus one (i.e. Equation 4.16). Each length value is an independent variable which is represented by its layer number and the additional variable **S** is an array made up of the inter-dependent spacing values.

$$NoV = NoG + 1 \qquad 4.16$$

In this paper the lower and upper bounds for the decision variables of type l (i.e. reinforcement length) are set to 1m and 10 m respectively. Applying the terms upper and lower bound for the array **S** does not make a clear sense as S contains a set of inter-dependent spacing-related variables (d). However, the lower and upper bounds for the dependent variables can be defined. The minimum and maximum values for the individual spacing values are considered to be 0.2 m and 1.5 m, respectively. These numbers were picked to be consistent, for result comparison purposes, with Mahdavi et al. (2007). In addition, these limit values can be applied to d-values so that the spacing values are allowed to vary within a specified range.

One of the challenging tasks, faced in this study, was how to assign the inter-dependent d values and form an optimized vector **S**. One way this task could be accomplished is by combining the gradient descent method with Harmony Search Algorithm and finding the optimum value of the **S** vector. Another, yet simpler, way is to discretize the domain of d into a few finite values and design a probabilistic method to find the optimum vector **S**. In the later approach, any possible combination of the discretized values of the domain -with a fixed summation equaling to the height of the wall- will have an equal probability of being chosen to make up the vector **S**. To elaborate on this, let's assume that the continuous range of d values (i.e. [0.2, 1.5]) is to be discretized into a certain number of distances (i.e. NoD). The difference between each discretized value in the given range is kept constant and less than a specified value. In this paper, DV refers to this value and the NoD is then given as:

$$NoD = \left| \frac{S_{max} - S_{min} + DV}{DV} \right| \tag{4.17}$$

The exact value of the difference between each discretized value within the domain is found by dividing the range by NoD. Once calculated, the discretized values are set in a vector. A random combination of the $NoG + 1$ number of the discretized values -with a fixed summation equaling to the height of the wall- can be assumed as a possible solution for the vector **S**.

The values for the length of geosynthetic layers (i.e. l values) are independently selected with a stochastic process. The ranges from which the algorithm

picks values for the NoG and l values are set based on experience and validated literature.

4.6.2 Step 2: Initialization of initial Harmony Memory (HM).

In this step, the initial HM matrix is populated with as many randomly generated individuals as the HMS and the corresponding Objective Function value of each set of random individuals $F(\mathbf{S}, l_1, l_2, \dots, l_N)$. The initial Harmony Memory is formed as follows:

$$HM = \left[\begin{array}{ccccc|c} \mathbf{S^1} & l_1^1 & R_2^1 & \cdots & l_N^1 & F(R^1) \\ \vdots & \vdots & \vdots & \cdots & \vdots & \vdots \\ \mathbf{S}^{HMS-1} & l_1^{HMS-1} & l_2^{HMS-1} & \cdots & l_N^{HMS-1} & F(R^{HMS-1}) \\ \mathbf{S}^{HMS} & l_1^{HMS} & l_2^{HMS} & \cdots & l_N^{HMS} & F(R^{HMS}) \end{array}\right] \quad 4.18$$

After the variables are assigned, the IHS algorithm solves the problem such that the Objective Function is optimized by minimizing its value. Upon the process of optimization, to minimize the Objective Function, Cost values associated with each set of individuals are arranged in a numerically ascending order.

4.6.3 Step 3: Improvisation for a New Harmony:

In this step, a New Harmony vector $F'(\mathbf{S}', l'_1, l'_2, \dots, l'_N)$., is improvised based on three mechanisms:

(1) Memory Consideration

(2) Random Selection

(3) Pitch Adjustment

4.6.3.1 Harmony Memory Consideration:

$HMCR$ and $1 - HMCR$ are defined as the rate of choosing one value from previously stored values in HM and the rate of randomly selecting one value from the possible range for variables respectively. For the i^{th} iteration and the j^{th} variable in each harmony vector we can write the following:

$$\text{For j} = 1: \quad \mathbf{S}_i' \leftarrow \begin{cases} \mathbf{S}_i' \in \{\mathbf{S^1}, \mathbf{S^2}, \dots, \mathbf{S^{HMS}}\} & \text{with probability } HMCR \\ \mathbf{S}' \in A\ new\ combination\ of\ H & \text{with probability } (1 - HMCR) \end{cases} \tag{4.19}$$

$$\text{For j} > 1: \quad l_{ij}' \leftarrow \begin{cases} l_{ij}' \in \{l_j^1, l_j^2, \dots, l_j^{HMS}\} & \text{with probability } HMCR \\ l_i' \in [l_{min}, l_{max}] & \text{with probability } (1 - HMCR) \end{cases} \tag{4.20}$$

For an instance, assuming $HMCR$ equal to 0.95, HSA selects the new variables from values stored in HM with a probability of 95%.

4.6.3.2 Pitch Adjustment:

In this step, each decision variable associated with the new individual is pitch-adjusted with a probability that was assigned to that variable. The main difference between HSA and IHS is observed when the pitch adjustment rate (PAR) is assigned to each variable in each step. In IHS a lower and upper level is defined for PAR. With

progressive iterations, PAR linearly changes from low to high values. Variation of PAR with iteration in IHS was expressed by Mahdavi et al. (2007) as:

$$PAR_i = PAR_{min} + \frac{PAR_{max} - PAR_{min}}{NI} \times i \qquad 4.21$$

Where i is the iteration number and NI is the maximum number of iterations as defined previously. The justification for this linear relationship was that small PAR values significantly increase the number of iterations Mahdavi et al. (2007). However, small PAR values are essential in first iterations to prevent the algorithm from being trapped in local optimums.

IHS bases itself on the dynamic interaction between PAR and BW. This dynamic interaction is manifest as the magnitude (distance) of the adjustment made to each variable, on each harmony, in the Pitch Adjustment operator. Generating high values of BW during the first iterations helps the algorithm to evaluate higher distances. This in turn augments the search capability of the algorithm. As the number of iterations increases, the system examines closer neighborhoods (distances from the newly obtained and assigned variables) and optimize their results further. The values of the BW which are bounded by lower and upper limits (i.e. BW_{min} and BW_{max}), are set to decrease exponentially from BW_{max} to BW_{min}. Mahdavi et al. (2007) proposed the following equation for BW in each iteration:

$$BW_i = BW_{max} + \exp(c \times i) \qquad 4.22$$

Where c is a coefficient given by:

$$c = \frac{\ln\left(\frac{BW_{min}}{BW_{max}}\right)}{NI} \tag{4.23}$$

Pitch Adjustment is applied to two kinds of variables. These are: (i) A vector of dependent variables (i.e. vector **S** made of the spacing values), and (ii) A set of independent variables (i.e. lengths).

4.6.3.2.1 Pitch adjustment for the vector S

In this study, the values of 0.35 and 0.99 are considered for PAR_{min}, $PAR_{max,}$ respectively. Having calculated the PAR_i, within the range [PAR_{min}, PAR_{max}], for each iteration from Equation (4.21), one can adjust the values of the vector **S** with the probability of PAR_i, as:

$$\text{Pitch adjusdting decision for } \mathbf{S}_i' \leftarrow \begin{cases} Yes & \text{with probability } PAR_i \\ \text{No} & \text{with probability } (1 - PAR_i) \end{cases} \tag{4.24}$$

Two simple methods can be adopted to define neighborhoods for vectors which are made of inter-dependent individual variables whose summation must remain constant (e.g. Vector **S**). The first method uses a small noise vector of the same number of elements and adds these elements with that of the original vector. Assume that $\mathbf{S}_{S+N}$ is a vector made by summing elements of the random noise vector (scaled by $BW1$) and elements of vector **S**.

$$\mathbf{S}_{S+N} \leftarrow= \mathbf{S} + BW1_i \times (a\ normal\ random\ noise\ vector) \quad 4.25$$

Where $BW1_i \in [BW1_{min}, BW1_{max}]$ is distance (neighborhood) bandwidth for vector **S** and can be calculated from Equation (4.22) for each iteration. $BW1_i$ is introduced to the IHS in order to assist the algorithm pick an optimal path in the close neighborhoods of vector S. Note that the sum of the elements of the vector defined in Equation (4.25) does not add up to a value equal to the height of the wall. In order to bring the summation to a value equaling the height of the wall, one needs to assess the locus of such vectors which takes the shape of a hyper-diamond. If the sum of the elements of $\mathbf{S}_{S+N}$is designated by V_{sum}, a new pitch adjusted neighborhood for the vector **S** (i.e. $\mathbf{S}'_i$) located on the hyper-diamond can be defined as:

$$\mathbf{S}'_{\boldsymbol{i}} \leftarrow= (S_s\ \mathbf{S}_{S+N})/V_{sum} \quad 4.26$$

Where S_s represents the sum of the elements of vector **S**.

This method, however, does not accommodate for any definite arrangement and order in framing the neighborhoods. There is an alternative approach that enables the algorithm to have an arranged set of vectors. In this method the neighborhoods of a vector can be defined by adding a set of defined vectors that add a small value to some elements and subtract it from other elements so as to keep the summation of the elements fixed. Each row of the matrix presented below shows some vectors that can be used to manipulate vector **S** and produce a new neighborhood:

$$\mathrm{N}_{set} = \underbrace{\begin{bmatrix} BW1_i & -BW1_i & 0 & 0 & 0 & 0 & \cdots \\ BW1_i \times 2 & -BW1_i \times 2 & 0 & 0 & 0 & 0 & \cdots \\ BW1_i \times 2 & -BW1_i & -BW1_i & 0 & 0 & 0 & \cdots \\ -BW1_i \times 2 & BW1_i & BW1_i & 0 & 0 & 0 & \cdots \\ BW1_i \times 3 & BW1_i \times 2 & BW1_i & -BW1_i & -BW1_i \times 2 & -BW1_i \times 3 & \cdots \\ -BW1_i \times 2 & -BW1_i & BW1_i & BW1_i \times 2 & 0 & 0 & \cdots \\ BW1_i & BW1_i & -BW1_i & -BW1_i & 0 & 0 & \cdots \\ \vdots & \vdots & \vdots & \vdots & \vdots & \vdots & \vdots \end{bmatrix}}_{Number\ of\ elements\ of\ \mathbf{S}} \quad 4.27$$

In Equation (4.27), each row of $\mathbf{N}_{\mathrm{set}}$ is a vector that contains scaled $BW1$ values that can be used in defining a neighborhood for vector **S**. Each row can be added to (or subtracted from) vector **S** to produce a new neighborhood. All permutations of the elements in each row of $\mathbf{N}_{\mathrm{set}}$ need to be considered in the calculation in order to have accurate estimate of the neighborhood vectors. Similar to the first method discussed above, this approach assigns values for $BW1_i$ within a range bounded by a minimum and maximum. In this study the lower and upper limits for $BW1$ are set to 0.009 and 0.2 respectively. These boundary values are set to attain an increased accuracy while running iterations for the spacing values that add up to give the height of the wall. Using the second approach, a set of random neighborhoods for the vector **S** can be generated using the following equation.

$$\mathbf{S}_i' \leftarrow= \mathbf{S} + N_{set} \quad 4.28$$

In this paper, all close neighborhoods are: generated using the second method; evaluated with the probability of PAR_i; and stored in a matrix ready to be evaluated with other adjusted harmonies.

4.6.3.2.2 Pitch adjustment for lN:

The values of PAR_{min} and PAR_{max} are the same for independent variables (lengths). Pitch adjustment for the lengths is done with the probability of PAR_i:

$$\text{Pitch adjusdting decision for } l_i' \leftarrow \begin{cases} Yes & \text{with probability } PAR_i \\ \text{No} & \text{with probability } (1 - PAR_i) \end{cases} \quad 4.29$$

The lengths are modified to their neighboring values with the probability of $PAR1$. For the problem discussed in this paper, Pitch Adjustment is applied for length (l_i) as described by the following expression:

$$l_i' \leftarrow= l_i' \pm (a\ normal\ random\ value) \times BW2_i \quad 4.30$$

Where $BW2_i$ for each step is calculated from Equation (4.22). The values of $BW2_{min}$ and $BW2_{max}$ are given by Equation (4.31).

$$[BW2_{min}, \quad BW2_{max}] = [0.009, \quad 0.05 \times (l_{max} - l_{min})] \quad 4.31$$

Where l_{min} and l_{max} are the lower and upper limits for the range defined for lengths of geosynthetics which are equal to 1 m and 10 m, respectively. The random value in Equation (4.30) is determined using the Gaussian Membership Function which covers a higher range for the random value and gives a small possibility to higher values to be chosen. If Pitch Adjustment causes a variable to fall outside the given range, an alternative value must be replaced for the outlier. This alternative value can be the minimum or maximum of the range assigned to the variable.

4.6.3.3 Permutation evaluation for the vector S

In this study, a set of random number of permutations of the vector **S** is also evaluated with the probability of PER to increase the chance of the **S** vectors that have small probability of random selection. This evaluation is done after Pitch Adjustment for the produced **S** vectors. The number of these permutations is randomly chosen from 1 to 10.

4.6.4 Step 4: Updating the Harmony Memory.

If the newly generated Harmony Vector is better than any of the stored Harmony Vectors in the *HM* (i.e. results in a better Objective Function value than that for the stored individuals), it will replace the old stored vector in the *HM*. Otherwise, the algorithm enters the next loop (iterating between Steps 3 and 4) without any replacement.

4.6.5 Step 5: Evaluation of the Termination Rule.

Steps 3 and 4 continue to repeat until the Termination Rule is satisfied. The last solution vector that meets the requirements of the Termination Rule is reported as the optimized solution for the problem under consideration. Undoubtedly, the maximum number of generations could be different from problem to problem depending on the desired accuracy. In this study, The Termination rule is considered to be satisfied, when the values of Cost Function, *F*, are equal up to ten decimal places

for 200 consecutive iterations. Figure 4.3 shows the reduction in cost with iterations for 9 meter Geogrid-Wrap Wall with A_m=0 and overburden pressure equal to q_s=10. It can be seen that the Mean Cost Values in the *HM* converge to the best cost, after 300 iterations. Further iteration causes slight changes in the variables, however, the changes in cost function will be insignificant.

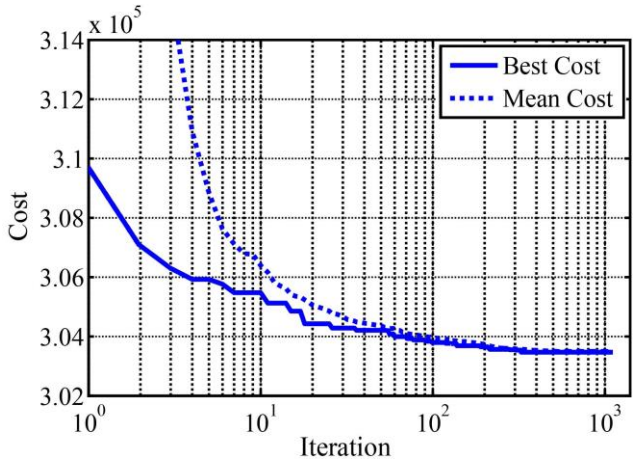

Figure 4.3 Reduction in cost with iterations for 9 meter Geogrid-Wrap Wall with A_m=0, q_s=10

4.7 Results and Discussions

As was discussed in Section 6, an Improved Harmony Search *(IHS)* was modified into a novel searching algorithm by incorporating a permutation-based optimization technique to handle non-uniform length and spacing of geosynthetic reinforcements. The analyses discussed herein and the associated results were compared to the work by Manahiloh et al. (2015). As such, the parameters, system geometry and load configurations were made, by design, similar to that of Manahiloh

et al. (2015) The input parameters used in defining each problem are presented in Table 4.2.

Table 4.2 Input design parameters (after Manahiloh et al. (2015))

Parameter	**value**
Height of Wall (H)	5-9 m
Minimum embankment of the fill (h_e)	0.45
Angle of internal friction of the backfill (ϕ_f)	30°
Unit weight of the backfill (γ_f)	18 kN/m^3
Angle of internal friction of the fill (ϕ_b)	35°
Unit weight of the fill (γ_b)	20 kN/m^3
Ultimate tensile strength of the geosynthetic (T_u)	<60 kN/m
Allowable tensile strength of the geosynthetic (T_a)	$T_a = T_u/1.5$ kN/m
Surcharge slope angle (β)	0°
Minimum length of the reinforcement ($l_{e\,min}$)	1.0 m

Table 4.3 shows the summary of results, obtained for uniform length and spacing values, that had been referred to in comparing the results of this study with that of Manahiloh et al. (2015). The results obtained for problems solved in different modes (i.e. Geotextile-wrap, Geogrids with; Static loading, Dynamic(seismic) loads) and their comparison with the results obtained by Manahiloh et al. (2015) are presented in Table 4.4 through Table 4.9.

Table 4.3 Summary of results for uniform length and spacing values (modified from Manahiloh et al. (2015))

Geotextile												
	A_m = 0 , q_s = 0				**A_m = 0 , q_s = 10 kPa**				**A_m = 0.05 , q_s = 0**			
H_t (m)	***NoG***	***l*(m)**	**T_a-max(KN/m)**	**Total Cost($)**	***NoG***	***L*(m)**	**T_a-max(KN/m)**	**Total Cost($)**	***NoG***	***l* (m)**	**T_a-max(KN/m)**	**Total Cost($)**
5	3	3.23	26.5	116826.2	3	3.24	30	117066	3	3.62	32	120390.5
7	5	4.34	38.5	175045.2	6	4.43	36.75	178993.7	6	4.83	40	184432.2
9	10	5.59	37.8	253864.8	11	5.62	37.1	258287.4	12	6.15	37.84	271914.3
Geogrid												
	A_m = 0 , q_s = 0				**A_m = 0 , q_s = 10 kPa**				**A_m = 0.05 , q_s = 0**			
H_t (m)	***NoG***	***L*(m)**	**T_a-max(KN/m)**	**Total Cost($)**	***NoG***	***L*(m)**	**T_a-max(KN/m)**	**Total Cost($)**	***NoG***	***l* (m)**	**T_a**	**Total Cost($)**
5	3	3.233	26.5	159262.7	3	2.238	30	159510.6	3	3.62	32	162693.4
7	5	4.341	38.5	232052.6	6	4.43	36.75	235405.1	6	4.83	40	240560.5
9	10	5.59	37.8	322755.3	11	5.626	37.1	326459.7	12	6.15	37.84	338650.2

Table 4.4 Optimum design values for Geotextile-wrap walls A_m=0, q_s=0

$H_t(m)$	Ta-max (kN/m)	l_{min}	l_{max}	Cost($)	Saving with respect to equal lengths and spacings (%)
5	36.5	1 m	10 m	113705.6	2.67

Lengths	l_1	l_2	l_3	l_4	distances	d_1	d_2	d_3	d_4	d_5
	4.62	2.04	1.26	1.11		1.5	1.5	1.5	0.29	0.21

$H_t(m)$	Ta-max (kN/m)	l_{min}	l_{max}	Cost($)	Saving with respect to equal lengths and spacings (%)
7	55.86	1 m	10 m	166944.58	4.62

Lengths	l_1	l_2	l_3	l_4	l_5	distances	d_1	d_2	d_3	d_4	d_5	d_6
	7.97	3.1	2.3	1.5	1.11		1.5	1.5	1.5	1.5	0.79	0.21

$H_t(m)$	Ta-max (kN/m)	l_{min}	l_{max}	Cost($)	Saving with respect to equal lengths and spacings (%)
9	60	1 m	10 m	229028.5	9.8

Lengths	l_1	l_2	l_3	l_4	l_5	l_6	l_7	distances	d_1	d_2	d_3	d_4	d_5	d_6	d_7	d_8
	10	6.7	4.1	2.6	2.1	1.5	1.2		1.5	1.5	1.5	1.5	0.96	1.15	0.53	0.35

Table 4.5 Optimum design values for Geogrid-reinforced walls A_m=0, q_s=0

$H_t(m)$	Ta-max (kN/m)	l_{min}	l_{max}	Cost($)	Saving with respect to equal lengths and spacings (%)
5	36.5	1 m	10 m	156217.1	1.91

Lengths	l_1	l_2	l_3	l_4	distances	d_1	d_2	d_3	d_4	d_5
	4.62	2.04	1.26	1.11		1.5	1.5	1.5	0.3	0.2

$H_t(m)$	Ta-max (kN/m)	l_{min}	l_{max}	Cost($)	Saving with respect to equal lengths and spacings (%)
7	54.8	1 m	10 m	225120.5	2.98

Lengths	l_1	l_2	l_3	l_4	l_5	l_6	distances	d_1	d_2	d_3	d_4	d_5	d_6	d_7
	8	3.1	2.3	1.5	1.2	1.1		1.5	1.5	1.5	1.5	0.59	0.21	0.2

$H_t(m)$	Ta-max (kN/m)	l_{min}	l_{max}	Cost($)	Saving with respect to equal lengths and spacings (%)
9	59.9	1 m	10 m	301860.6	6.47

Lengths	l_1	l_2	l_3	l_4	l_5	l_6	l_7	l_8	distances	d_1	d_2	d_3	d_4	d_5	d_6	d_7	d_8	d_9
	10	6.7	4	2.66	2.11	1.65	1.3	1.16		1.5	1.5	1.5	1.47	1	1	0.6	0.2	0.23

The results for No Earthquake and No Surcharge Load (i.e. A_m=0, q_s=0) presented in Table 4.4 and Table 4.5 indicates that the amount of saving increases as the height of the wall increases. As was expected, the cost savings were higher for larger wall heights that involve larger volume of excavation. For smaller heights, the amount of saving is higher for Geotextile-wrap walls as compared to that of Geogrid-reinforced walls. The tensile strength required for the reinforcement was found to be higher for he cases involving taller wall heights. A decreasing trend, for both spacing and length values, was observed from upper to lower geosynthetic layers.

As shown in Table 4.6 and Table 4.7, higher saving was obtained for the case of No Earthquake and Surcharge of 10 kPa (A_m=0 and qs=10 kPa) as compared to the cases presented in Tables 4.4 & 4.5. A general increasing trend in the percentage of cost reduction was observed.

The total saving in the presence of seismic loads was found to be lower (Table 4.8 and Table 4.9) compared to the other modes of analyses. This reduction in total saving can be related to the extent of seismic load considered in analysis. The inertial force was assumed to act over a zone of width equaling half of the wall height. This assumption indeed leads to a conservative design. The total saving for Geotextile-Wrapped Walls was found to be higher than that of Geogrid-reinforced Walls.

Table 4.6 Optimum design values for Geotextile-wrap walls A_m=0, q_s=10 kPa

$H_t(m)$	Ta-max (kN/m)	l_{min}	l_{max}	Cost($)	Saving with respect to uniform lengths and spacing (%)
5	40	1 m	10 m	115006.56	1.76

Lengths	l_1	l_2	l_3	l_4	Distances	d_1	d_2	d_3	d_4	d_5
	5.1	2.1	1.38	1.11		1.33	1.49	1.48	0.5	0.2

$H_t(m)$	Ta-max (kN/m)	l_{min}	l_{max}	Cost($)	Saving with respect to uniform lengths and spacing (%)
7	60	1 m	10 m	167738.5	6.29

Lengths	l_1	l_2	l_3	l_4	l_5	Distances	d_1	d_2	d_3	d_4	d_5	d_6
	8.1	3.1	2.3	1.54	1.12		1.49	1.5	1.49	1.47	0.82	0.22

$H_t(m)$	Ta-max (kN/m)	l_{min}	l_{max}	Cost($)	Saving with respect to uniform lengths and spacing (%)
9	60	1 m	10 m	231288.1	10.45

Lengths	l_1	l_2	l_3	l_4	l_5	l_6	l_7	l_8	Distances	d_1	d_2	d_3	d_4	d_5	d_6	d_7	d_8	d_9
	10	7.5	3.49	2.74	2.2	1.59	1.3	1.17		1.5	1.5	1.5	1.4	0.88	1.14	0.54	0.33	0.2

Table 4.7 Optimum design values for Geogrid-reinforced walls A_m=0, q_s=10 kPa

$H_t(m)$	Ta-max (kN/m)	l_{min}	l_{max}	Cost($)	Saving with respect to uniform lengths and spacing (%)
5	39.8	1 m	10 m	157449.7	1.29

Lengths	l_1	l_2	l_3	l_4	Distances	d_1	d_2	d_3	d_4	d_5
	5.23	2.2	1.44	1.11		1.2	1.48	1.47	0.63	0.22

$H_t(m)$	Ta-max (kN/m)	l_{min}	l_{max}	Cost($)	Saving with respect to uniform lengths and spacing (%)
7	56.55	1 m	10 m	225458.7	4.22

Lengths	l_1	l_2	l_3	l_4	l_5	Distances	d_1	d_2	d_3	d_4	d_5	d_6
	9.26	3.41	2.63	1.85	1.4		0.88	1.5	1.5	1.5	0.87	0.75

$H_t(m)$	Ta-max (kN/m)	l_{min}	l_{max}	Cost($)	Saving with respect to uniform lengths and spacing (%)
9	59.8	1 m	10 m	303382.37	7.1

Lengths	l_1	l_2	l_3	l_4	l_5	l_6	l_7	l_8	Distances	d_1	d_2	d_3	d_4	d_5	d_6	d_7	d_8	d_9
	9.99	6.49	4.53	2.7	2.23	1.77	1.27	1.16		1.5	1.5	1.5	1.45	0.84	1.02	0.69	0.3	0.2

Table 4.8 Optimum design values for Geotextile-wrap walls A_m=0.05, q_s=0

$H_t(m)$	Ta-max (kN/m)	l_{min}	l_{max}	Cost($)	Saving with respect to equal lengths and spacings (%)
5	39.3	1 m	10 m	118560.7	1.52

Lengths	l_1	l_2	l_3	l_4	distances	d_1	d_1	d_1	d_4	d_5
	5.92	2.14	1.27	1.1		1.5	1.5	1.49	0.31	0.2

$H_t(m)$	Ta-max (kN/m)	l_{min}	l_{max}	Cost($)	Saving with respect to equal lengths and spacings (%)
7	56.55	1 m	10 m	225458.7	4.22

Lengths	l_1	l_2	l_3	l_4	l_5	l_6	distances	d_1	d_2	d_3	d_4	d_5	d_6	d_7
	9.53	4.64	2.36	1.54	1.2	1.11		1.5	1.5	1.5	1.5	0.6	0.2	0.2

$H_t(m)$	Ta-max (kN/m)	l_{min}	l_{max}	Cost($)	Saving with respect to equal lengths and spacings (%)
9	59.9	1 m	10 m	248689.4	8.54

Lengths	l_1	l_2	l_3	l_4	l_5	l_6	l_7	l_8	distances	d_1	d_2	d_3	d_4	d_5	d_6	d_7	d_8	d_9
	10	9.54	7.2	4.16	2.16	1.76	1.34	1.2		1.48	1.49	1.49	1.14	1.22	0.83	0.89	0.25	0.21

Table 4.9 Optimum design values for Geogrid-reinforced walls A_m=0.05, q_s=0

$H_t(m)$	Ta-max (kN/m)	l_{min}	l_{max}	Cost($)	Saving with respect to equal lengths and spacings (%)
5	39.34	1 m	10 m	160904.7	1.1

Lengths	l1	l2	l3	l4	distances	d_1	d_1	d_1	d_4	d_5
	5.9	2.13	1.26	1.11		1.5	1.5	1.5	0.3	0.2

$H_t(m)$	Ta-max (kN/m)	l_{min}	l_{max}	Cost($)	Saving with respect to equal lengths and spacings (%)
7	58.16621	1 m	10 m	234729.7	2.42

Lengths	l_1	l_2	l_3	l_4	l_5	l_6	distances	d_1	d_2	d_3	d_4	d_5	d_6	d_7
	9.99	3.77	2.49	1.55	1.22	1.12		1.5	1.5	1.5	1.5	0.6	0.2	0.2

$H_t(m)$	Ta-max (kN/m)	l_{min}	l_{max}	Cost($)	Saving with respect to equal lengths and spacings (%)
9	59.78175	1 m	10 m	319736.72	5.58

Lengths	l_1	l_2	l_3	l_4	l_5	l_6	l_7	l_8	distances	d_1	d_2	d_3	d_4	d_5	d_6	d_7	d_8	d_9
	10	9.96	6.3	3.74	2.65	1.73	1.58	1.32		1.5	1.5	1.46	1.28	1.05	0.93	0.7	0.22	0.36

The total saving in the presence of seismic loads was found to be lower (Table 4.8 and Table 4.9) compared to the other modes of analyses. This reduction in total saving can be related to the extent of seismic load considered in analysis. The inertial force was assumed to act over a zone of width equaling half of the wall height. This assumption indeed leads to a conservative design. The total saving for Geotextile-Wrapped Walls was found to be higher than that of Geogrid-reinforced Walls.

The range for the length of geosynthetic layers, for the results presented in all of the cases discussed in Tables 4.4 –4.9, was [l_{min}, l_{max}] = [1m, 10m]. This range was selected to be consistent with a previous study done for uniform length and spacing values (Manahiloh et al. 2015). However, the authors would like to note that this range can be altered to increase the overlap of the geosynthetic layers which helps in enhancing the integrity of the reinforced zone. To compare the results with smaller ranges for lengths of geosynthetic and justify the arrangement of layers obtained by *IHS* Algorithm, the optimization program is repeated for the 9m Geogrid-reinforced wall with $A_m=0$ and $q_s=10$ kPa. The lower bound is kept as 1 meter and the upper bound is changed to 9 and 5.7 meters which is close to the optimum value of length for the case of equal length and spacing. The results are presented in Table 4.10

.

Table 4.10 9m Geogrid-reinforced Wall with $A_m=0$ and $q_s=10\ kPa$ with two different range for lengths.

l_{max}	Ta-max (kN/m)	Cost($)	Saving with respect to uniform lengths and spacings (%)
8 m	60	305999.9	6.2

Lengths	l_1	l_2	l_3	l_4	l_5	l_6	l_7	l_8	Distances	d_1	d_2	d_3	d_4	d_5	d_6	d_7	d_8	d_9
	8	7.8	6.2	3.5	2.35	1.58	1.3	1.18		1.5	1.47	1.49	1.47	0.8	1.2	0.54	0.21	0.32

l_{max}	Ta-max (kN/m)	Cost($)	Saving with respect to uniform lengths and spacings (%)
5.7 m	60	311696.3	4.5

Lengths	l_1	l_2	l_3	l_4	l_5	l_6	l_7	l_8	Distances	d_1	d_2	d_3	d_4	d_5	d_6	d_7	d_8	d_9
	5.7	5.69	5.65	5.64	5.41	4.7	2.99	2.98		1.5	1.5	1.5	1.42	0.84	1.17	0.54	0.23	0.3

It was obtained that, with decrease in l_{max}, the amount of saving reduced. Figure 4.4 shows the arrangement of geothynsetics for 9m Geogrid-Wrap Wall with $A_m=0$ and $q_s=10$ *kPa*, and for three different l_{max}. It is inferred that reducing the range over which the length of geosynthetic layers can vary, increases the length of geosynthetic for lower layers. Figure 4.4 (c) shows the arrangement for maximum length equal to 5.7 meter which was equal to the optimum length of geosynthetics for the case of same lengths and spacing (Manahiloh et al. 2015). Table 4.10 also indicates that, using variable lengths and spacing values, the total cost is higher compared to the case of equal lengths and spacing values (Manahiloh et al. 2015) with same maximum length for both cases. It can be inferred from Figure 4.4 that the overall trend for spacing and length is decreasing for lower layers. This trend is same for all heights and static and seismic analysis (see Table 4.4 to Table 4.9)

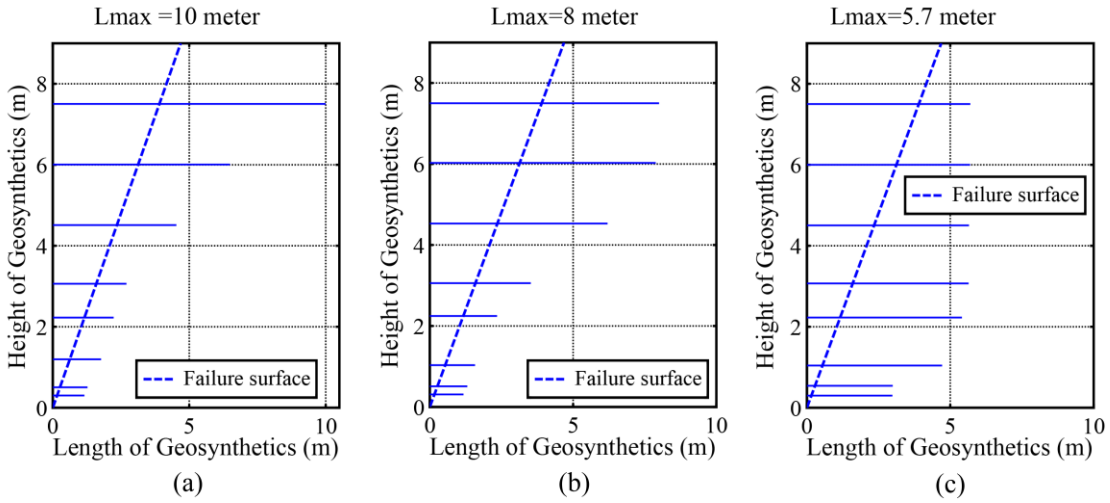

Figure 4.4 Arrangement of geosynthetics for 9m Geogrid-Wrap Wall with A_m=0 and q_s=10 kPa with three different range for lengths

The range of spacing and lengths in this study are chosen to be equal to the previous study was performed by Manahiloh et al. (2015). This study mainly performed to examine the applicability of the mentioned method, however, it is desirable to decrease the spacing and increase the overlapping between layers that ensures the integrity of the reinforced zone.

4.8 Conclusions

In this study the principles involving different constrained optimization methods were highlighted. A novel Improved Harmony Search Algorithm (*IHS)* was developed and used to optimize the design of Geosynthetic-reinforced walls with non-uniform lengths and spacing values. Heuristic methods were employed to modify the traditional Harmony Search Algorithms and extend their capability to add a vector - composed of dependent variables- as a single variable in the process of defining the optimization problem. In each layer, the *IHS* algorithm was enabled to confine the strength of the geosynthetics to allowable values set using constraints. While strength requirements are met at each layer, the optimum tensile strength of the geosynthetics were set to correspond to those values that result in reduced overall cost of construction. In addition to the cost of geosynthetic itself, the big proportion of cost reduction came from the reduction of the volume of fill and the associated reduction in the length of reinforcements for lower layers.

The newly developed *IHSA* was applied to optimize the construction of geosynthetic reinforced earth walls of height 5, 7 and 9 meters. Various cases

considered were: geotextile vs. geogrid reinforcement; static ($A_m = 0$) vs. dynamic ($A_m = 0.05$) loading conditions; and the presence ($q_s = 10\ kPa$) vs. absence ($q_s = 0$) of a surcharge load. The geometrical and loading values were selected to be consistent with a previous work with which relative observations were made. Cost savings were reported in comparison to the work done by Manahiloh et al. (2015) using the "classic" *HSA.*

For geotextile-reinforced wall construction: for the case of no dynamic and no surcharge loads, the cost of construction of the 5, 7, and 9 meter walls showed a reduction of 2.67%, 4.62%, and 9.8% respectively; for the case where no dynamic load and q_s=10 kPa were considered, the corresponding cost savings were found to be equal to 1.76%, 6.29%, and 10.45% respectively; and for the case where dynamic analysis is performed with $A_m = 0.05$ in the absence of surcharge, the cost reductions were 1.52%, 4.22%, and 8.54% respectively. In all cases, it was observed that the rate of cost saving increased with the height of the walls. For Geogrid-reinforced walls the cost savings was about 30% less than that of Geotextile-reinforced walls. In addition, the spacing between adjacent geosynthetic layers and the corresponding lengths were observed to decrease from top to bottom of the walls. The authors believe that the ideas implemented in this newly improved algorithm could be used towards optimizing the design of other geotechnical projects that involve variable parameters in their design.

Chapter 5

SUMMARY, CONCLUSIONS, AND RECOMMENDATIONS

Two commonly used Harmony Search Algorithms were utilized to optimize the cost of construction for MSE walls reinforced with geosynthetic layers. Quantitative comparisons and specific conclusions were made in the appropriate sections of Chapters 3 and 4. In this chapter, a general summary of the findings is presented.

Harmony search algorithm was shown to be one of the newly developed, mathematically less complicated, search algorithms that benefits from the concept of memory. The utilization of this method, for engineering problems where absolute deterministic results are not required, is highly recommended. In this study, it was shown that the results obtained from HSA (for the design of MSE walls) are very close to those of the deterministic optimization approaches. The HSA optimization was modified in such a way that it always succeeded in finding global optimum, without the threat of getting trapped by the local optimums.

The optimal design of conventional MSE walls, reinforced with uniform geosynthetic layers, was presented in Chapter 3. The length and vertical spacing of the reinforcements were assumed to be fixed over all reinforcement layers. The results of this study were compared with that of Basudhar et al. (2008). The maximum cost reduction was 9%. This much cost reduction was found to be very significant, taking

into consideration the big-scale of retaining wall construction. The cost function was assumed to be the cost of construction and the simple general form of the harmony search algorithm was used in optimizing the overall cost of the construction. This study showed that, even the simple form of the HSA was successful in searching the optimum design variables.

Improved Harmony Search Algorithm (IHSA) was utilized to optimize the cost of construction for MSE walls with non-uniform geosynthetic layers. The length and vertical spacing of the layers were allowed to vary across different reinforcement layers. To account for constructability, one additional constraint was added to the optimization problem. This constraint limits the length of the reinforcements in a given layer to be equal or less than that of the top layer. It was shown that a set of variables of the same type could be introduced to IHSA as a single vector-type variable. In addition, a new permutation adjustment was introduced to the pitch-adjustment-step of the optimization for such a vector-type variable. The cost of construction was shown to reduce by 10% compared to the HSA optimization result obtained with the assumption of uniform length and spacing of reinforcement (i.e., Chapter 3).

The over conservative design outcomes that result from the use of high factors of safety can be significantly be improved by using optimization methods. The complexity of geotechnical engineering problems and their constraints (most importantly factors of safety) can benefit from adopting metaheuristic methods of obtaining optimal design. Based on the results obtained by this work, the application

of HSA algorithm is highly recommended for the optimization of geotechnical engineering designs.

REFERENCES

AASHTO (1996). Standard Specifications for Highway Bridges, with 2000 Interims. Washington, D.C., USA, 686 p., *American Association of State Highway and Transportation Officials*, Fifteenth Edition.

Abdollahi, A. and M. Shams (2015a). "Optimization of shape and angle of attack of winglet vortex generator in a rectangular channel for heat transfer enhancement." *Applied Thermal Engineering* 81: 376-387.

Abdollahi, A. and M. Shams (2015b). "Optimization of heat transfer enhancement of nanofluid in a channel with winglet vortex generator." *Applied Thermal Engineering* 91: 1116-1126.

Alimoradi, H. and M. Shams (2017). "Optimization of subcooled flow boiling in a vertical pipe by using artificial neural network and multi objective genetic algorithm." *Applied Thermal Engineering* 111: 1039-1051.

Ayvaz, T. (2007). "Simultaneous determination of aquifer parameters and zone structures with fuzzy c-means clustering and meta-heuristic harmony search algorithm." *Advances in Water Resources* 30: 2326–2338.

Basha, B. M. and G. L. S. Babu (2012). "Target reliability-based optimisation for internal seismic stability of reinforced soil structures." *Geotechnique* 62(1): 55-68.

Basha, B. M. and K. V. N. S. Raviteja (2016). "Optimum Tensile Strength of Geomembrane Liner for V-Shaped Anchor Trenches Using Target Reliability Approach." *Geotechnical and Geological Engineering* 34(6): 1995-2018.

Basudhar, P. K., et al. (2008). "Cost Optimization of Reinforced Earth Walls." *Geotechnical and Geological Engineering* 26: 1-12.

Ben, L. (2014). "Limit Analysis Optimization of Design Factors for Mechanically Stabilized Earth Wall-Supported Footings." *Transportation Infrastructure Geotechnology* 1(2): 111-128.

Box, M. J. (1965). "A New Method of Constrained Optimization and a Comparison With Other Methods." *The Computer Journal* 8(1): 42-52.

Ceylan, H., et al. (2008). "Transport energy modeling with metaheuristic harmony search algorithm, an application to Turkey." *Journal of Energy Policy* 36: 2527–2535.

Coello, C. A. C. (2002). "Theoretical and Numerical Constraint-Handling Techniques used with Evolutionary Algorithms : A survey of the state of the art." *Computer Methods in Applied Mechanics and Engineering* 191(11-12): 1245-1287.

Das, B. M. (2007). Principles of Foundation Engineering, *Cengage learning*.

Degertekin, S. O. (2008). "Optimum design of steel frames using harmony search algorithm." *Struct. Multidiscip. Optim.* 36: 393–401.

Dorigo, M. and T. Stützle (2004). Ant Colony Optimization, *Bradford Company*.

Elias, V., et al. (2001). Mechanically stabilized earth walls and reinforced soil slopes design & construction guidelines.

Gao, X. Z., et al. (2015). "Harmony Search Method: Theory and Applications." *Computational Intelligence and Neuroscience* 2015: 258491.

Geem, Z. W. (2000). Optimal design of water distribution networks using harmony search. Department of Civil and Environmental Engineering, *Korea University*. Doctor of Philosophy.

Geem, Z. W. (2006). "Optimal cost design of water distribution networks using harmony search." *Eng. Optim.* 38: 259 – 280.

Geem, Z. W. (2008). "Novel derivative of harmony search algorithm for discrete design variables." *Applied Mathematics and Computation* 199(1): 223-230.

Geem, Z. W. and H. Hwangbo (2006). Application of harmony search to multi-objective optimization for satellite heat pipe design. *Proceeding of the US-Korea Conference on Science, Technology, and Entrepreneur ship* (UKC 2006), Teaneck, NJ, USA, Korean-American Scientists and Engineers Association.

Geem, Z. W., et al. (2001). "A New Heuristic Optimization Algorithm: Harmony Search." *SIMULATION* 76(2): 60-68.

Geem, Z. W., et al. (2002). "Harmony search optimization: Application to pipe network design." *Int. J. Model. Simulat.* 22: 125.

Geem, Z. W. and K. B. Sim (2010). "Parameter-setting-free harmony search algorithm." *Applied Mathematics and Computation* 217(8): 3881-3889.

Glover, F. and M. Laguna (1997). Tabu Search, *Kluwer Academic Publishers*.

Guin, J. A. (1968). "Modification of the Complex method of constraint optimization." *Computer Journal* Volume 10: pages 416-417.

Hasancebi, O. (2008). "Adaptive evolution strategies in structural optimization: Enhancing their computational performance with applications to large-scale structures." *Comput. Struct.* 86: 119.

Hasancebi, O., et al. (2009). "Performance evaluation of metaheuristic search techniques in the optimum design of real size pin jointed structures." *Comput. Struct.* 87: 284.

Holland, J. H. (1992). Adaptation in Natural and Artificial Systems: An Introductory Analysis with Applications to Biology, Control and Artificial Intelligence, *MIT Press*.

Jamali Keisari, S. and M. Shams (2016). "Shape optimization of nucleating wet-steam flow nozzle." *Applied Thermal Engineering* 103: 812-820.

Karahan, H., et al. (2013). "Parameter Estimation of the Nonlinear Muskingum Flood-Routing Model Using a Hybrid Harmony Search Algorithm." *Journal of Hydrologic Engineering* 18(3): 352-360.

Kayhan, A. H., et al. (2011). "Selecting and scaling real ground motion records using harmony search algorithm." *Soil Dyn. Earthq. Eng.* 31: 941-953.

Kennedy, J. and R. Eberhart (1995). Particle swarm optimization. *In Proceedings of the IEEE international conference on neural networks IV*, pp. 1942-1948 Piscataway: IEEE.

Kim, J. H., et al. (2001). "Parameter estimation of the nonlinear Muskingum model using harmony search." *J. Am. Water Resour. Assoc* 37: 1131–1138.

Kirkpatrick, S., et al. (1983). "Optimization by Simulated Annealing." *Science* 220(4598): 671.

Koerner, M. R. and T. Soong (2001). "Geosynthetic reinforced segmental retaining walls." *Journal of Geotextiles and Geomembrane* 19: 359-386.

Kosugi, K. and Y. Nakayama (1997). "A method for estimating unsaturated hydraulic properties of vertically heterogeneous soils from transient capillary pressure profiles." *Agricultural and Forest Meteorology* 84(1): 37-50.

Lamberti, L. (2008). "An efficient simulated annealing algorithm for design optimization of truss structures." *Computers & Structures* 86(19–20): 1936-1953.

Lawrence, C. (2014). High Performance Textiles and their Applications, *Woodhead Publishing*: 256–350.

Lee, K. S. and Z. W. Geem (2004). "A new structural optimization method based on the harmony search algorithm." *Composite Structures* 82: 781-798.

Lee, K. S., et al. (2005). "The harmony search heuristic algorithm for discrete structural optimization." *Engineering Optimization* 37(663–684).

Levenberg, K. (1944). "A METHOD FOR THE SOLUTION OF CERTAIN NON-LINEAR PROBLEMS IN LEAST SQUARES." *Quarterly of Applied Mathematics* 2(2): 164-168.

Mahdavi, M., et al. (2007). "An improved harmony search algorithm for solving optimization problems." *Applied Mathematics and Computation* 188: 1567-1579.

Manahiloh, K. N., et al. (2015). "Optimization of Design Parameters and Cost of Geosynthetic-Reinforced Earth Walls Using Harmony Search Algorithm." *Int. J. of Geosynth. and Ground Eng.*: 1:15.

Marquardt, D. W. (1963). "An Algorithm for Least-Squares Estimation of Nonlinear Parameters." *Journal of the Society for Industrial and Applied Mathematics* 11(2): 431-441.

Mattsson, H., et al. (2001). "Optimization routine for identification of model parameters in soil plasticity." *International Journal for Numerical and Analytical Methods in Geomechanics* 25(5): 435-472.

Meyerhof, G. G. (1953). The bearing capacity of foundation under eccentric and inclined loads. *Third International Conference on Soil Mechanics and Foundation Engineering*, Zurich.

Mouritz, A. P. and A. G. Gibson (2006). Fire properties of polymer composite materials, *Springer*.

Murty, K. G. (1983). Linear programming, *Wiley*.

Nazari, T., et al. (2013 (a)). "WWER core pattern enhancement using adaptive improved harmony search." *J. Nuclear Engineering and Design* 254: 23-32.

Nazari, T., et al. (2013 (b)). "Investigation of PWR core optimization using harmony search algorithms." *Journal Annals of Nuclear Energy* 57: 1-15.

Nicholson, P. G. (2015). Chapter 14 - Geosynthetic Reinforced Soil. Soil Improvement and Ground Modification Methods. *Boston*, *Butterworth-Heinemann*: 343-369.

Omran, M. G. H. and M. Mahdavi (2008). "Global-best harmony search." *Applied Mathematics and Computation* 198(2): 643-656.

Paik, K., et al. (2005). "A conceptual rainfall-runoff model considering seasonal variation." *Hydrol. Process* 19: 3837–4385.

Parncutt, R. (1989). Harmony: A psychoacoustical approach. *Berlin*, *Springer Science & Business Media*.

Pham, D. T., et al. (2005). "The bees algorithm. Technical note." *Manufacturing Engineering Centre, Cardiff University, UK*: 1-57.

Pourbaba, M., et al. (2013). "A Chaotic Imperialist Competitive Algorithm for Optimum Cost Design of Cantilever Retaining Walls." *KSCE Journal of Civil Engineering* 17(5): 972-979.

Prakash, S. and S. Saran (1971). "Bearing capacity of eccentrically loaded footings." *ASCE J Soil Mech Found Div* 97(97-117).

Pucker, T. and J. Grabe (2011). "Structural optimization in geotechnical engineering: basics and application." *Acta Geotechnica* 6(1): 41-49.

Robinson, J. D., et al. (2016). "Multi-objective traction optimization of vehicles in loose dry sand using the generalized reduced gradient method." *Journal of Terramechanics* 64: 46-57.

Rosenbrock, H. H. (1963). "Some general implicit processes for the numerical solution of differential equations." *The Computer Journal* 5(4): 329-330.

Serpik, I. N., et al. (2016). "Algorithm for Evolutionary Optimization of Reinforced Concrete Frames Subject to Nonlinear Material Deformation." *Procedia Engineering* 150: 1311-1316.

Shahrokhabadi, S. and M. M. Toufigh (2013). "The solution of unconfined seepage problem using Natural Element Method (NEM) coupled with Genetic Algorithm (GA)." *Applied Mathematical Modelling* 37(5): 2775-2786.

Shahrokhabadi, S., et al. (2016). "Integration of Thiele Continued Fractions and the method of fundamental solutions for solving unconfined seepage problems." *Computers & Mathematics with Applications* 71(7): 1479-1490.

Shi, W. W., et al. (2013). "A Hybrid Genetic Algorithm Based on Harmony Search and its Improving." *Informatics and Management Science I* 204: 101-109

Simunek, J., et al. (1998). "Parameter estimation of unsaturated soil hydraulic properties from transient flow processes1." *Soil and Tillage Research* 47(1–2): 27-36.

Storn, R. and K. Price (1997). "Differential Evolution – A Simple and Efficient Heuristic for global Optimization over Continuous Spaces." *Journal of Global Optimization* 11(4): 341-359.

Terzaghi, K. (1943). Theoretical Soil Mechanics, *Wiley, New York*.

Vahedifard, F., et al. (2016). "Geosynthetic-reinforced soil structures with concave facing profile." *Geotextiles and Geomembranes* 44(3): 358-365.

Wang, C. M. and Y. F. Huang (2010). "Self-adaptive harmony search algorithm for optimization." *Expert Systems with Applications* 37(4): 2826-2837.

Wang, L. and L. P. Li (2013). "An effective differential harmony search algorithm for the solving non-convex economic load dispatch problems." *Electrical Power and Energy Systems* 44(2013): 832-843.

Wang, L., et al. (2011). "A hybrid harmony search algorithm for the blocking permutation flow shop scheduling problem." *Comput Ind Eng* 61: 76-83.

Wu, B., et al. (2012). "Hybrid harmony search and artificial bee colony algorithm for global optimization problems." 64(8): 2621-2634.

Yang, X. S. (2009). Harmony Search as a Metaheuristic Algorithm. *Music-Inspired Harmony Search Algorithm: Theory and Applications*, Berlin, Springer.

Yang, X. S. (2014). Nature-Inspired Optimization Algorithms, *Elsevier Science Publishers B. V.*

Yang, X. S. and S. Deb (2009). Cuckoo search via Levy flights. *Proceeding of World Congress on Nature & Biologically Inspired Computing*, India. NaBIC, (December 2009), pp. 210-214, IEEE Publications, USA.

Yoo, H., et al. (2007). "Evaluation of Pullout and Drainage Properties of Geosynthetic Reinforcements in Weathered Granite Backfill Soils." *Fibers and Polymers* 8(6): 635-641.

Zarei, O., et al. (2008). "Optimization of multi-pass face-milling via harmony search algorithm." *J. Mater. Process. Technol.* 209: 2386–2392.

Zentar, R., et al. (2001). "Identification of soil parameters by inverse analysis." *computers and geotechnics* 28(2): 129-144.

Zhang, J., et al. (2011). "Reliability-Based Optimization of Geotechnical Systems." *Journal of Geotechnical and Geoenvironmental Engineering* 137(12): 1211-1221.

Zhang, M. X., et al. (2006). "Analysis of geosynthetic reinforced soil structures with orthogonal anisotropy." *Geotechnical and Geological Engineering* 24: 903–917.

Zhang, Y., et al. (2009). "Simulation-based calibration of geotechnical parameters using parallel hybrid moving boundary particle swarm optimization." *computers and geotechnics* 36(4): 604-615.

Zou, D., et al. (2010). "A novel global harmony search algorithm for reliability problems." *Comput Ind Eng* 58(2): 307-316.

Appendix A

THE CODE FOR UNIFORM REINFORCEMENT ARRANGEMENT (USED IN CHAPTER 3)

In Appendix A the Matlab code used for optimization of design for an earth wall with uniform geosynthetic layers is presented. Firstly the main body of the code is presented and then the two subroutines to get the required parameter and calculate the cost of the construction is mentioned.

A.1 The Main Body of the Code

```
%% Problem Definition

% Cost Function:
CostF(NoG,A,Hd,alfa,e,c1,qs,Ke,Ki,delta,Nf,Nq,teta,J,k,gg,h,I,CoG);
% Cost Function
[a1,alfa,qs,b,c1,d,e,gg,h,I,J,k,Nf,Nq,teta,Hd,delta,Ke,Ki]=getpar();
% Get the parameters

%% Harmony Search Parameters

    prompt = {'Maximum Iteration:',...
              'Harmony Memory Size:',...
              'New Memory Size:',...
              'Harmony Memory Consideration Rate:',...
              'Pitch Adjustment Rate:',...
              'Fret Width Damp Ratio:'};

            pause(0.01);

    dlg_title1 = 'Assign the height of the wall and specify a range
for geosynthetic spacing and length:';


    num_lines1 = 1;
```

```
    def1 = {'5000','20','20','0.5','0.5','0.9995'};

    options.Resize='on';
    options.WindowStyle='normal';
    options.Interpreter='tex';

    answer = inputdlg(prompt,dlg_title1,num_lines1,def1,options);

    CCC = cell2mat(answer(1));
    MaxIt = str2double(CCC);            % Maximum Number of
Iterations

    DDD = cell2mat(answer(2));
    HMS = str2double(DDD);              % Harmony Memory Size

    EEE = cell2mat(answer(3));
    nNew = str2double(EEE);             % Number of New Harmonies

    FFF = cell2mat(answer(4));
    HMCR = str2double(FFF);             % Harmony Memory
Consideration Rate

    GGG = cell2mat(answer(5));
    PAR = str2double(GGG);              % Pitch Adjustment Rate

    HHH = cell2mat(answer(6));
    FW_damp = str2double(HHH);          % Fret Width Damp Ratio


%% if both of the Spacings and lengths are constant along the wall
height:



    nVar=2;                 % Number of Decision Variables
    VarSize=[1 nVar];       % Decision Variables Matrix Size

    prompt = {'Smin:',...
              'Smax:',...
              'Lmin:',...
              'Lmax:'};

            pause(0.01);

    dlg_title1 = 'specify ranges for geosynthetic spacing and
length:';
```

```
    num_lines1 = 1;

    def1 = {'0.5','1.2','1','7'};

    options.Resize='on';
    options.WindowStyle='normal';
    options.Interpreter='tex';

    answer = inputdlg(prompt,dlg_title1,num_lines1,def1,options);

    AA = cell2mat(answer(1));
    Smin = str2double(AA);

    BB = cell2mat(answer(2));
    Smax = str2double(BB);

    CC = cell2mat(answer(3));
    Lmin = str2double(CC);

    DD = cell2mat(answer(4));
    Lmax = str2double(DD);


%Maximum and minimum number of Geosynthetics:

NN1=(round(Hd/Smin))-1;
NN2=(round(Hd/Smax))-1;

%Band Widthes:


FW1=0.02*(Smax-Smin);     % Fret Width (Bandwidth) for Spacings
FW2=0.02*(Lmax-Lmin);     % Fret Width (Bandwidth) for lengths

%% Cost of Geosynthetics:

    prompt = {'Cost of Geosynthetic (2.6 for geotextile & 2 for
geogrid):'};

            pause(0.01);

    dlg_title1 = 'Cost of Geosynthetic:';


    num_lines1 = 1;

    def1 = {'2.6'};
```

```
    options.Resize='on';
    options.WindowStyle='normal';
    options.Interpreter='tex';

    answer = inputdlg(prompt,dlg_title1,num_lines1,def1,options);

    AAA = cell2mat(answer(1));
    CoG = str2double(AAA);

    %% Cost of Geosynthetics:

    prompt = {['Choose between ' num2str(NN2) ' and ' num2str(NN1) '
:']};

            pause(0.01);

    dlg_title1 = 'Number of Geosynthetic:';

    num_lines1 = 1;

    def1 = {num2str(NN2)};

    options.Resize='on';
    options.WindowStyle='normal';
    options.Interpreter='tex';

    answer = inputdlg(prompt,dlg_title1,num_lines1,def1,options);

    BBB = cell2mat(answer(1));
    NoG = str2double(BBB);


%% Initialization

% Empty Harmony Structure
empty_harmony.NoG=[];
empty_harmony.NoS=[];
empty_harmony.Length=[];
empty_harmony.Spacing=[];
empty_harmony.Cost=[];
empty_harmony.CoV=[];

% Initialize Harmony Memory
HM=repmat(empty_harmony,HMS,1);

% Create Initial Harmonies
```

```
for i=1:HMS

    % assign length to harmony position
    HM(i).NoG=NoG;                                  %Assign a random
value for GeoS numbers;
    HM(i).NoS=NoG+1;
    HM(i).Spacing=Hd/HM(i).NoS;
    HM(i).Length=unifrnd(Lmin,Lmax,[1 NoG]);        %Uniform random
values for Lengths;

    %the costs of initial harmonies:

[HM(i).CoV,HM(i).Cost]=CostF(HM(i).Length,HM(i).Spacing,HM(i).NoG,Hd,
alfa,e,c1,qs,Ke,Ki,delta,Nf,Nq,teta,J,k,gg,h,I,CoG);
end


% Sort Harmony Memory
[BbBb, SortOrder]=sort([HM.Cost]);
HM=HM(SortOrder);

% Update Best Solution Ever Found
BestSol=HM(1);

% Array to Hold Best CoV
BestCoV=zeros(MaxIt,1);

% Array to Hold Best Cost Values
BestCost=zeros(MaxIt,1);

% Array to Hold Mean Cost Values
MeanCost=zeros(MaxIt,1);

HMit=repmat(empty_harmony,nNew+HMS,1);


%% Harmony Search Main Loop

for it=1:MaxIt

    % Initialize Array for New Harmonies
    NEW=repmat(empty_harmony,nNew,1);

    % Create New Harmonies

    for kk=1:nNew

    NEW(kk).NoG=NoG;                                %Assign a random
value for GeoS numbers;
```

```
    NEW(kk).NoS=NoG+1;
    NEW(kk).Spacing=HM(kk).Spacing;


    % Create New Harmony Position and set Probability analysis
        NEW(kk).Length=unifrnd(Lmin,Lmax,[1 NoG]);   %Uniform random
values for Lengthes;
        for j=1:NoG
            if rand<=HMCR
                % Use Harmony Memory
                i=randi(1,1,[1,HMS]);
                    NEW(kk).Length(1,j)=HM(i).Length(1,j);
            end

            % Pitch Adjustment
            if rand<=PAR
                          % Length
                %DELTA=FW2*unifrnd(-1,+1);     % Uniform
                 DELTA=FW2*randn();            % Gaussian (Normal)
                 NEW(kk).Length(1,j)=NEW(kk).Length(1,j)+DELTA;

                % Apply Variable Limits

                     % Length

NEW(kk).Length(1,j)=max(NEW(kk).Length(1,j),Lmin);

NEW(kk).Length(1,j)=min(NEW(kk).Length(1,j),Lmax);

            end

        end

        % Evaluation

[NEW(kk).CoV,NEW(kk).Cost]=CostF(NEW(kk).Length,NEW(kk).Spacing,NEW(k
k).NoG,Hd,alfa,e,c1,qs,Ke,Ki,delta,Nf,Nq,teta,J,k,gg,h,I,CoG);

    end

    % Merge Harmony Memory and New Harmonies
    HMit=[HM
        NEW];

    % Sort Harmony Memory
    [AaAa, SortOrder]=sort([HMit.Cost]);
    HMit=HMit(SortOrder);

    % Truncate Extra Harmonies
    HM=HM(1:HMS);
```

```
    % Update Best Solution Ever Found
    BestSol=HM(1);

    % Store Coefficient of violation Ever Found
    BestCoV(it)=BestSol.CoV;

    % Store Best Cost Ever Found
    BestCost(it)=BestSol.Cost;

    % Store Mean Cost
    MeanCost(it)=mean([HM.Cost]);

    % Show Iteration Information
    disp(['Iteration ' num2str(it) ': Best Cost = '
num2str(BestCost(it))   ': Best CoV = ' num2str(BestCoV(it))]);

    % Damp Fret Width
    FW1=FW1*FW_damp;
    FW2=FW2*FW_damp;

end

%% Results

figure;
semilogy(BestCost,'r','LineWidth',2);
hold on;
semilogy(MeanCost,'b:','LineWidth',2);
hold off;
xlabel('Iteration');
legend('Best Cost','Mean Cost');
```

A.2 Subroutine Used to Get the Input Parameters

In this subroutine the value of different parameters used in design of the MSE Walls reinforced by geosynthetics, acquired by an input user interface.

```
function [a,b,c,d,e,f,g,h,i,j,k,l,m,n,o,p,q,r,s]=getpar(x)


prompt = {'H(m):',...
                'peak acceleration coefficient:',...
```

```
                'Surcharge(KN/M):',...
                'Angle of internal friction of the
fill(phi,degree):',...
                'Unit weight of the fill(KN/m3):',...
                'Angle of internal friction of the
backfill(phi,degree):',...
                'Unit weight of the backfill(KN/M3):',...
                'FS(ovd,min):',...
                'FS(sld,min):',...
                'FS(bcd,min):',...
                'FS(std,min):',...
                'FS(pld,min):',...
                'Nf:',...
                'Nq:'};

            pause(0.01);

    dlg_title1 = 'inter the input parameters:';

    num_lines1 = 1;

    def1 =
{'5','0','0','34','20','30','18','2','1.5','2','1.5','2','41.06','29.
44'};

    options.Resize='on';
    options.WindowStyle='normal';
    options.Interpreter='tex';

    answer = inputdlg(prompt,dlg_title1,num_lines1,def1,options);

    AA = cell2mat(answer(1));
    a = str2double(AA);

    BB = cell2mat(answer(2));
    b = str2double(BB);

    CC = cell2mat(answer(3));
    c = str2double(CC);

    DD = cell2mat(answer(4));
    d = str2double(DD);

    EE = cell2mat(answer(5));
    e = str2double(EE);

    FF = cell2mat(answer(6));
    f = str2double(FF);

    GG = cell2mat(answer(7));
```

```
    g = str2double(GG);

    HH = cell2mat(answer(8));
    h = str2double(HH);

    II = cell2mat(answer(9));
    i = str2double(II);

    JJ = cell2mat(answer(10));
    j = str2double(JJ);

    KK = cell2mat(answer(11));
    k = str2double(KK);

    LL = cell2mat(answer(12));
    l = str2double(LL);

    MM = cell2mat(answer(13));
    m = str2double(MM);

    NN = cell2mat(answer(13));
    n = str2double(NN);

%failure wedge slopes at an angle(teta):
o=(d/2)+45;
%Design height:
p=a+.45;
%friction between soil and reinforcement:
q=(2*d)/3;
%('Kae=');
r=(1-sind(f))/(1+sind(f));
%('Kai=');
s=(1-sind(d))/(1+sind(d));

%[a1,alfa,qs,b,c1,d,e,gg,h,I,J,k,Nf,Nq,teta,Hd,delta,Ke,Ki]=getpar()
```

A.3 Subroutine Used to Calculate the Cost of the Wall

The cost of construction is calculated and compared to the method of non-uniform reinforcement layers. The penalty function is also applied in this subroutine.

```
Function
[CCC,CostF]=CostF(A,SpS,NoG,Hd,alfa,e,c1,qs,Ke,Ki,delta,Nf,Nq,teta,J,
k,gg,h,I,CoG)


%Initial spacings and length of Geosynthetics

% A   = a vector of lengths
% SpS = spacing
% NoG = Number of Geosynthetics

Amax=max(A);

%% Factors of safety:

%pseudo static external force:
Fe=(.375*alfa*e*(Hd^2))*.5+.5*(alfa*c1*Hd*Amax);

%pseudo static internal force:
Fi=.5*alfa*Amax*Hd*c1;

%FS overturning
Fo=((3*(c1*Hd+qs))*(Amax^2))/(Ke*(Hd^2)*(e*Hd+3*qs)+Fe);

%FS sliding
Rs=(c1*Hd+qs)*Amax*tand(delta);
Pa=.5*Ke*e*(Hd^2)+Ke*qs*Hd;
Fsl=Rs/(Pa+Fe);

%FS bearing capacity
e1=(Ke*(Hd^2)*(e*Hd+3*qs))/(6*(c1*Hd+(qs/Amax)));
qmax=(c1*Hd+qs)*(1+((6*e1)/Amax));
qnet=.5*c1*Nf*Amax+qs*Nq;
Fb=qnet/(qmax+Fe);

%FS pullout

zi=zeros(1,NoG);
le=zeros(1,NoG);
leSum=0;

for i=1:NoG
    zi(i)=i*SpS;
    le(i)=A(i)-((Hd-zi(i))/tand(teta));
    leSum=leSum+le(i);
end

g=zeros(1,NoG);
G=zeros(1,NoG);
```

```
for i=1:NoG
         g(i)=Ki*(qs+e*zi(i))*SpS;
%required strength geosynthetic

G(i)=(2*(c1*zi(i)+qs)*(tand(delta)*(le(i))))/(g(i)+(Fi*(le(i)/leSum))
);                %FS Pullout
end


%% constraints


E=zeros(1,NoG);
pp=zeros(1,NoG);
ll=zeros(1,NoG);

SumPP=0;
SumE=0;
Sumll=0;

for j=1:NoG

      if (g(j)/(60/J))-1<=0,      % C for Ta<60
       E(j)=0;
      else
       E(j)=(g(j)/(60/J))-1;
       SumE=SumE+E(j);
      end
       if 1-(G(j)/k)<=0,          % C for Pull out
       pp(j)=0;
       else
       pp(j)=1-(G(j)/k);
       SumPP=SumPP+pp(j);
       end
       if 1-(le(j))<=0,          %C For effective length >1
      ll(j)=0;
       else
       ll(j)=1-(le(j));
       Sumll=Sumll+ll(j);
       end
 end


if 1-(Fo/gg)<=0,         %C for F overturning
    C1=0;
else
    C1=1-(Fo/gg);
end
if 1-(Fsl/h)<=0,            %C for F slide
```

```
    C2=0;
else
    C2=1-(Fsl/h);
end
if 1-(Fb/I)<=0,     %C for f bearing
    C3=0;
else
    C3=1-(Fb/I);
end



%cost of geosynthetic

  Gcst=zeros(1,NoG);
  Gcstall=0;

for j=1:NoG
    Gcst(j)=((g(j)*0.03)+CoG)*A(i);    %CoG = Cost of geot=2.6  geog=2
    Gcstall=Gcstall+Gcst(j);
end

%Coefficient of violation

CCC=C1+C2+C3+SumPP+Sumll+SumE;

  %Cost Function
   CostF=((3*20*Hd*Amax/9.81)+Gcstall+10+80*Hd)*200*(1+10*CCC);
```

Appendix B

THE CODE FOR NON-UNIFORM REINFORCEMENT ARRANGEMENT (USED IN CHAPTER 4)

In Appendix B the Matlab code used for optimization of design for an earth wall with non-uniform geosynthetic layers is presented. First, the main body of the code is presented and then the two subroutines to get the required parameter and calculate the cost of the construction is mentioned.

B.1 The Main Body of the Code

```
%% Input parameters
[H0,alfa,qs,b,c1,d,e,gg,h,I,J,k,Nf,Nq,teta,Hd,delta,Ke,Ki]=getpar();


CoG=2.6;
NoG=8;


%% Problem Definition

% Cost Function:
CostF(NoG,A,Hd,alfa,e,c1,qs,Ke,Ki,delta,Nf,Nq,teta,J,k,gg,h,I,CoG);
% Cost Function


%% Harmony Search Parameters

MaxIt=1200;      % Maximum Number of Iterations

HMS=20;          % Harmony Memory Size

nNew=20;         % Number of New Harmonies
```

```
%% if both of the Spacings and lengths are constant along the wall
height:



    Smin = 0.2;

    Smax = 1.5;

    Lmin = 1;

    Lmax = 10;



%for NoG=6:10


    SoG=NoG+1;
    nVar=NoG+1;                 % Number of Decision Variables
    VarSize=[1 nVar];       % Decision Variables Matrix Size

%Maximum and minimum number of Geosynthetics:

max_NoG=(round(Hd/Smin))-1;
min_NoG=(round(Hd/Smax))-1;

%% define IHS parameters:

HMCR=0.95;       % Harmony Memory Consideration Rate

% For L:

PARmaxL=0.99;        % Pitch Adjustment Rate
PARminL=0.35;
PARminLIt=PARminL;

FWminL=0.009;
FWmaxL=0.05*(Lmax-Lmin);
FWmaxLIt=FWmaxL;

C_FWL=(log(FWminL/FWmaxL))/MaxIt;

% For S:

PARmaxS=0.99;        % Pitch Adjustment Rate
```

```
PARminS=0.35;
PARminSIt=PARminS;

FWminS=0.009;
FWmaxS=0.2;
FWmaxSIt=FWmaxS;

C_FWS=(log(FWminS/FWmaxS))/MaxIt;

DscrtV=0.1;          % Discretization value for S
Prmt_S=100;          % Number of permutations considered
PAR1=0.5;            % Permutation Consideration Probability


%% Applicability

Limit1=SoG*Smin;
Limit2=SoG*Smax;

  if Limit1 > H0 || Limit2 < H0
   error(['Error, inappropriate NoG. Please choose between '
num2str(min_NoG) ' and ' num2str(max_NoG)])
  end



%% For NN2:NN1

Diff=max_NoG-min_NoG+1;

%% Initialization

% Empty Harmony Structure

empty_harmony.PositionL=[];
empty_harmony.PositionS=[];
empty_harmony.NoG=[];
empty_harmony.Cost=[];
empty_harmony.CoV=[];
empty_harmony.Ti=[];
empty_harmony.MAXT=[];
empty_harmony.Saving=[];
empty_harmony.CCC=[];
HMtwo=[];

% Initialize Harmony Memory
HM=repmat(empty_harmony,HMS,1);
```

```
%what is initial spacing and length? (I assigned equal spacing and
equal length)


% Create Initial Harmonies

for i=1:HMS

    HM(i).NoG=NoG;
    %     ============================== TOP      |                   |
    %     ##                   | S1                |                   |
    %     ##                   |                   |                   |
    %     -------------------------                |                   |
    %     ##              | S2                     |                   |
    %     ##              |                        |                   |
    %     -------------------------                |                   |
    %     ##            | S3                       |H0                 |
    %     ##            |                          |                   |
    %     -------------------------                |                   |
Hd
    %     ##        | S4                           |                   |
    %     ##        |                              |                   |
    %     ------------------------                 |                   |
    %     ##     | S5                              |                   |
    %     ##     |                                 |                   |
    %     ============================             |                   |
    %     ##        |                                                  |
    %     ##      0.45                                                 |
    %     ##        |                                                  |

        [XX]=q2(Smin,Smax,DscrtV,NoG+1,H0);
        HM(i).PositionS=XX(1,:);

        HM(i).PositionL(1,1)=unifrnd(Lmin,Lmax);
%A=unifrnd(Lmin,Lmax);
            for L1st=2:NoG

HM(i).PositionL(1,L1st)=unifrnd(Lmin,HM(i).PositionL(1,L1st-1));
%A=unifrnd(Lmin,Lmax);
            end

[HM(i).CCC,HM(i).MAXT,HM(i).Ti,~,HM(i).CoV,HM(i).Cost]=CostFN(HM(i).P
ositionL,XX,NoG,Hd,alfa,e,c1,qs,Ke,Ki,delta,Nf,Nq,teta,J,k,gg,h,I,CoG
);

end


% Sort Harmony Memory
```

```
[~, SortOrder]=sort([HM.Cost]);
HM=HM(SortOrder);

HMone=HM;

% Update Best Solution Ever Found
BestSol=HM(1);

% Array to Hold Best CoV
BestCoV=zeros(MaxIt,1);

% Array to Hold Best Cost Values
BestCost=zeros(MaxIt,1);

% Array to Hold Mean Cost Values
MeanCost=zeros(MaxIt,1);

HMit=repmat(empty_harmony,nNew+HMS,1);

%% Harmony Search Main Loop

for it=1:MaxIt

    % Initialize Array for New Harmonies
    NEW=repmat(empty_harmony,nNew,1);

% Create New Harmonies
 for kk=1:nNew

    NEW(kk).NoG=NoG;
        [ZZ]=q2(Smin,Smax,DscrtV,NoG+1,H0);
            NEW(kk).PositionS=ZZ(1,:);

            NEW(kk).PositionL(1,1)=unifrnd(Lmin,Lmax);
%A=unifrnd(Lmin,Lmax);
            for L1st=2:NoG

NEW(kk).PositionL(1,L1st)=unifrnd(Lmin,NEW(kk).PositionL(1,L1st-1));
%A=unifrnd(Lmin,Lmax);
            end


[NEW(kk).CCC,NEW(kk).MAXT,NEW(kk).Ti,~,NEW(kk).CoV,NEW(kk).Cost]=Cost
FN(NEW(kk).PositionL,ZZ,NoG,Hd,alfa,e,c1,qs,Ke,Ki,delta,Nf,Nq,teta,J,
k,gg,h,I,CoG);


NEWJ_HMCR=repmat(NEW(kk),nVar,1);
NEWJ_PAR1=repmat(NEW(kk),nVar,1);
```

```
NEWJ_PAR2=repmat(NEW(kk),nVar,1);
NEWJ_PAR3=repmat(NEW(kk),Prmt_S,1);

        for j=1:nVar
%% Harmony Memory Consideration
P_HMCR=rand;
            if P_HMCR<=HMCR
                % Use Harmony Memory
                i=randi([1 HMS]);
              if j==1
                NEW(kk).PositionS=HM(i).PositionS;
              else
                NEW(kk).PositionL(1,j-1)=HM(i).PositionL(1,j-1);
              end

              %Multiple Evaluation (1)

[NEWJ_HMCR(j).CCC,NEWJ_HMCR(j).MAXT,NEWJ_HMCR(j).Ti,~,NEWJ_HMCR(j).Co
V,NEWJ_HMCR(j).Cost]=CostFN(NEW(kk).PositionL,NEW(kk).PositionS,NoG,H
d,alfa,e,c1,qs,Ke,Ki,delta,Nf,Nq,teta,J,k,gg,h,I,CoG);
               NEWJ_HMCR(j).PositionL=NEW(kk).PositionL;
               NEWJ_HMCR(j).PositionS=NEW(kk).PositionS;
               NEWJ_HMCR(j).NoG=NoG;
            end


 Cpar1=0;
 Cpar2=0;
 Cpar3=0;

%% Pitch Adjustment
P_PAR=rand;


                if j==1
                    if P_PAR<=PARminSIt

[YY]=Vicinity_H(NEW(kk).PositionS,Smin,Smax,FWmaxSIt,SoG);
                           S3=size(YY);
                           NEWD1=repmat(empty_harmony,S3(1,1),1);

                               for ww3=1:S3(1,1)

[NEWD1(ww3).CCC,NEWD1(ww3).MAXT,NEWD1(ww3).Ti,~,NEWD1(ww3).CoV,NEWD1(
ww3).Cost]=CostFN(NEW(kk).PositionL,YY(ww3,:),NoG,Hd,alfa,e,c1,qs,Ke,
Ki,delta,Nf,Nq,teta,J,k,gg,h,I,CoG);

NEWD1(ww3).PositionL=NEW(kk).PositionL;
                                    NEWD1(ww3).PositionS=YY(ww3,:);
                                    NEWD1(ww3).NoG=NoG;
                               end
```

```
                            [~, SortOrder2]=sort([NEWD1.Cost]);
                             NEWD1=NEWD1(SortOrder2);
                             NEW(kk)=NEWD1(1);

                        %Multiple Evaluation (2)

[NEWJ_PAR1(j).CCC,NEWJ_PAR1(j).MAXT,NEWJ_PAR1(j).Ti,~,NEWJ_PAR1(j).Co
V,NEWJ_PAR1(j).Cost]=CostFN(NEW(kk).PositionL,NEW(kk).PositionS,NoG,H
d,alfa,e,c1,qs,Ke,Ki,delta,Nf,Nq,teta,J,k,gg,h,I,CoG);
                         NEWJ_PAR1(j).PositionL=NEW(kk).PositionL;
                         NEWJ_PAR1(j).PositionS=NEW(kk).PositionS;
                         NEWJ_PAR1(j).NoG=NoG;
                         HCount=1;
                        end
                    end

                   if j>1
                       if P_PAR<=PARminLIt
                        %DELTA=FW*unifrnd(-1,+1);    % Uniform
                         DELTA=FWmaxLIt*randn();            % Gaussian
(Normal)
                         NEW(kk).PositionL(1,j-1)=NEW(kk).PositionL(1,j-
1)+DELTA;
                         %% Apply Variable Limits
                         NEW(kk).PositionL(1,j-
1)=max(NEW(kk).PositionL(1,j-1),Lmin);
                         NEW(kk).PositionL(1,j-
1)=min(NEW(kk).PositionL(1,j-1),Lmax);

                         %Multiple Evaluation (3)

[NEWJ_PAR2(j).CCC,NEWJ_PAR2(j).MAXT,NEWJ_PAR2(j).Ti,~,NEWJ_PAR2(j).Co
V,NEWJ_PAR2(j).Cost]=CostFN(NEW(kk).PositionL,NEW(kk).PositionS,NoG,H
d,alfa,e,c1,qs,Ke,Ki,delta,Nf,Nq,teta,J,k,gg,h,I,CoG);
                         NEWJ_PAR2(j).PositionL=NEW(kk).PositionL;
                         NEWJ_PAR2(j).PositionS=NEW(kk).PositionS;
                         NEWJ_PAR2(j).NoG=NoG;
                       end
                   end
           end

P_PAR2=rand;
           if P_PAR2<=PAR1

               SC1=0;
               for CparC=1:Prmt_S
                       SC1=SC1+1;
                       ranC2=randperm(SoG);

[NEWJ_PAR3(SC1).CCC,NEWJ_PAR3(SC1).MAXT,NEWJ_PAR3(SC1).Ti,~,NEWJ_PAR3
(SC1).CoV,NEWJ_PAR3(SC1).Cost]=CostFN(NEW(kk).PositionL,NEW(kk).Posit
```

```
ionS(ranC2),NoG,Hd,alfa,e,c1,qs,Ke,Ki,delta,Nf,Nq,teta,J,k,gg,h,I,CoG
);
                    NEWJ_PAR3(SC1).PositionL=NEW(kk).PositionL;

NEWJ_PAR3(SC1).PositionS=NEW(kk).PositionS(ranC2);
                    NEWJ_PAR3(SC1).NoG=NEW(kk).NoG;
            end
        end

                NEW_Total=[NEWJ_HMCR
            NEWJ_PAR1
            NEWJ_PAR2
            NEWJ_PAR3];

       [~, SortOrder3]=sort([NEW_Total.Cost]);
       NEW_Total=NEW_Total(SortOrder3);
       NEW(kk)=NEW_Total(1);


end

    % Merge Harmony Memory and New Harmonies
    HMit=[HM
        NEW];

    if it==1
        HMtwo=[HM
            NEW(1)];
    [~, SOr]=sort([HMtwo.Cost]);
    HMtwo=HMtwo(SOr);
    end

    % Sort Harmony Memory
    [~, SortOrder2]=sort([HMit.Cost]);
    HMit=HMit(SortOrder2);

    % Truncate Extra Harmonies
    HM=HMit(1:HMS);



    % Update Best Solution Ever Found
    BestSol=HM(1);

    % Store Coefficeient of violation Ever Found
    BestCoV(it)=BestSol.CoV;

    % Store Best Cost Ever Found
    BestCost(it)=BestSol.Cost;
```

```
    % Store Mean Cost
    MeanCost(it)=mean([HM.Cost]);

    % Show Iteration Information
    disp(['Iteration ' num2str(it) ': Best Cost = '
num2str(BestCost(it))    ': Best CoV = ' num2str(BestCoV(it))]);

    % Damp Fret Width for Length
    PARminLIt=PARminL+((PARmaxL-PARminL)*it/MaxIt);

    FWmaxLIt=FWmaxL*exp(C_FWL*it);

    % Damp Fret Width for Length
    PARminSIt=PARminS+((PARmaxS-PARminS)*it/MaxIt);

    FWmaxSIt=FWmaxS*exp(C_FWS*it);

end

%% Results


figure;
semilogx(BestCost,'r','LineWidth',8);
hold on;
semilogx(MeanCost,'b:','LineWidth',8);
hold off;
xlabel('Iteration');
ylabel('Cost');
legend('Best Cost','Mean Cost');


if CoG==2

PMKD=['D:\Paper-Works\HArmony 2\A' num2str(alfa) 'q' num2str(qs) '-
gg\excel-' num2str(H0) 'm\'];
mkdir(PMKD, [ num2str(H0) '-' num2str(NoG) '-' num2str(MaxIt) 'NoG'])
PMKDfig1=['D:\Paper-Works\HArmony 2\A' num2str(alfa) 'q' num2str(qs)
'-gg\excel-' num2str(H0) 'm\' num2str(H0) '-' num2str(NoG) '-'
num2str(MaxIt) 'NoG\' 'CstIt.fig'];
savefig(PMKDfig1)

end

if CoG==2.6

PMKD=['D:\Paper-Works\HArmony 2\A' num2str(alfa) 'q' num2str(qs) '-
gt\excel-' num2str(H0) 'm\'];
mkdir(PMKD, [ num2str(H0) '-' num2str(NoG) '-' num2str(MaxIt) 'NoG'])
```

```
PMKDfig1=['D:\Paper-Works\HArmony 2\A' num2str(alfa) 'q' num2str(qs)
'-gt\excel-' num2str(H0) 'm\' num2str(H0) '-' num2str(NoG) '-'
num2str(MaxIt) 'NoG\' 'CstIt.fig'];
savefig(PMKDfig1)

end

%% Calculate the saving

if CoG==2.6

    if H0==5
       if alfa==0 && qs==0
          CTC=116826.2;
       elseif alfa==0 && qs==10
          CTC=117066;
       else
          CTC=120390.5;
       end
    end

    if H0==7
       if alfa==0 && qs==0
          CTC=175045.2;
       elseif alfa==0 && qs==10
          CTC=178993.7;
       else
          CTC=184432.2;
       end
    end

    if H0==9
       if alfa==0 && qs==0
          CTC=253864.8;
       elseif alfa==0 && qs==10
          CTC=258287.4;
       else
          CTC=271914.3;
       end
    end

end


if CoG==2

    if H0==5
       if alfa==0 && qs==0
          CTC=159262.7;
       elseif alfa==0 && qs==10
```

```
            CTC=159510.6;
        else
            CTC=162693.4;
        end
    end

    if H0==7
        if alfa==0 && qs==0
            CTC=232052.6;
        elseif alfa==0 && qs==10
            CTC=235405.1;
        else
            CTC=240560.5;
        end
    end

    if H0==9
        if alfa==0 && qs==0
            CTC=322755.3;
        elseif alfa==0 && qs==10
            CTC=326459.7;
        else
            CTC=338650.2;
        end
    end
end

Perc_C=(CTC-BestSol.Cost)/CTC;
disp(['Saving(%): ' num2str(Perc_C) '% '])
disp(['Previous Cost value($): ' num2str(CTC)])

for iS=1:HMS
    HM(iS).Saving=Perc_C;
end


%% plot the arrangement of reinforcements

FIGLSUM=0;
figure;
for i=1:NoG
    FIGZ=HM(1).PositionS(1,i);
    FIGL=HM(1).PositionL(1,i);
    FIGLSUM=FIGLSUM+FIGZ;
    FIGH=H0-FIGLSUM;
    FIGX=[0 FIGL];
    FIGY=[FIGH FIGH];
    plot(FIGX,FIGY);
    hold on;
end
```

```
FIGX=[0 H0/tand(teta)];
FIGY=[0 H0];
plot(FIGX,FIGY);

hold off;
xlabel('Length of Geosynthetics (m)');
ylabel('Height of Geosynthetics (m)');
axis([0 HM(1).PositionL(1,1)+0.5 0 FIGLSUM+HM(1).PositionS(1,SoG)])
```

B.2 Subroutine Used to Get the Input Parameters

In this subroutine the value of different parameters used in design of the MSE Walls reinforced by geosynthetics, acquired by an input user interface.

```
function
[H0,alfa,qs,b,c1,d,e,gg,h,I,J,k,Nf,Nq,teta,Hd,delta,Ke,Ki]=getpar()


prompt = {'H(m):',...
%H0       1
                'peak acceleration coefficient:',...
%alfa     2
                'Surcharge(KN/M):',...
%qs       3
                'Angle of internal friction of the
fill(phi,degree):',...          %b       4
                'Unit weight of the fill(KN/m3):',...
%c1       5
                'Angle of internal friction of the
backfill(phi,degree):',...      %d       6
                'Unit weight of the backfill(KN/M3):',...
%e        7
                'FS(ovd,min):',...
%gg       8
                'FS(sld,min):',...
%h        9
                'FS(bcd,min):',...
%I        10
                'FS(std,min):',...
%J        11
                'FS(pld,min):',...
%k        12
                'Nf:',...
%Nf       13
                'Nq:'};
%Nq       14
```

```
            pause(0.01);

    dlg_title1 = 'inter the input parameters:';

    num_lines1 = 1;

    def1 =
{'9','0','10','35','20','30','18','2','1.5','2','1.5','2','41.06','29
.44'};

    options.Resize='on';
    options.WindowStyle='normal';
    options.Interpreter='tex';

    answer = inputdlg(prompt,dlg_title1,num_lines1,def1,options);

    AA = cell2mat(answer(1));
    H0 = str2double(AA);

    BB = cell2mat(answer(2));
    alfa = str2double(BB);

    CC = cell2mat(answer(3));
    qs = str2double(CC);

    DD = cell2mat(answer(4));
    b = str2double(DD);

    EE = cell2mat(answer(5));
    c1 = str2double(EE);

    FF = cell2mat(answer(6));
    d = str2double(FF);

    GG = cell2mat(answer(7));
    e = str2double(GG);

    HH = cell2mat(answer(8));
    gg = str2double(HH);

    II = cell2mat(answer(9));
    h = str2double(II);

    JJ = cell2mat(answer(10));
    I = str2double(JJ);

    KK = cell2mat(answer(11));
    J = str2double(KK);
```

```
    LL = cell2mat(answer(12));
    k = str2double(LL);

    MM = cell2mat(answer(13));
    Nf = str2double(MM);

    NN = cell2mat(answer(13));
    Nq = str2double(NN);

%failure wedge slopes at an angle (teta):
teta=(b/2)+45;
%Design height:
Hd=H0+.45;
%friction between soil and reinforcement:
delta=(2*b)/3;
%('Kae=');
Ke=(1-sind(d))/(1+sind(d));
%('Kai=');
Ki=(1-sind(b))/(1+sind(b));

%[a1,alfa,qs,b,c1,d,e,gg,h,I,J,k,Nf,Nq,teta,Hd,delta,Ke,Ki]=getpar()
```

B.3 Subroutine Used to Calculate the Cost of the Wall

The cost of construction is calculated and compared to the method of non-uniform reinforcement layers. The penalty function is also applied in this subroutine.

```
function
[CCCC1,MAXT,g,SpS,CCC,CostF]=CostFN(A,SpS,NoG,Hd,alfa,e,c1,qs,Ke,Ki,d
elta,Nf,Nq,teta,J,k,gg,h,I,CoG)

%Initial spacings and length of Geosynthetics

% Ys  = an array of Yns
% A   = an array of Lengths
% SpS = a vector of spacings
% NoG = Number of Geosynthetics

A_min=min(A);

%% Factors of safety:

%pseudo static external force:
Fe=(.375*alfa*e*(Hd^2))*0.5+0.5*(alfa*c1*((Hd-0.45)^2));
```

```
%pseudo static internal force:
Fi=0.5*alfa*((Hd-0.45)^2)*c1;

%% FS overturning

MVo=0;
MVoNoG=zeros(1,NoG);

for i=1:NoG
    if i==1
        MVoNoG(i)=(SpS(i)+(SpS(i+1)/2))*A(i)*c1*(A(i)/2);
    elseif i==NoG
        MVoNoG(i)=((SpS(i)/2)+SpS(i+1)+0.45)*A(i)*c1*(A(i)/2);
    else
        MVoNoG(i)=((SpS(i)+SpS(i+1))/2)*A(i)*c1*(A(i)/2);
    end
   MVo=MVo+MVoNoG(i);
end

MVototal=(qs*(A(1)^2)/2)+MVo;

Mo=Ke*c1*(Hd^3)*(1/6)+Ke*qs*(Hd^2)*(1/2)+Fe;

Fo=MVototal/Mo;

% for same length and same spacings:
% Fo=((3*(c1*(Hd-0.45)+qs))*(A_max^2))/(Ke*((Hd-0.45)^2)*(e*(Hd-
0.45)+3*qs)+Fe);

%% FS sliding

%total valume of the soil to be excavated:

VolT=0;
SVolT=zeros(1,NoG);

for i=1:NoG
    if i==1
        SVolT(i)=(SpS(i)+(SpS(i+1)/2))*A(i);
    elseif i==NoG
        SVolT(i)=((SpS(i)/2)+SpS(i+1)+0.45)*A(i);
    else
        SVolT(i)=((SpS(i)+SpS(i+1))/2)*A(i);
    end
   VolT=VolT+SVolT(i);
end

% calculate the FSsliding
```

```
Rs=( (c1*(Hd))*A_min + (VolT-(A_min*Hd))*c1 + qs*A(1) )*tand(delta);
Pa=0.5*Ke*e*(Hd^2)+Ke*qs*Hd;
Fsl=Rs/(Pa+Fe);

%% FS bearing capacity

SigmaMV2=0;
MV2=zeros(1,NoG);

%Moment of extra lengths more than A(NoG)

for i=1:NoG
    if i==1
        MV2(i)=(SpS(i)+(SpS(i+1)/2))*(A(i)-
A_min)*c1*((A(i)+A_min)/2);
    elseif i==NoG
        MV2(i)=((SpS(i)/2)+SpS(i+1)+0.45)*(A(i)-
A_min)*c1*((A(i)+A_min)/2);
    else
        MV2(i)=((SpS(i)+SpS(i+1))/2)*(A(i)-
A_min)*c1*((A(i)+A_min)/2);
    end
   SigmaMV2=SigmaMV2+MV2(i);
end

Driving_Moments=(1/3)*(0.5)*Ke*e*(Hd)^3+(qs*(Hd)^2*Ke)*0.5;
Resisting_Moments=SigmaMV2;
Vert_Load=VolT*c1+A(1)*qs;

%e1=(Ke*(Hd^2)*(e*Hd+3*qs))/(6*(c1*Hd+(qs/A_max)));
e1=(Driving_Moments-Resisting_Moments)/Vert_Load;
%qmax=(c1*Hd+qs)*(1+((6*e1)/A(NoG)));
qmax=(A(1)*qs+VolT*c1)/(A_min-2*e1);
qnet=.5*c1*Nf*A_min+qs*Nq;
Fb=qnet/(qmax+Fe);

%% FS pullout

zi=zeros(1,NoG);
le=zeros(1,NoG);
leSum=0;
SpSc=0;
for i=1:NoG
    SpSc=SpSc + SpS(i);
    zi(i)=SpSc;
    le(i)=A(i)-((Hd-0.45-zi(i))/tand(teta));
    leSum=leSum+le(i);
end

g=zeros(1,NoG);
G=zeros(1,NoG);
```

```
for i=1:NoG

g(i)=(Ki*(qs+c1*zi(i))*((SpS(i)+SpS(i+1))/2))+(Fi*(le(i)/leSum));
%required strength geosynthetic

G(i)=(2*(c1*zi(i)+qs)*(tand(delta)*(le(i))))/(g(i)+(Fi*(le(i)/leSum))
);                %FS Pullout
end

 %% constraints

E=zeros(1,NoG);
pp=zeros(1,NoG);
ll=zeros(1,NoG);

SumPP=0;
SumE=0;
Sumll=0;

for j=1:NoG

      if (g(j)/(60/J))-1<=0,      % C for Ta<60
       E(j)=0;
      else
       E(j)=(g(j)/(60/J))-1;
       SumE=SumE+E(j);
      end
       if 1-(G(j)/k)<=0,          % C for Pull out
       pp(j)=0;
       else
       pp(j)=1-(G(j)/k);
       SumPP=SumPP+pp(j);
       end
       if 1-(le(j))<=0,          %C For effective length >1
      ll(j)=0;
       else
       ll(j)=1-(le(j));
       Sumll=Sumll+ll(j);
       end
 end

if 1-(Fo/gg)<=0,         %C for F overturning
    C1=0;
else
    C1=1-(Fo/gg);
end
if 1-(Fsl/h)<=0,            %C for F slide
    C2=0;
else
    C2=1-(Fsl/h);
```

```
end
if 1-(Fb/I)<=0,     %C for f bearing
    C3=0;
else
    C3=1-(Fb/I);
end

%% cost of geosynthetic

  Gcst=zeros(1,NoG);
  Gcstall=0;
  MAXT=zeros(1,NoG);

for j=1:NoG
    Gcst(j)=((g(j)*.03)+CoG)*A(j);    %Cost geos=2.6  geog=2
    MAXT(j)=g(j)*1.5;
    Gcstall=Gcstall+Gcst(j);
end

C4=0;

for koli=2:NoG
    if A(koli) >= A(koli-1)
        C4=C4+0.1;
    end
end

%% Coefficient of violation

CCC=C1+C2+C3+C4+SumPP+Sumll+SumE;

CCCC1=[C1 C2 C3 C4 SumPP Sumll SumE];

%% Cost function:

  %Cost Function
  if CoG==2.6
   CostF=((3*c1*VolT/9.81)+Gcstall+10+80*Hd)*200*(1+6*CCC);
  elseif CoG==2
   CostF=((3*c1*VolT/9.81)+Gcstall+10+120*Hd)*200*(1+6*CCC);
  end

  % If g(i) is negative:

  if CostF<=0
      CostF=CostF*(-900);
  end
```